Ph. D. Thesis

FINGERPRINT IMAGE COMPRESSION AND GENDER CLASSIFICATION: AN APPROACH USING OPTIMIZED WAVELET COEFFICIENTS

Submitted by

SHANAVAZ K.T.

DIVISION OF ELECTRONICS ENGINEERING
SCHOOL OF ENGINEERING
COCHIN UNIVERSITY OF SCIENCE AND TECHNOLOGY
KOCHI – 682 022
INDIA

SEPTEMBER 2015

FINGERPRINT IMAGE COMPRESSION AND GENDER CLASSIFICATION: AN APPROACH USING OPTIMIZED WAVELET COEFFICIENTS

A thesis submitted by

SHANAVAZ K.T.

for the award of the degree of

DOCTOR OF PHILOSOPHY
(Faculty of Engineering)

Under the guidance of

Dr. P. MYTHILI

DIVISION OF ELECTRONICS ENGINEERING
SCHOOL OF ENGINEERING
COCHIN UNIVERSITY OF SCIENCE AND TECHNOLOGY
KOCHI – 682 022
INDIA

SEPTEMBER 2015

FINGERPRINT IMAGE COMPRESSION AND GENDER CLASSIFICATION: AN APPROACH USING OPTIMIZED WAVELET COEFFICIENTS

Ph. D. Thesis in the field of Image Processing

Author

SHANAVAZ K.T.
Research scholar
Division of Electronics Engineering
School of Engineering
Cochin University of Science and Technology
Kochi - 682 022, Kerala, INDIA
E-mail: shanavazkt@gmail.com

Research Advisor

Dr. P. MYTHILI
Associate Professor
Division of Electronics Engineering
School of Engineering
Cochin University of Science and Technology
Kochi - 682 022, Kerala, INDIA
E-mail: mythili@cusat.ac.in

September 2015

"Does man think that WE Cannot assemble his bones? Nay, WE are able to put Together in perfect order The very tips of his fingers."

[AL-QUR'AN 75:3-4]

CERTIFICATE

This is to certify that the thesis entitled "**Fingerprint Image Compression and Gender Classification : An Approach using Optimized Wavelet Coefficients**" is a bonafide record of research work carried out by Mr. Shanavaz K.T. under my supervision and guidance in the Division of Electronics Engineering, School of Engineering, Cochin University of Science and Technology, Kochi, Kerala, India and that no part of this thesis has been presented for the award of any other degree from any other university.

Kochi
22nd September 2015

Dr. P. Mythili, Ph. D.

(Supervising Guide)
Associate Professor
Division of Electronics Engineering
Cochin University of Science and Technology
Kochi, Kerala, INDIA

DECLARATION

I hereby declare that the work presented in the thesis entitled "**Fingerprint Image Compression and Gender Classification: An Approach using Optimized Wavelet Coefficients**" is based on the original work done by me under the supervision of Dr. P. Mythili, Associate Professor, Division of Electronics Engineering, School of Engineering, Cochin University of Science and Technology, Kochi, Kerala, India as Research guide and that no part of this thesis has been presented for the award of any other degree from any other institution.

Kochi **Shanavaz K.T.**
22nd September 2015

ACKNOWLEDGEMENT

First and foremost, I would like to thank God Almighty for providing me inspiration, wisdom, strength, health and patience to start and accomplish my goal.

I wish to put on record my deep sense of gratitude and thanks to my guide Dr. P. Mythili, Associate Professor, Division of Electronics Engineering, School of Engineering, Cochin University of Science and Technology (CUSAT), who has been the key source of motivation. Her valuable guidance and inspiration throughout this research work have been of the greatest help in carrying out this work in its present form. Her constant advice, discussions, support and encouragement have been so helpful that they made me complete the work successfully.

I am very much grateful to Dr. R. Gopikakumari, Professor, Division of Electronics Engineering, School of Engineering, Cochin University of Science and Technology, for the encouragement, support and suggestions offered to me during the research work.

I am very much indebted to Dr. Binu Paul, Head of the Department, Division of Electronics Engineering, School of Engineering, Cochin University of Science and Technology, for her support in pursuing my Ph.D. programme in the department.

I would like to extend my sincere gratitude to Dr. Rekha K. James and Dr. Deepa Sankar, Associate Professors , Division of Electronics Engineering, School of Engineering, Cochin University of Science and Technology, for their valuable suggestions and support given to me during the research work.

I acknowledge Dr. Bhadran V., Principal, College of Engineering, Attingal, Dr. Sunilkumar K., Associate Professor, Model Engineering College, Ernakulam, Mr. Renjith R., Technical Assistant, Department of Computer Science, Cochin University of Science and Technology, for helping and inspiring me in doing the research work.

My sincere thanks are due to Mr. Baby Paul, Mr. Anjith T.A. and Mrs. Rema N. R., Research Scholars, Division of Electronics Engineering, School of

Engineering, Cochin University of Science and Technology, for giving me inspiration for the timely completion of the work.

I specially thank Mr. Pradeep M. and Mr. Manilal D.L., Research Scholars, Department of Computer Science, Cochin University of Science and Technology, and Dr. Praveen M., former Research Scholar, Department of Electronics, for caring me and providing hardware facility for running some of the computer programs.

I would like to express my sincere thanks to all Faculty and Staff of Division of Electronics Engineering, School of Engineering, Cochin University of Science and Technology for their support and cooperation during the entire research work.

I am extremely obliged to my parents, who always stood behind me and offered me all the facilities in my life. I am grateful to my father-in-law, my brothers, sisters and their in-laws and other relatives for their timely help and support throughout the research work.

And above all, I would like to convey my deepest gratitude to my wife and daughters, for their love, care, understanding, patience and sacrifice to enable me to achieve this target, without which this endeavor would have been worth nil.

Shanavaz K.T.

ABSTRACT

The gigantic and radical developments in the field of Science and Technology and the associated improvements in the living standards of people demand to protect data to evade stealing of confidential information in applications, such as forensic, government, commercial, health-care, traveling and immigration, etc. Therefore, it is necessary to have an accurate and secure automatic identification and personal verification system. Biometrics has the potential to turn out to be the main automatic personal identification.

Fingerprints are the most widely used biometrics capable of identifying individuals because of their high immutability, acceptability and uniqueness. Fingerprints form a specific class of images having distinct characteristics which can differentiate them from other types of images.

Massive secondary storage devices that are needed to store fingerprint database are of great concern in fingerprint image processing. To reduce the rising demand on storage space, efficient image compression techniques are required. Wavelet based image coders are the state of art in image compression. The Federal Bureau of Investigation (FBI) fingerprint compression standard uses the cdf 9/7 classical wavelet filters. The filter coefficients used for wavelet transformation of the specific class of images like fingerprints can be optimized using evolutionary algorithms, resulting in better compression performance. The wavelet lifting scheme is an effective technique to represent classical wavelets with lesser number of coefficients. So, wavelet lifting filter coefficients can be optimized at a faster rate by using evolutionary techniques, which can then be used for performing compression in a lesser time.

Fingerprint classification takes a key role in any fingerprint identification system as it considerably decreases the time taken in identifying an individual. The database for searching an individual can be narrowed down by performing gender classification, as it calls for searching either a female or male database alone. This can

reduce the time required for searching an individual in a huge database. Discrete Wavelet Transform (DWT), Singular Value Decomposition (SVD) and Principal Component Analysis (PCA) techniques can be employed to derive feature vectors from fingerprints for gender classification using Neural Network (NN) classifiers. Again, by employing evolutionary techniques, the feature vectors formed by wavelet lifting coefficients and other parameters of the classifiers can be optimized for more accurate and faster gender classification.

Thus, the major contribution of this research include the development of :

- A novel fast and efficient algorithm for the compression of fingerprint images using wavelet lifting coefficients optimized by employing Genetic Algorithm (GA) -
  - (i) under quantization condition of transform coefficients. (It is a dual-objective problem that requires the maximization of both Peak Signal to Noise Ratio and Compression Ratio simultaneously. Here, the transform coefficients are subjected to uniform scalar quantization).
  - (ii) under thresholding condition of transform coefficients. (It is a single-objective problem with a fixed Compression Ratio that requires the maximization of Peak Signal to Noise Ratio alone. Here, the largest 1/16 transform coefficients are retained and the remaining values are discarded).
- A new algorithm for identifying gender more accurately and at a faster rate from fingerprints by employing -
  - (i) GA optimized wavelet lifting coefficients and neural networks using lesser number of DWT, SVD and PCA transform components.
  - (ii) a multilevel decision based hybrid gender classifier derived from the above individual classifiers.

Performances of the compression algorithms were evaluated using the metrics, Peak Signal to Noise Ratio (PSNR) and Compression Ratio (CR). The fingerprint images for optimizing and evaluating the compression algorithms were taken from the fingerprint database DB1_B of FBI's Fingerprint Validation

Competition (FVC) 2000. Other fingerprint databases used in FVC 2000, FVC 2002, FVC 2004, NIST fingerprint images and the set collected using NITGEN USB Fingkey Hamster (HFDU 01) were employed for testing the algorithm.

Performances of the gender classification systems were measured in classification accuracy and the algorithms were evaluated on the fingerprint data set collected using NITGEN USB Fingkey Hamster (HFDU 01) fingerprint scanner.

The outcome of the research work shows that the proposed algorithms are highly useful in those forensic, government, commercial, health-care and traveling and immigration applications, where effective storage of fingerprint database and gender classification for ease of personal identification are very much required.

****

CONTENTS

LIST OF FIGURES

Page No.

LIST OF TABLES

Page No.

LIST OF SYMBOLS AND ABBREVIATIONS

SYMBOLS

$\alpha,\beta,\gamma,\delta$	-	Lifting filter coefficients
ζ	-	Lifting scaling factor
C_b	-	Compressed bit stream
d_j	-	High pass filtered image (detail) coefficients
$g(n)$	-	High pass synthesis filter
$\tilde{g}(n)$	-	High pass analysis filter
$h(n)$	-	Low pass synthesis filter
$\tilde{h}(n)$	-	Low pass analysis filter
I_j	-	Disjoint intervals on the real line
$p(z)$	-	Lifting scheme predict filter
P	-	Pareto optimal set
P_c	-	Crossover rate
P_m	-	Mutation rate
P_{size}	-	Population size
$Q(.)$	-	Quantization mapping
$Q^{-1}(.)$	-	De-quantization mapping
$q[l_1,l_2]$	-	Two dimensional sequence of quantization indices
R_b	-	Bit-rate
s_j	-	Low pass filtered image (approximation) coefficients
s_{j+1}	-	Original / higher level image data
$u(z)$	-	Lifting scheme update filter
$\downarrow 2$	-	Down sample by 2
$\uparrow 2$	-	Up sample by 2
Δ	-	Quantization step-size

ABBREVIATIONS

ACO	-	Ant Colony Optimization
AFIS	-	Automatic Fingerprint Identification System
ANN	-	Artificial Neural Network
ANS	-	Artificial Neural System

ARSC	-	Arctic Regional Supercomputer Center
BP	-	Back Propagation
BPNN	-	Back Propagation Neural Network
CA	-	Cultural Algorithms
CDF	-	Cohen Daubechies Feauveau
CMA-ES	-	Evolution Strategy with Covariance Matrix Adaptation
CR	-	Compression Ratio
CS	-	Compression Speed
CWT	-	Continuous Wavelet Transform
DCT	-	Discrete Cosine Transform
DWT	-	Discrete Wavelet Transform
EA	-	Evolutionary Algorithm
ES	-	Evolutionary Strategy
EZW	-	Embedded Zerotree Wavelet
FBI	-	Federal Bureau of Investigation
FCM	-	Fuzzy- C Means
FIC	-	Fingerprint Image Compression
FP	-	Finger Print
FT	-	Fourier Transform
FVC	-	Fingerprint Verification Competition
GA	-	Genetic Algorithm
GLCM	-	Gray Level Co-occurrence Matrix
GP	-	Genetic Programming
IDP	-	Interlaced Derivative Patterns
IE	-	Information Entropy
JPEG	-	Joint Photographic Experts Group
KNN	-	K-Nearest Neighbor
LBP	-	Local Binary Pattern
LDA	-	Linear Discriminant Analysis
LS	-	Lifting Scheme
LTI	-	Linear Time Invariant
MOO	-	Multi Objective Optimization
MOP	-	Multi Objective Problem
MRA	-	Multiresolution Analysis
MSE	-	Mean Square Error

NN	-	Neural Network
NOA	-	Natural Optimization Algorithm
NZ	-	Number of Zeros
PCA	-	Principal Component Analysis
PE	-	Processing Element
PF	-	Pareto Front
PSO	-	Particle Swarm Optimization
PSNR	-	Peak Signal to Noise Ratio
PSSVM	-	Polynomial Smooth Support Vector Machine
RE	-	Retain Energy
RMSE	-	Root Mean Squared Error
RTVTR	-	Ridge Thickness to Valley Thickness Ratio
SA	-	Simulated Annealing
SOFM-VQ	-	Self-Organizing Feature Map Vector Quantization
SPIHT	-	Set Partitioning In Hierarchical Trees
SSIM	-	Structural Similarity
STFT	-	Short Time Fourier Transform
SQ	-	Scalar Quantization
SVD	-	Singular Value Decomposition
SVM	-	Support Vector Machine
TF	-	Total Fitness
TIS	-	Training Image Set
UQI	-	Universal Quality Index
VQ	-	Vector Quantization
WBCT	-	Wavelet Based Contourlet Transform
WFT	-	Windowed Fourier Transform
WSQ	-	Wavelet Scalar Quantization
WT	-	Wavelet Transform

Chapter 1

Introduction

Image compression plays a major role in the effective storage of fingerprint images in digital archives and their efficient transmission through communication channels. Fingerprint is one of the most common biometric traits used for personal identification. Image processing techniques can be employed on fingerprint images to identify the gender of a person. A brief introduction to the research is presented in this chapter. Fundamentals of fingerprint biometrics, fingerprint image compression and image compression using the state-of-the-art Wavelet Transform (WT) technique are discussed. Basic ideas of gender classification system using fingerprints are also highlighted. This chapter gives the objective and motivation behind the proposed research work. The main contributions of the present research and organization of the thesis are also highlighted.

1.1 Biometrics

The science of identifying or verifying a person by measuring the distinctive physiological and behavioral characteristics is known as biometrics. The popular biometric technologies that have been in use rely on the physiological characteristics such as face, fingerprint, hand geometry, hand, vein, iris, retinal pattern, facial thermogram, etc. and the behavioral characteristics such as signature, voiceprint, etc. **(**Nanavati, Thieme & Nanavati, 2002; Jain, Ross & Prabhakar, 2004). The biometric technologies can check an individual's identity by automating the process of using a physiological or behavioral characteristic. It is very much associated with issues related to information security as well as criminology. Commercial, government and forensic applications such as medical, banking and finance, security, law and order, immigration control, communications, access control, etc. exemplify the areas on which the contemporary biometric use mainly focuses on.

1.1.1 Fingerprint Biometrics

Fingerprints are impressions made by the ridges, whorls and valleys patterns on the surface of a person's fingertip. They form at about 7 months of fetus development. Any physiological or behavioral trait of a person can qualify as a biometric identifier if it meets the requirements such as (Maltoni, Maio, Jain & Prabhakar, 2009),

- *Universality*: each human being should have a biometric trait.
- *Uniqueness*: the biometric traits should be different from person to person.
- *Permanence*: biometric trait should not change over time.
- *Collectability*: ease of measurement of biometric trait.

The other desirable properties of biometric traits are:

- *Performance*: accuracy, speed, resource requirements, and robustness of the technology used.
- *Acceptability*: degree of user's willingness to accept the biometric technology.
- *Circumvention*: ease of avoiding fraudulent methods in the biometric system.

The fingerprint possesses a good balance among all the desirable requirements. Every person has fingers and hence fingerprints. They are unique and permanent. The availability of accurate live scan fingerprint scanners with affordable cost price facilitates the collection of high quality fingerprint images. Each and every biometric technology is noted for its special features and it is used in specific applications. A comparison of various biometric traits is provided in Table 1.1. Note that among all biometric traits, fingerprints provide the most reliable personal identification systems (Shoniregun & Crosier, 2008).

Table 1.1 Comparison of biometric traits.

Biometric trait	**Universality**	**Uniqueness**	**Permanence**	**Collectability**	**Performance**	**Acceptability**	**Circumvention**
Face	H	L	M	H	L	H	H
Fingerprint	M	H	H	M	H	M	M
Hand geometry	M	M	M	H	M	M	M
Hand/finger vein	M	M	M	M	M	M	L
Iris	H	H	H	M	H	L	L
Signature	L	L	L	H	L	H	H
Voice	M	L	L	M	L	H	H

H=high, M=medium, L=low.

The fingerprint pattern shows various types of features as shown in Figures 1.1 and 1.2. The global features (level 1 or Galton level features) are ridge line flow pattern and singular points (called loop and delta). The ridge lines enfold these singular points. The ridge endings and ridge bifurcations, called minutiae are the local ridge characteristics that make the local features (level 2 features). A ridge ending is the point at which a ridge ends abruptly. At a ridge bifurcation the ridge diverges into branch ridges. The intra-ridge details including shape, curvature, width, edge contours of ridges, sweat pores, etc. are the fine level features (level 3 features).

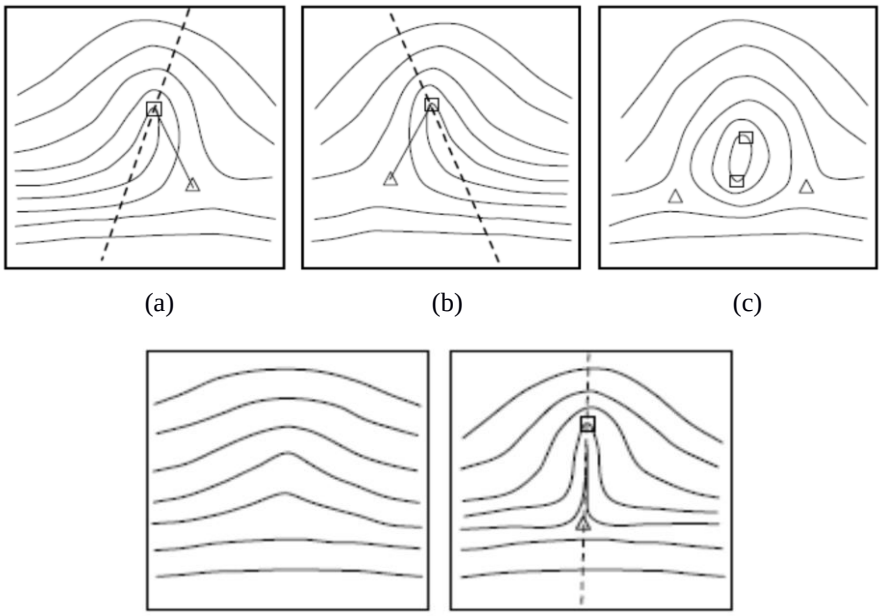

Figure 1.1 Fingerprint patterns: (a) left loop, (b) right loop, (c) whorl, (d) arch, and (e) tented arch. Squares and triangles represent loop-type and delta-type singular points respectively (Courtesy: Maltoni et al., 2009).

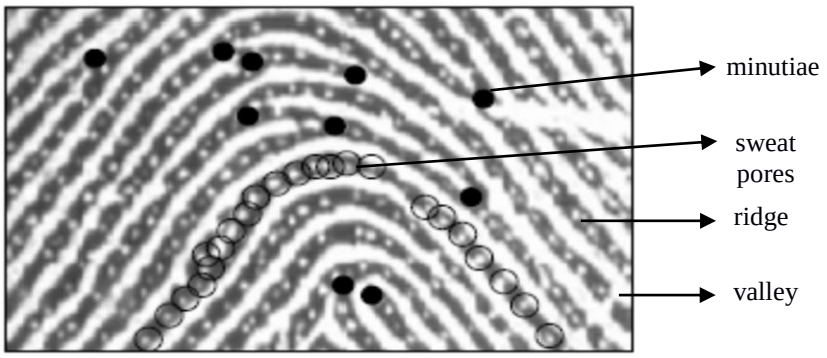

Figure 1.2 A section of fingerprint image marked with ridge lines (black lines), valley (white lines), minutiae (black circles), and sweat pores (blank circles) on a single ridge line (Courtesy: Maltoni et al., 2009).

The width of ridge varies from 100 μm to 300 μm. Ridges and valleys form interleaved pattern with ridge/valley cycle period about 500 μm. A detailed view of

the different minutiae types showing discontinuity of ridges can be had from Figure 1.3. The uniqueness and other desirable properties qualify the fingerprint as a good biometric trait for classification and indexing.

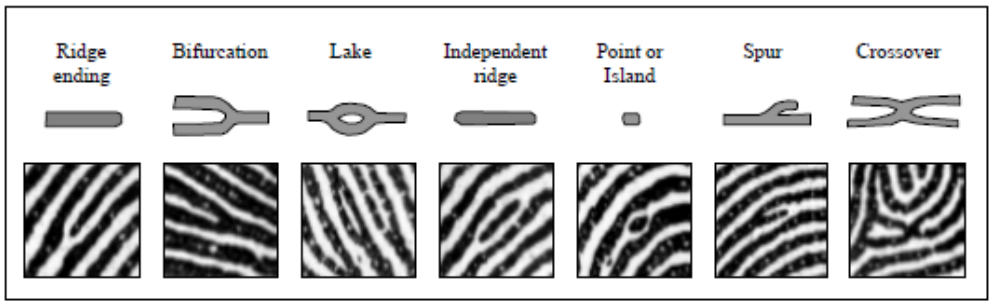

Figure 1.3 Common minutiae types (Courtesy: Maltoni et al.,2009).

Separate studies have been made by several researchers among various populations in different countries to know about the differences in male and female fingerprints. Difference in fingerprint features has been reported by the researchers from different parts of the world. Significant variations have been noted in ridge counts and ridge densities among male and female. The women have higher number of fingerprint ridges and ridge densities than the men.

1.1.1.1 A Brief History of Fingerprints

Fingerprints, the oldest and the most commonly used biometric trait, are the impressions of the friction ridges on the surfaces of the hand. In most of the applications the basic interest lies in the ridges above the end joints on the front of the fingers. Fingerprints have been used as personal marks or signatures for identifying people in several parts of the world for many years.

In July 1858 Sir William Herschel, a British Administrator in Hooghly District of Bengal in India, collected fingerprints in Bengal to check people's identity while signing contracts. Dr. Henry Faulds, a missionary doctor in Japan published an article on fingerprints in '*Nature'* in 1880. He demonstrated that latent or partial fingerprints present at a crime scene can be matched with a persona to support a 'criminal investigation'. In 1892 Juan Vucetich, an Argentine Police Officer, initiated

the first fingerprint files based on Galton pattern types and successfully identified a criminal. Sir Francis Galton, a British Anthropologist, published his book *Finger Prints* in 1892, which declared the permanence and uniqueness of fingerprints for the first time. "Galton's Details", the unique characteristics of fingerprints identified by Galton, had become known as minutiae. A criminal case in Bengal in 1898 is believed to be the foremost case wherein fingerprint proof was used to secure a conviction. In 1901 Sir Edward Henry, the Inspector General of Police in Bengal, India, developed the fingerprint classification system for the first time and it was documented in his book, *Classification and Uses of Finger Prints*. Henry's classification system was based on three fingerprint classes: loop, arch, and whorl. The use of this system quickly spread throughout the world. Alphonse Bertillon, in 1902 solved the first murder in Europe with the use of fingerprint evidence alone. In 1902, Dr. Henry P. de Forest of the New York Civil Service Commission bagged the credit for the first systematic usage of the fingerprints in U.S. By 1903, the Fingerprint Bureau had been started at the State Bureau of Prisons in New York. In October 1904, Inspector Ferrier and Major M. W. McClaughry began the U.S. Government's fingerprint collection by recording fingerprints of all inmates in a prison. In 1905, latent fingerprints (latent fingerprints are marks, formed by sweat and oil on the skin's surface left at a crime scene that may not be straight away visible to the bare eye) were adopted for use in a British criminal case for the first time.

FBI set up its fingerprint identification division in 1924 with a database of 810,000 fingerprint cards. In 1980s, an Automated Fingerprint Identification System (AFIS) based exclusively on the computerized extraction of minutiae was developed. The FBI introduced its national Integrated Automated Fingerprint Identification System (IAFIS) in 1999, which was responsible for the mandatory standard for the interchange of fingerprint images and the Image Quality specification (IQS) for live-scans, card scanners, monitors and printers. Today fingerprint biometric system has become one among the most commonly used personal identification systems in many diverse applications throughout the world (Woodward, Orlans & Higgins, 2003; Holder, Robinson, Laub & National Institute of Justice (U.S.), 2011).

1.2 Image Compression

Image compression is one of the most essential and useful technologies in the area of digital image processing. The aim of image compression is to gain the best possible image quality at an allotted storage facility. It is needed for easy archiving and faster transmission of images over band-limited communication channels. Fingerprint image compression finds a significant role in some vital areas like forensic, medical applications, law enforcement and border security.

A gray scale image can be represented by way of a 2-D light intensity function $f(x,y)$, where x and y are spatial coordinates. The brightness or value of the gray level at a point (x,y) is the value of f at that point in the image. A digital image is a matrix and each element in this matrix is called a picture element or pixel. Rows and columns of the digital image matrix are represented by x and y respectively, that are used to locate a pixel in the image with a value indicating the gray level or brightness of that pixel. A digital image of size $L \times M$ is typically represented as in equation (1.1). An 8-bit gray scale digital image has 256 (i.e., 2^8) intensity levels ranging from 0 to 255.

$$f(x,y) = \begin{bmatrix} f(0,0) & f(0,1) & \cdots & f(0,M-1) \\ f(1,0) & f(1,1) & \cdots & f(1,M-1) \\ \vdots & \vdots & \vdots\vdots & \vdots \\ f(L-1,0) & f(L-1,1) & \cdots & f(L-1,M-1) \end{bmatrix} \tag{1.1}$$

Digital image compression techniques (Gonzalez & Woods, 2008; Jain, 1989; Castleman, 1996; Chanda & Majumder, 2000) exploit the data redundancy present in image data. In general, removal of redundant information results in image compression. From the mathematical point of view, image compression is considered as transformation of the 2-D pixel array into a statistically uncorrelated data set. The three types of data redundancies identified in image intensity matrix are:

1) ***Coding Redundancy*:** The 8-bit codes representing the intensity values may be more than what is required to represent them.

2) ***Spatial and Temporal Redundancy:*** Neighbouring pixels may be similar to or dependent on each other causing spatial correlation and hence redundancy.

3) ***Irrelevant Information:*** Some of the information contained in the intensity arrays may be unnoticed by human vision. In some other cases there may be information irrelevant to the expected use of the image.

Reduction or elimination of any one or more of these redundancies achieves image compression.

Compression algorithms can be classified into two broad categories: *lossless algorithm* and *lossy algorithm*. Lossless compression algorithm permits exact reproduction of the original data and provides low compression ratios. For instance, text compression should be lossless since a small information loss can result in unlike statements with completely different meanings. Astronomical imaging for galaxies and stars, medical imaging, etc. are a few examples in which lossless compression finds wide applications. Some of the main techniques used in lossless compression are the Run Length Encoding and variable length coding like Huffman coding, Arithmetic coding, etc.

In lossy or irreversible compression algorithm some information is lost. As an example, in common image compression applications, the exact reconstruction of the original image is not needed. The amount of information loss depends upon the quality required for the compressed image. There are many lossy compression techniques available in literature that provides high quality compressed images at high compression ratios. In fact, the fundamental difference among the lossless and lossy compression schemes is the presence or absence of quantizer units.

Fractal compression and transform coding are the popular lossy compression methods. Fractal image compression scheme gives high Compression Ratio (CR) with good quality, particularly in images having high degree of self-similarity. However, the fractal scheme suffers from two serious problems. The first drawback is that the encoding is computationally complex and hence slow. The second issue is that unlike transform methods, the size of encoded data grows very large during perfect reconstruction of certain images. For example, a regular pattern such as alternating

white and black blocks are poorly coded as it actually takes more space in its compressed form than its raw form **(**Fisher, 1995).

In transformation coding, spatial image pixel values are converted into a transform domain (frequency domain) to get transform coefficients. These coefficients possess an important property called energy compaction property, which forms the basis for accomplishing compression. By this property the energy of the original data concentrates in a few significant transform coefficients. Discarding the insignificant coefficients leads to image compression. Several transform techniques such as discrete Fourier, Karhonen-Loeve, Walsh-Hadamard, discrete cosine, and the state-of-the-art wavelets have been used for image coding.

1.2.1 Measures of Performance of Image Compression Algorithms

Performance of image compression algorithms can be measured in several ways. The quantity of compression achieved, compression speed and closeness of the qualities of the reconstructed image to the original input image are the important criteria for evaluating the performance of a compression algorithm.

1.2.1.1 Compression Ratio (CR)

CR is defined as the ratio of the size of the original image to the size of the compressed image (Khalid, 2006). The image is represented as a stream of bits. So, CR is expressed as,

$$CR = \frac{Number\ of\ bits\ in\ the\ original\ image}{Number\ of\ bits\ in\ the\ compressed\ image} \tag{1.2}$$

This ratio shows the amount of image compression achieved. CR is inversely proportional to the picture quality of the compressed image. In general, the quality of the compressed image becomes poorer as CR increases. So, there should be a compromise between CR and picture quality while compressing images.

For an image having height M and width N in pixels, the CR is given as,

$$CR = \frac{M.N.B}{C_b} \quad (1.3)$$

where, B is the number of bits required to represent one pixel and C_b is the number of bits in the compressed image.

An equivalent measure of compression performance is the compressed bit-rate or simply bit rate, expressed as

$$R_b = \frac{C_b}{M.N} \quad (1.4)$$

where, R_b is the bit rate in bits per sample (bps) or bits per pixel (bpp). The major objective of image compression is to get the compressed image with best image quality at a specified bit rate.

For example, consider a gray scale image of size 512 x 512 pixels. For storing this image 512 x 512 or 262,144 bytes, taking one byte for each pixel, are needed. Let the compressed image takes 32,768 bytes. Then the CR is 8:1 and the bit rate is 1 bpp. Another way of representing compression performance is as a percentage. The percentage of compression can be calculated by using the expression:

$$Percentage\ compression = 100 \times (1 - (1/compression\ ratio))\ \% \quad (1.5)$$

In this example the percentage compression is calculated as 87.5% (i.e., the savings in the storage requirement is 87.5%), which means that the compressed image takes only 12.5% of the size of the original image.

1.2.1.2 Compression Speed (CS)

CS tells how fast the compression and decompression of the image is performed. A higher compression speed means that the time taken for compression and decompression is lesser. It is dependent on the particular compression algorithm, image type and efficiency of the hardware used for compression.

1.2.1.3 Root Mean Square Error (RMSE)

Mean Square Error (MSE) measures the average of the square error between the

original and the compressed image. The square root of MSE is termed as RMSE. The expression for RMSE of gray scale image is given as,

$$RMSE = \sqrt{\frac{1}{M.N}\sum_{x=0}^{N-1}\sum_{y=0}^{M-1}\left[f(x,y) - \tilde{f}(x,y)\right]^2} \tag{1.6}$$

where, $f(x,y)$ and $\tilde{f}(x,y)$ represent a pixel at location (x,y) of the original and the reconstructed image respectively with size M x N. For a good quality reconstructed image the RMSE is low.

1.2.1.4 Peak Signal to Noise Ratio (PSNR)

PSNR represents the ratio of maximum possible power of a signal and the power of the distorted signal corrupted by noise. PSNR in dB is given as,

$$PSNR = 20\log_{10}\frac{P_{max}}{RMSE}\ \ dB \tag{1.7}$$

where, P_{max} stands for the maximum pixel intensity value. For a two level image P_{max} is 1. For a gray scale image with peak level pixel value of 255, the PSNR is,

$$PSNR = 20\log_{10}\frac{255}{RMSE}\ \ dB \tag{1.8}$$

For good-quality reconstructed image, the PSNR is high. For lossy image compression, typical values of the PSNR range from 30 to 50 dB. PSNR above 40 dB are generally taken as very good and those under 20 dB are generally not acceptable (Bull, 2014).

1.2.1.5 Structural Similarity (SSIM)

SSIM index is a recently proposed method for image quality assessment based on human visual perception. It is an approach for measuring the similarity between two images. The SSIM is intended to improve on conventional metric such as PSNR and MSE. SSIM considers degradation of the image as perceived change in its structural

information. The SSIM index is usually computed on windows *x* and *y* of sizes 8 x 8 pixels of the image (Wang, Bovik, Sheikh & Simoncelli, 2004).

$$SSIM(x,y) = \frac{(2\mu_x \mu_y + c_1)(2\sigma_{xy} + c_2)}{(\mu_x^2 + \mu_y^2 + c_1)(\sigma_x^2 + \sigma_y^2 + c_2)} \tag{1.9}$$

where, μ_x and μ_y are the averages of x and y , σ_x^2 and σ_y^2 are their variances and σ_{xy} is their covariance. $c_1 = (k_1 L)^2$ and $c_2 = (k_2 L)^2$ are variables with k_1=0.01 and k_2=0.03. L is the dynamic range of the pixel-values (equal to 255 for gray scale images). SSIM index value ranges between -1 and 1. For two identical images the value of SSIM is 1.

1.3 Image Compression using Wavelet Transforms

Wavelet based image coders are the state of art in image compression. It is a transform coding technique where WT of the image is modified. A reversible, linear transform such as WT is used to map the image into a set of transform coefficients, which are then quantized and coded to minimize inter-coefficient and coding redundancies. Figure 1.4 shows a typical WT based image compression system.

The encoder at the transmitting side de-correlates the input image pixels by performing the forward transform operation. The quantization is an irreversible

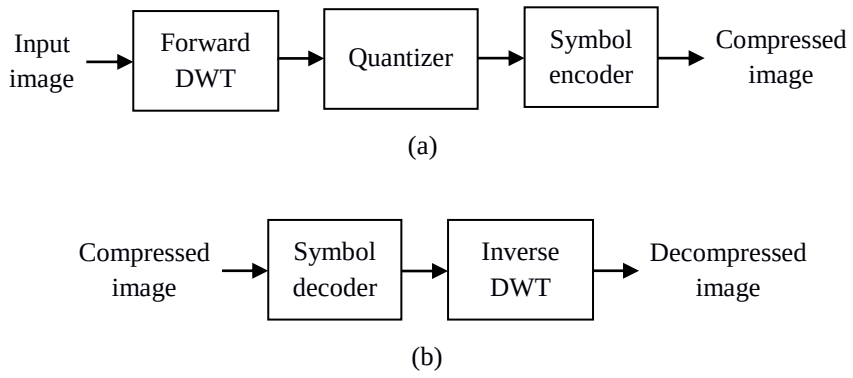

Figure 1.4 A typical transform based image compression system: (a) encoder, (b) decoder.

operation that coarsely quantizes the transform coefficients. Finally, the quantized coefficients are coded using a symbol encoder (usually a variable length coder) to get

the compressed image data. The decoder at the receiving end performs the reverse sequence of operations (except quantization, which cannot be reversed exactly) to output the decompressed image. The DWT is usually performed by subband coding technique, which converts the original image to horizontal, vertical and diagonal decomposition coefficients. A detailed discussion on DWT and subband coding is presented in chapter 3.

1.3.1 Quantization

Quantization is the main part of lossy compression schemes (Khalid,2006). It is a many-to-one mapping as it substitutes a group of data values with a single representative value. In lossy image compression, the quantization process converts the continuous range of intensity values of the input image data into a finite and smaller set of values to achieve compression. The quantization is a noninvertible process. The compression scheme is said to be lossy since the original input image cannot be reconstructed exactly after quantization. The system which performs quantization of data is known as a quantizer. The error or loss introduced by quantization is called quantization error, quantization noise or quantization distortion, which is due to the difference between the original input image data and quantized data output. It is evident that a good quantizer approximates the original input image with minimum loss. In image compression applications the quantization is usually performed on the transform domain of images.

1.3.1.1 Scalar Quantization (SQ)

In SQ, the set of inputs and outputs are scalars and such quantizers are known as scalar quantizers. There exist two mappings in a quantizer, the encoder mapping and the decoder mapping. The encoder partitions the range of input data values into certain intervals and different codewords are associated with different intervals. The range of input values that come within a particular interval is encoded by the codeword corresponding to that interval. Thus there will be a finite, smaller set of data values that represent the original data. After quantization these codewords only be known, from which the exact data value cannot be recovered since the codeword

represents only the interval containing the data value. This causes the quantization to be an irreversible process.

As explained, the quantizer uses a succession of quantization indices to approximate the input two dimensional image data samples (Taubman & Marcellin, 2002). The quantization process is denoted as,

$$q[I_1, I_2] = Q(x) \tag{1.10}$$

where, $Q(.)$ represents the quantization mapping of the input sample $x[I_1, I_2]$ and $q[I_1, I_2]$, the corresponding quantization index. Obviously, the count of quantization indices will be lesser than the count of input samples and hence $Q(.)$ causes distortion at its output. So, the exact input data is irretrievable. However, a reverse mapping, $Q^{-1}(.)$ can be used to de-quantize the quantized data samples to get back an approximated input data as $Q^{-1}(Q(x))$.

In SQ, each quantization index $q[I_1, I_2]$ corresponds to an interval on the real line represented by input sample $x[I_1, I_2]$, which is indicated by

$$q[I_1, I_2] = j \qquad if \qquad x[I_1, I_2] \in I_i \tag{1.11}$$

where, I_i are disjoint intervals on the real line. At the reconstruction side, the de-quantizer map the quantization index, $q[I_1, I_2]$, to certain value in the corresponding interval, $\tilde{x}[I_1, I_2]$. Figure 1.5 shows the mapping of input data samples to 8 discrete values of quantization indices.

Figure 1.6 shows the encoder mapping for a 3-bit quantizer having eight reconstruction levels. Here, each reconstruction level is represented by a 3-bit number. The input data values in the range from a_1 to a_2 are assigned 001, the codeword of the quantized value corresponding to that range. Similarly the input data values in the range from a_2 to a_3 are assigned 010, the codeword related to that range, and so on. As a result, all the input data values will be represented by

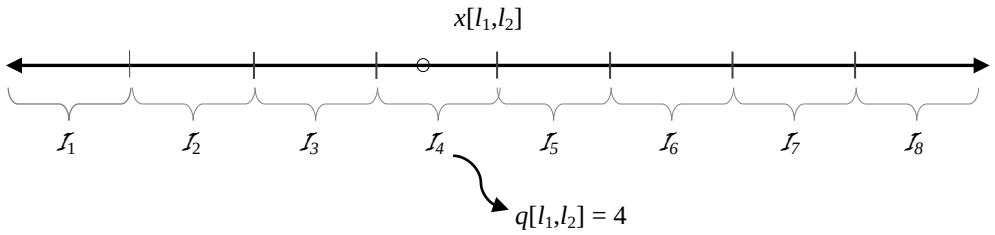

Figure 1.5 Scalar quantizer with eight discrete output levels.

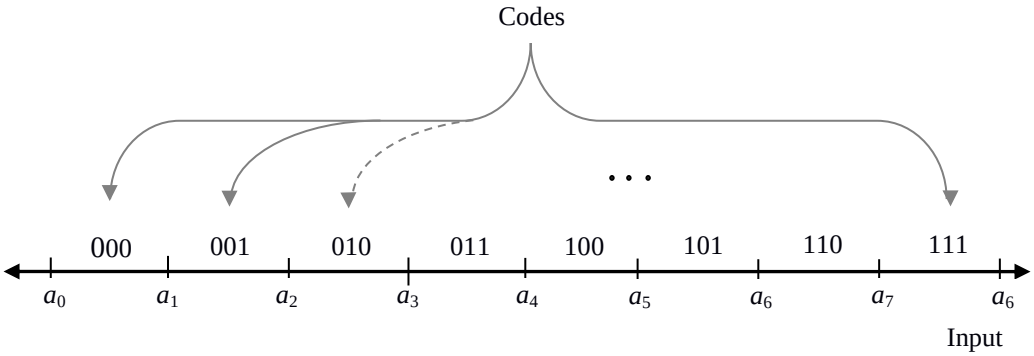

Figure 1.6 Encoder mapping for a 3-bit quantizer.

codewords corresponding to the respective intervals to which the input data belong. The inputs falling in the range of values less than a_1 will be assigned the codeword 000 and that falling in the range of values above a_7 will be assigned the codeword 111 (Zeng, Yu & Lin, 2006). The scalar quantizers are broadly classified into uniform and non-uniform quantizers.

1.3.1.2 Uniform Scalar Quantization

In the uniform SQ technique all intervals are of constant size. The system which performs uniform SQ is called a uniform scalar quantizer. In this, the input data intervals and the quantization levels are separated evenly. Usually, the centre points of the intervals correspond to their respective reconstruction levels. It is due to this constant spacing the uniform scalar quantizer is said to have constant step size Δ. In fact, Figure 1.6 and Table 1.2 represent the encoder and decoder mapping, respectively, for a 3-bit uniform scalar quantizer.

The input-output mapping of a typical uniform scalar quantizer is shown in Figure 1.7. Here, the input range (-0.5, 0.5) is represented by the output quantized value 0.0 (i.e., the mid-point of the input range), (0.5,1.5) by 1.0 and (-1.5,-0.5) by -1.0 and so on.

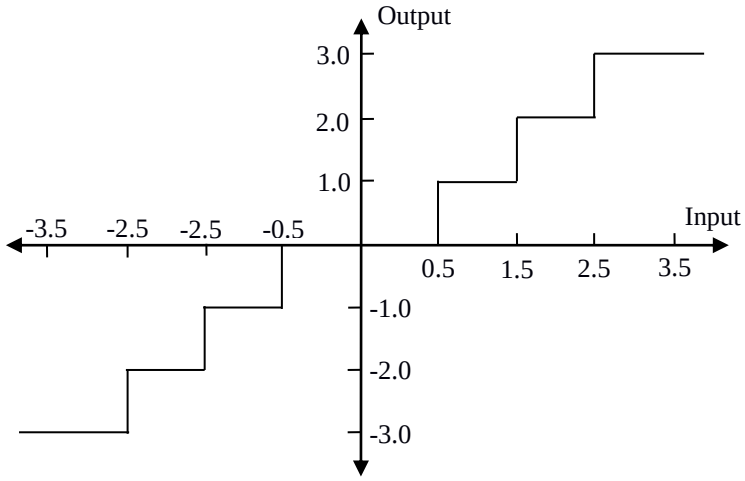

Figure 1.7 The input-output mapping of a typical uniform scalar quantizer.

1.3.1.3 Non-uniform Scalar Quantization

A non-uniform scalar quantizer is a system that performs SQ at non- uniform intervals. The particular use of non-uniform scalar quantization is in quantizing the input data, which are distributed in non-uniform fashion. In the input regions of high probability, a better approximation of input can be done. This is accomplished by using smaller intervals I_j or smaller quantization step size in such regions, so as to reduce the quantization error. The regions with lower probabilities are given worse approximations by employing larger quantization step sizes. Thus, the average quantization error is reduced.

1.4 Fingerprint Image Compression

The familiar lossless compression techniques were inadequate as it typically provided a CR = 2:1 on gray scale fingerprint images. The famous Joint Photographic Experts

Group (JPEG) compression technique using Discrete Cosine Transform (DCT) was also not preferred since, at the FBI target compression ratio or at higher compression ratios it produced blocking artifacts caused by the independent compression of image blocks formed by 8 x 8 pixels. Hence, among the various compression techniques proposed, Wavelet Scalar Quantization (WSQ) technique has been adopted as a standard by the FBI. In WSQ, the fingerprint image is decomposed into a number of spatial frequency subbands by using cdf 9/7 biorthogonal wavelet. It can compress fingerprint images at CRs of 10 to 25. As higher CRs caused undesirable degradation of the fingerprint image, a typical factor of 10 to 15 seems to be most suitable. The well-known JPEG 2000 compression also is based on WT using cdf 9/7 wavelet for its lossy compression.

1.4.1 Need for Fingerprint Image Compression

The FBI's IAFIS is a national fingerprint and criminal history system of USA which provides automated fingerprint storage and search capabilities.

In any AFIS catering forensic and non-forensic applications, the size of the fingerprint database is huge. With a database of more than 810,000 fingerprint cards, the FBI set up its fingerprint identification division in 1924. Since then the fingerprint recognition in forensics is expanding fast, and the FBI fingerprint databases have been growing so large. The database now contains more than 200 million fingerprints and is expanding at the rate of 30,000 to 50,000 new cards per day. It was estimated that the FBI fingerprint card archive containing over 200 million fingerprints, takes up an acre of filing cabinets in the J. Edgar Hoover building in Washington, DC. Digital archiving of fingerprint cards is a solution. However the size of the digital archive is also becoming too large. For example, digital representation of an image of size 768 x 768 pixels at 256 gray levels digitized at 500 dpi took 589,824 bytes and approximately 10 megabytes were required to encode one fingerprint card. Thus, 200 million fingerprints required the huge storage facility of 2,000 terabytes.

The long delay involved in transmitting fingerprint images over band-limited communication channels was also a problem. Over a 9600 baud communication

channel almost 3 hours was needed for transmitting only one image. These problems created urgent necessity of an effective technique for compressing fingerprint images.

1.5 Gender Classification

Visual information has a major role in the interaction of human beings. While looking at someone's face we also try to get other information about the person, such as gender, age and the present mood through expressions. Gender classification is important, as there is vital dependence on the notion of right gender in many social dealings. It is a simple job for human beings, but a difficult one for computers. Automated gender classification is a field of remarkable importance in human-computer interaction. It offers several applications in basic and applied research areas. Security, law enforcement, study on demography, man-machine interaction, medical, education and telecommunication name a few application areas of gender recognition or classification. Needless to say, only a few works in gender classification have been reported so far (Rai & Khanna, 2012).

1.5.1 Gender Classification using Fingerprints

There exist several features of the human body that can be used to estimate sex difference in humans (Brown, Hines, Fane & Breedlove, 2002). There are lots of biometric techniques available nowadays, using biometric traits and other characteristics of human such as face, fingerprint, gait, body, length ratios of pairs of fingers on each hand and toes on each foot, etc., which can be used for gender classification (McFadden & Shubel, 2002; Ng, Tay & Goi, 2012). Since fingerprints are distinctive and not forged, they are widely accepted well preferred biometric features and have become very well accepted in personal identification and verification applications. It has been reported by several researchers from different parts across the world that there is significant difference in fingerprint features such as ridge counts and ridge densities among male and female. These features can be made use of for performing the gender classification. Figure 1.8 shows the block diagram of a basic gender classification system using fingerprints.

The basic gender classification system consists of feature extraction and classifier blocks. The feature extraction block extracts features of reduced size that are useful for gender classification. In the training phase the classifier is trained using the training set of fingerprints whose gender is already known. In the testing phase the trained classifier classifies the testing fingerprint images based on their features to get the final decision as either male or female (Rai & Khanna, 2012).

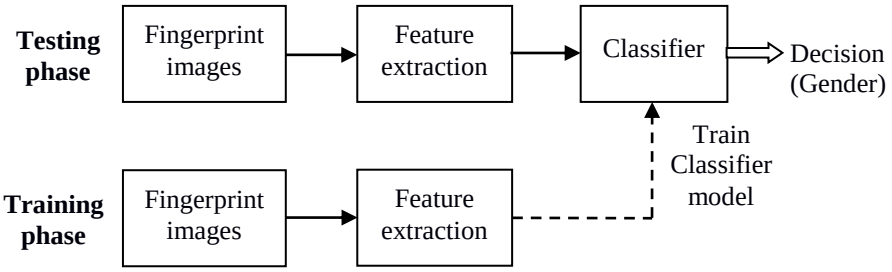

Figure 1.8 Block diagram of a basic gender classification system using fingerprints.

1.6 Objective of the Research

The objective of this research work is:

- To develop algorithms to optimize wavelet coefficients at a faster rate for fingerprint image compression.
- To develop algorithms for optimizing wavelet lifting coefficients for fingerprint image compression to obtain maximum PSNR between the input and the compressed output images.
- To develop algorithms to optimize wavelet coefficients and the initial seed values of the classifier networks for gender classification.
- To classify fingerprints into male and female categories using the optimized wavelet coefficients and the initial seed values.

Cdf 9/7 biorthogonal wavelet based techniques are employed in the present works. Feed forward Back Propagation Neural Network (BPNN) is used for gender classification.

1.7 Motivation

In any AFIS used in Government and commercial applications for forensic and non-forensic purposes, the quantity of fingerprints in the database is day by day becoming large and large. Also, the original images impose large delay during their transmission over band-limited communication channels. To reduce the storage space required to keep the digital fingerprint archive and to avoid long delays in communication channels better compression schemes are required. Even though the-state-of-the-art wavelet based compression scheme basically provides good compression performance, there is a need for improving the techniques to get even better results.

As the fingerprint images form a specific class of images having specific patterns, the wavelet coefficients can be optimized for better compression. A few researchers evolved optimized wavelet coefficients from cdf 9/7 classical wavelets (the one used in FBI fingerprint compression standards) to get improved results, compromising the hefty computational complexity and hence long time delay. The delay is mainly due to the time taken to evolve coefficients similar to classical wavelet coefficients that are more in number. The size and number of the fingerprint images in the training database also cause problems. Therefore, lifting wavelet scheme representing classical wavelets with lesser number of coefficients and optimized training image sets can be used for obtaining faster evolution of optimized coefficients for better fingerprint image compression.

Gender classification is a very helpful preprocessing step in personal identification and verification. Gender classification using fingerprint features is an active research area. WT coefficients, Singular Value Decomposition (SVD) and Principal Component Analysis (PCA) components with BPNN classifiers have been used by researchers giving better classification of male and female genders. These conventional classification techniques, mostly employed feature vectors comprised of the complete set of WT coefficients, SVD and PCA components in the classifiers are causing very slow classification speed.

However, the classification accuracy can be further improved by employing optimized wavelet coefficients and initial seed values of Neural Network (NN) classifiers. The classification speed can also be improved by using feature vectors of reduced size.

1.8 Contribution of the Thesis

The main contributions of this research include the development of-

- A novel fast and efficient algorithm for the compression of fingerprint images using wavelet lifting coefficients optimized by employing Genetic Algorithm (GA),
  - (i) under condition such that the transform coefficients are subjected to uniform SQ. This is a dual-objective GA optimization problem that requires the simultaneous maximization of both PSNR and CR.
  - (ii) under condition such that the largest 1/16 transform coefficients are retained and the remaining are discarded. This is a single-objective GA optimization problem that requires the maximization of PSNR alone.
- A new algorithm for identifying gender more accurately and at a faster rate from fingerprints by employing
  - (i) GA optimized wavelet lifting coefficients and NNs using lesser number of DWT, SVD and PCA transform components.
  - (ii) multilevel decision based hybrid gender classifier derived from the above individual classifiers.

1.9 Organization of the Thesis

Chapter 2 summarizes the literature survey for the fingerprint image compression, wavelet based fingerprint image compression, gender classification and fingerprint based gender classification.

Chapter 3 is dedicated to the description of WT, optimization tools and classification tools used in this research work. The fundamental concepts and

mathematical background are detailed here.

Chapter 4 describes a multi-objective approach for fingerprint compression using GA optimized wavelet coefficients and quantization. The time taken for evolving optimized classical wavelet coefficients (cdf 9/7) is too large. So, to ensure faster evolution the equivalent wavelet Lifting Scheme (LS) is employed. Wavelet optimization techniques for single-level and three-level DWT based fingerprint image compression are discussed.

Chapter 5 deals with a single-objective approach for optimizing wavelet filter coefficients for fingerprint image compression using GA employing a single training image for single-level to four-level transforms. An optimum training fingerprint image set is developed which enables faster GA evolution as well as higher PSNR for the compressed image at various CRs. In addition, the performance of the proposed compression system with degraded and noisy fingerprint images is discussed.

Chapter 6 presents a fingerprint based gender classification system using GA. The chapter begins with developing individual gender classification systems using optimized numbers of SVD and PCA components and DWT coefficients of fingerprints as feature vectors. Further development of the system by combining the individual classifiers to build a hybrid system and its performance are presented in this chapter.

Chapter 7 provides the summary and conclusions based on the present work. A brief description on the future scope and possibility of the continuation of the present work are included in this chapter.

Chapter 2

Literature Survey

Many fingerprint image compression techniques have been studied, experimented and presented by a number of researchers. Several works have been carried out in the area of fingerprint image compression using WTs. Automated gender classification system is an active research topic for several years and fingerprint based gender classification is a promising one. This chapter provides a detailed survey of the published literature for setting up an innovative foundation to begin the work on evolutionary approach for fingerprint image compression and fingerprint based gender classification using DWT. A few literatures pertaining to both fingerprint image compression and gender classification using conventional methods are reviewed. The summary of the findings in the literatures connected to the works carried out in this thesis and the inspiration to prefer the proposed methodologies are also discussed.

2.1 Introduction

Image compression (Rabbani & Jones, 1991; Shi & Sun, 2000) has been a topic of great interest in digital image processing. It turns out to be more and more important for reducing the data redundancy to cut down storage space and transmission bandwidth. Several research papers with different compression algorithms employing techniques like DCT, Discrete Wavelet Transform (DWT), fractals, etc. (Topiwala, 1998; Welstead, 1999; Fisher, 1995; Watson, 1994) have been devoted to this. Wavelet compression is one of the most effective methods and it has been used for fingerprint image compression also.

2.2 General Survey of Fingerprint Image Compression

Erçal, Gokmen and Ersoy (1999) proposed a fingerprint image compression scheme based on the hybrid model of image. The scheme used various processing steps such as enhancement, binarization and thinning to encode fingerprint images. The ridge skeleton was coded by using differential chain codes. The ridge and valley skeletons were encoded using DCT. The algorithm offered high CRs like 63:l when applied on various fingerprint images. The algorithm has the advantages that the direct extraction of the original features like end and bifurcation points from the compressed image even at high CR could be possible. The reconstruction process involved many iterations and it became the shortcoming of their approach.

Ferreira and Figueiredo (2006) used Independent Component Analysis (ICA) to realize compression schemes adapted to the data-dependent nature of the ICA bases obtained from training images. The ICA bases were applied to specific image classes such as faces and fingerprints. They found that ICA was effective for learning a coder for a specific image class. For fingerprint images, the scheme performed close to the coder developed by the FBI.

A coding technique for fingerprint compression based on Contourlet transform and Self-Organizing Feature Map Vector Quantization (SOFM-VQ) was presented by Veerakumar, Esakkirajan, Sudhakar and Murugan (2007). They claimed that a better image reconstruction was possible with less number of bits by using

Contourlet transform and SOFM-VQ. Their results revealed the fact that SOFM-VQ is suitable for low bit rate image coding. The reconstructed image quality (i.e., PSNR) was comparable with that of WSQ and JPEG2000 only at high bit rates. In their work, selection of weight matrix, learning rate and the number of iterations have important part in influencing the reconstructed image quality.

Shahid, Dupont and Baskurt (2009) introduced a novel technique to transform the image in which basis functions trained by ICA were used. The image was transformed to the ICA domain using a greedy algorithm called Matching Pursuit (MP) followed by quantization and multistage entropy coding. For fingerprint image, the system outperformed JPEG and WSQ and gave results comparable to JPEG2000 with lesser complexity.

Perumal and Ramaswamy (2009) proposed a novel fingerprint compression scheme utilizing the Bezier curve and claimed considerable reduction in memory requirement for storing fingerprints, compromising some accuracy. At first, the ridges were extracted along with the associated coordinate values and then the control points were obtained for all the ridges by viewing each ridge as a Bezier curve and stored. Using Bezier curves the fingerprint image could be reconstructed from the stored control points. The proposed scheme offered better compression at the expense of accuracy.

Zhou, Guo and Wu (2010) proposed a matrix optimization model for fingerprint compression and reconstruction based on Two Dimensional Ridgelet Non-negative Matrix Factorization (TDR-NMF). The method could provide a good PSNR.

A progressive fingerprint image compression using ridge detection was proposed by Lakshmi, Chandulal and Patro (2012). The image was decomposed into a primary component containing the ridges and bifurcations and a secondary component containing the textures and the features. The proposed method gave a CR = 50:1.

A fingerprint compression algorithm based on sparse representation was

introduced by Shao, Wu, Yong, Liuand Guo (2014). The given fingerprint was sliced into small patches. An overcomplete dictionary obtained from a set of fingerprint patches enabled them to represent as a sparse linear combination of dictionary atoms. The algorithm showed higher complexities as a result of the block by block processing steps involved.

Apart from the various techniques presented by the various researchers in their papers, the traditional wavelet algorithms are currently used in state of the art signal processing systems including image compression. Wavelet compression scheme provides significant enhancements in picture quality of the compressed images at higher CRs. For the past few years, a number of potent and sophisticated image compression algorithms using WTs have been developed and realized. Owing to the many advantages, wavelet based compression algorithms are still employed in the current image compression including fingerprint compression standards. For example, the FBI wavelet scalar quantization gray scale fingerprint image compression specification (version 3.1) sets the latest standard for the exchange of fingerprint images in law enforcement and other biometric communities. WSQ (Bradley, Brislawn & Hopper, 1993; Criminal Justice Information Services, 1997) is the standard for exchanging 8 bit, 500 ppi fingerprint images (Planetbiometrics, n.d.). Moreover, “Profile for 1000 ppi Fingerprint Compression” is a standard published by FBI for compressing and formatting 1000 ppi fingerprint and palm images. This involves the use of the general purpose standards like JPEG2000 (Aware Biometric Software, n.d.; Orandi et al., 2014). All these standards use wavelet based compression algorithm.

The Unique Identification Authority of India (UIDAI) set up by the Government of India for issuing Unique Identification (UID) numbers to the residents in the country also recommended JPEG2000 or WSQ based on WT coders as the fingerprint compression standard. They preferred these standards on account of their wide acceptance and also considering the past experiences of the US and Europe with biometrics (UIDAI Committee on Biometrics, 2009).

Thus, being the technique used in the globally accepted latest standard for the compression of fingerprint images, this study mainly concentrated in WT based fingerprint image compression and its scope for further improvement in the quality of compressed image.

2.3 Wavelet Based Fingerprint Image Compression

Li and Kuo (1995) proposed an embedded wavelet packet coding algorithm for fingerprint image compression. As claimed by the authors the proposed method offered 1 dB PSNR gain compared to FBI WSQ standard, and 2 to 3 dB PSNR gain above the JPEG standard for fingerprint image compression. The preprocessing and post-processing techniques for embedded coding at lower bit rates were a problem under consideration.

Sherlock and Monro (1996) presented optimized biorthogonal and orthonormal wavelets for compression of fingerprint images using Embedded Zero-Tree Wavelet (EZW) compression scheme. The optimization was performed by simulated annealing over the wavelet filter coefficients. RMSE between original and reconstructed images was used as the cost function to be minimized. Compared with classical wavelets and wavelets optimized using general images, linear phase biorthogonal wavelets optimized for fingerprint image compression offered significant enhancement in fidelity.

Kasaei, Deriche and Boash (2002) proposed a compression algorithm for fingerprint images using wavelet packets and lattice vector quantization. The model was based on the generalized Gaussian distribution. The proposed algorithm was developed to improve the rate-distortion function by adapting to the characteristics of the subimages. It was reported that the proposed algorithm offered compressed images of higher quality for identical bit rates compared to the other available algorithms. The higher computational cost of wavelet packet is a drawback.

Gornale, Humbe, Manza and Kale (2008) applied wavelet packet transform based on Haar, Daubechies (db1) and Symlet (sym2) on fingerprint images. They applied three-level transforms on noisy and noiseless fingerprint images of size

374 x 388. On analyzing the results on the basis of retain energy and number of zeros present in the compressed image it was observed that higher CR was achieved for noiseless fingerprint image compared to noisy images for all the transforms. But, the computational requirement is higher in wavelet packet transform. Selection of an optimal threshold value to get better compression with minimum loss to images is difficult.

Funk, Arnold, Busch and Munde (2005) evaluated the effect of JPEG, JPEG2000 and WSQ compression algorithms on the performance of fingerprint recognition algorithms. The effect of the JPEG algorithm on fingerprint recognition was comparable to that of JPEG2000 and WSQ, above a CR of 0.056. For higher CRs WSQ and JPEG2000 were better.

A fingerprint compression scheme to obtain improved quality and higher CR via multiwavelet transform was proposed by Sudhakar and Jayaraman (2008). Embedded coding of multiwavelet coefficients was performed through Set Partitioning In Hierarchical Trees (SPIHT) algorithm. They pointed out that multiwavelets provide better PSNR as they have the properties such as orthogonality, symmetry, short support and higher approximation order for better in compression performance, which the scalar wavelets do not meet altogether. However, multiwavelets have some disadvantages: preprocessing and post-processing operations are required for the discrete multiwavelet transform. Also, the theory turns out to be more complicated (Keinert, 2003).

In the paper published by Gornale, Manza, Humbea and Kale (2007) it was reported that they applied Daubechies, Symlet and Coiflet wavelet transforms through different orders at 1 to 5 transform levels on the fingerprint images. It was found that the Coiflet4 (4th order) wavelet filter was more fit for lossy fingerprint image compression. However, Coiflets have a major shortcoming: they have a much wider support. The support with N vanishing moments is 6N - 1 for Coiflets compared to 2N - 1 for orthonormal wavelets. Compared to Coiflets the filter coefficients of biothogonal bases are easier to compute and give perfect symmetric wavelets too (Kobayashi, 1998).

Kampfer, Stogner and Uhl (2007) used five different general purpose image compression algorithms including three transform based algorithms: JPEG, JPEG2000, SPIHT, and two codebook-based schemes: Fractal image compression, Predictive Residual Vector Quantization (PRVQ – a special type of vector quantization). They reported that JPEG2000 and SPIHT (both wavelet based algorithms) clearly outperformed the remaining compression algorithms. But SPIHT coding is vulnerable to bit corruption, because a one bit error can cause significant image distortion depending on its location. Accurate bit synchronization is required, because loss in a bit during transmission can cause complete misinterpretation of the data (Santhi & Banu,2010).

Sung and Hsin (2007) proposed a hybrid Set Partitioning In Hierarchical Trees Embedded Block Coding (SPIHT-EBC) algorithm using the linear phase biorthogonal wavelet with 9/7-coefficient filter. The compression rate (bpp) and PSNR offered by the proposed algorithm were compared with that of the SPIHT and Embedded Block Coding with Optimized Truncation (EBCOT) algorithms. For fingerprint image it was noted that SPIHT-EBC without entropy coding was marginally preferable to SPIHT with entropy coding and SPIHT-EBC with entropy coding can provide further improvement compared with SPIHT and EBCOT.

A fingerprint compression algorithm called Wavelet Based Contourlet Transform (WBCT), which was based on WT and Directional Filter Banks (DFBs) was proposed by Zhao and Wang (2009). The DFBs were implemented using maximally flat filters and the scheme reduced frequency scrambling. Classes of WBCT coefficients were formed by a quadtree sorting procedure. It was reported that the proposed encoding algorithm offered improved performance over SPIHT.

A lossy fingerprint compression using wavelet and optimal re-quantization methodology was proposed by Muhsen, Dababneh and Nsour (2011). The technique employed 9/7 WT and the transformed coefficients were subjected to optimal re-quantization using re-quantization codebook. However, there could be additional computational cost due to the codebook generation.

Shakhakarmi (2012) performed multiscale analysis of fingerprint image compression using DCT, Fast Fourier Transform (FFT) and different wavelets. It was confirmed that the multiscale analysis at fourth level offered a better result for wavelet based compression system compared to FFT and DCT based systems.

Islam, Bulbul and Shanta (2012) employed Coiflet-type wavelets and wavelet packets for better compression of fingerprint image at three-level decomposition. They used 8-bit gray scale fingerprint image of size 480 × 400 as test image. They reported that the Coiflet 5 was much better than other Coiflet-type wavelets for wavelet based as well as wavelet packet based fingerprint image compression. For the wavelet packet transform there was improvement in the percentage of Retain Energy (RE) and percentage of Number of Zeros (NZ), showing better results for wavelet packet transform. However wavelet packet transform is computationally complex than WT.

From a review of different wavelet based fingerprint image compression algorithms, Emmanuel, Mu'azu, Sani and Garba (2014) observed that most of the prevailing techniques need codebooks or lookup tables, the generation of which causes extra computational complexity for implementation. They concluded that compared to the standard cdf 9/7 wavelet, biorthogonal coiflet wavelets can achieve superior performance in terms of better rate-distortion, better quality and lower computational complexity. They used fingerprint database of the National Institute of Standards and Technology (NIST), USA for experimentation and obtained better PSNR values at CR = 20:1. However, coiflets have a wider support.

Optimization of wavelet coefficients using Evolutionary Algorithms (EA) has been a significant approach in image compression. Several researchers have evolved wavelet coefficients using GA.

Moore, Marshall and Balster (2005) established an adaptive filtering methodology for the reconstruction of image with reduced MSE, which was previously forward transformed. They evolved classical wavelet coefficients similar to Daub4 and 2/6 (TS) wavelet coefficients for standard photographic image compression using a single training image and GA under quantization. Initial

population for GA was formed by randomly mutated copies of the coefficients of the selected classical wavelet. Reduction in MSE for single-level transformation with quantization step size, q = 64 and q = 32 was reported. The coefficients evolved for inverse DWT using a single training image performed well on other images from the test set. However, the work considered only reconstruction filters.

Grasemann and Mikkulainen (2005) employed the coevolutionary algorithm and properties of lifting by which specialized wavelets were evolved for fingerprint image compression. Coefficients taken randomly from a Gaussian distribution were used for initial population. Fingerprints from the first set of FVC2000 fingerprint database containing 80 black and white images of size 300 x 300 pixels, at 500 dpi resolution were used for training and testing. It was shown that the evolved wavelets consistently outperformed the classical wavelet used by FBI and that evolving wavelets adapted to specific classes of images could improve the compression performance of an image coder. Each individual had been evaluated 10 times on average. For a population size of 150 for each of the seven parallel sub-populations, it performed 1500 evaluations in each of the 500 generations in a run. The approach was highly time-consuming. The algorithm took 60 hours on a 3 GHz Xeon Processor. An average PSNR improvement of 0.75 dB was reported.

Peterson, Lamont and Moore (2006) expanded the previous approaches and reported that though MSE (or PSNR) is computationally a little faster than Universal Quality Index (UQI) and both perform well as fitness measure for GA evolution. SSIM measure was not qualified as an appropriate fitness measure for the optimization of image reconstruction filter. They evolved classical coefficients from random values obtained from the Daub4 wavelet for “fruits” image with q = 64. They explored the standard and local genetic search operators, and evolved coefficients that excelled the classical DWT for image reconstruction under quantization. They considered only reconstruction filters and that too at one and three MRA levels.

Babb, Moore and Marshall (2007) optimized wavelet coefficients for compression and reconstruction of images under quantization. They worked on Arctic Regional Supercomputer Center (ARSC) platforms to meet the huge computational

requirement and used 512 x 512 pixel “zelda.bmp” image for training purpose. Without any increase in the compressed file size the algorithm could achieve 1.126 dB improvement in PSNR at single-level decomposition, and more than 0.50 dB on average at three-level MRA compared to Daubechies-4 (D4) wavelet.

Babb (2007) described the evolution of wavelet coefficients for optimized transforms for fingerprint compression and reconstruction, surpassing the cdf 9/7 DWT. The initial population of GA for four-level MRA transform was built with randomly mutated copies of 9/7 wavelet coefficients. An individual chromosome in GA for four-level transform was represented by a total of 128 floating point values, with 16 forward and 16 inverse coefficients for each level. As a commonly used technique the first 1/16 transform values were retained and the rest were set to 0. The best transform produced 0.76 dB improvement in average PSNR over 80 fingerprint images. The experiments were done in ARSC supercomputer.

Babb and Moore (2007) reported that the cdf 9/7 wavelet coefficients optimized for four-level MRA transforms at one threshold level (or for one CR) performed well for a range of threshold levels (or for various CRs). According to them, the flexibility of the evolved transforms established them as the best fingerprint standard. While performing the GA evolution, the highest 6.25% (or 1/16) transform coefficients were retained (so that the CR = 16:1) and the remaining transform coefficients were set to zero. GA population at each generation was formed by 240 to 800 individual chromosomes each consisting of 128 floating numbers with initial population consisting of one exact copy of the cdf 9/7 wavelet coefficients and the remaining individuals were mutated copies of it. The training image consisted of four representative images from the fingerprint database. The GA used stochastic uniform selection operator, single-point heuristic crossover and elitism was set to 2. The number of generations in GA exceeded 15000. They used supercomputer for running the algorithm. There was an average PSNR improvement of 0.76 dB. The optimized coefficients offered improvements in average PSNR at other threshold levels also (for example, 0.794 dB at an approximate CR = 19:1).

An EA known as Covariance Matrix Adaptation Evolution Strategy (CMA-ES) was used by Babb, Moore and Peterson (2009a) for finding real-valued coefficients for matched forward and inverse transforms that outperformed the cdf 9/7 wavelet for satellite image compression and reconstruction under conditions subject to quantization error. For fingerprint compression at single-level MRA, compared to the cdf 9/7 wavelet, the optimized coefficients caused an average PSNR improvement by 3.00 dB at 64:1 quantization, allowing 4.36% increment in the average Information Entropy (IE). However, the increase in the number of coevolved real-valued coefficients with the number of multiresolution levels results in an exponential raise in the dimensionality of the problem. Babb, Moore and Peterson (2009b) evolved coefficients for three-level MRA which offered 0.54 dB average PSNR improvement in comparison to cdf 9/7 wavelet.

To improve image compression in embedded systems Salvador, Moreno, Riesgo and Sekanina (2011) presented a bioinspired, EA for optimizing WTs. The search algorithm was an easy version of an Evolution Strategy (ES), employing fixed point arithmetic. The optimization was done for two-level decomposition with single evolving population, one set of coefficients for all MRA levels and all high pass coefficients discarded. The average improvement in PSNR for two-level transform offered by the algorithm was 1.57 dB.

2.4 Gender Classification

Sex is the primary information that distinguishes between individuals. There are several features that discriminate male and female. Gender classification has important applications in areas where male-female recognition is significant. As an example, once a suspect’s sex is known it can limit its search among enrolled suspects to reduce decision time and get better recognition performance. Gender identification and classification has been extensively researched in literature. Researchers have attempted to do male-female classification using other discriminating information from face, hand, finger, voice, human gait, shape, etc.

A general survey of various human features other than fingerprint has been made and presented below.

Majority of the work has been done utilizing features collected from frontal face images. A multi-view gender classification method using both shape and texture information of facial image was presented by Lian and Lu (2006). For classification, Support Vector Machines (SVM) method was employed. An appearance based approach using features extracted from facial images by Gabor filter banks was used by Rahman, Chowdhury and Bashar (2013) to discriminate men and women. They also employed SVM classifier. A frontal face image based method was proposed by Nazir, Ishtiaq, Batool, Jaffar and Mirza (2010). DCT based feature extraction and K-Nearest Neighbor (KNN) classifier were employed. Shobeirinejad and Gao (2010) presented a derivative based technique called Interlaced Derivative Patterns (IDP) to extract facial features for gender classification. According to the authors the proposed method is more fast and accurate than Local Binary Patterns (LBP), and Local Derivative Patterns (LDP) techniques. Ravi and Wilson (2010) presented a gender classification strategy employing linear SVM classifier in color images under non-uniform background using facial image. Chen and Ross (2011) established the possibility of realizing gender from face images acquired in the near-infrared and thermal spectra. As stated by them Local Binary Pattern Histogram (LBPH) features together with discriminative classifiers provide a reasonable amount of gender classification accuracy. Li, Lian and Lu (2012) proposed a gender classification framework, which operates on features from facial components: forehead, eyes, nose, mouth and chin and also from hair and clothing. For each of these features separate SVM classifier with probabilistic output was used. According to the authors, their proposed framework improved classification accuracy, even at the presence of noise, occlusions, and changes in illumination. The work suffered from the problem of the dependence of hair feature on complex backgrounds and also the computation time for hair feature extraction was high. Perez, Tapia, Estevez and Held (2012) reported a gender classification method using features of frontal face images. It employed feature selection based on mutual information and fusion of features extracted from intensity, shape, texture, and from three different spatial scales. Basha and Jahangeer

(2012) used Continuous Wavelet Transforms (CWT) for selection of features from face images. Classification was performed using SVM with linear kernel. Shan (2012) investigated gender recognition on real-life faces using the database, the Labeled Faces in the Wild. He used LBPs to describe faces, Adaboost to select the discriminative LBPs features and obtained the performance of 94.81% by applying SVM. An approach for designing a fuzzy decision making system from shape and texture of face images for male and female classification was made by Moallem and Mousavi (2013). In addition to face shape features, Zernik moments which is considered as the probability of being male face image were also used to improve the result. They got 85.05% classification rate on the FERET face database. Jaswante, Khan and Gour (2013) used the geometric features of face, i.e., distance between eyebrow to eye, eyebrow to nose top, nose top to mouth, eye to mouth, left eye to right eye, width of nose and width of mouth. The features were fed to BPNN for classification. Maximum accuracy obtained was 98.40%. A gender classification technique employing a machine learning technique called decision trees was presented by Khan, Qureshi and Riaz (2013). The gender classification was performed based on frontal facial images. They could correctly classify gender with 97.33% accuracy.

Alrashed and Berbar (2013) proposed a gender classification system using features extracted from the eye and eyebrow region. 2D WT, Gray Level Co-occurrence Matrix (GLCM) and DCT techniques were used to extract features for an SVM classifier. They reported accuracy rate of 99.49% on gender recognition using 2D WT, 98.49% using GLCM and 99.62% with DCT on Faces94 database.

Pitch and formants extracted from speech samples and their combination were used by Kumar, Jakhanwal, Bhowmick and Chandra (2011) for gender determination. Based on three features such as energy entropy, short time energy and zero crossing rates from speech signal and using fuzzy logic and NN, a classifier to identify the gender of the speaker was proposed by Meena, Subramaniam and Gomathy (2013). DCT based features of both lip appearance and lip dynamics during

speech were used by Stewart, Pass and Zhang (2013) to discriminate gender. Lip appearance and dynamics were modeled by Gaussian mixture.

Yoo, Hwang and Nixon (2005) utilized human gait data and employed an SVM classifier for gender classification. Human gaits in image sequences were used by Shan, Gong and McOwan (2007) for gender classification. For improved performance gait and face features were used by them. Lu, Wang and Huang (2012) in their paper proposed a system to recognize gender from human gaits collected in an uncontrolled manner in which people could walk freely with time varying walking direction.

Mozaffari, Behravan and Akbari (2010) established a gender classification algorithm using combination of appearance based and geometric based features of a single frontal image per person. For better classification accuracy two appearance based features; DCT, LBP and one Geometric-based feature, i.e., Geometrical Distance Feature (GDF) were used. Based on the majority rule the gender was determined.

Wu and Yuan (2014) presented male-female classification technique based on geometry features of palm image. A Polynomial Smooth Support Vector Machine (PSSVM) was used for classification purpose. On a database of 180 palm images collected from 30 persons, their gender classification algorithm offered classification rate over 85%. Bansal, Agarwal and Sharma (2014) proposed an algorithm for predicting gender using iris images. Feature vector was created from the statistical and texture features of iris image using wavelets. Using SVM, they achieved a gender classification accuracy of 85.68%.

The gender classification schemes with the existing techniques which use other biometric traits such as face iris, hand shape, speech etc. have restricted use for crime investigation. Fingerprint analysis has a key role in convicting the person responsible for a crime.

2.5 Fingerprint Based Gender Classification

Fingerprint evidence is unquestionably the most dependable and legitimate proof till date in the court of law throughout the world. Gender classification from fingerprints is noteworthy move in forensic applications in order to shortlist the suspects in identifying a criminal. Extensive research works have been conducted in the field of fingerprint identification and classification (Maltoni & Jain, 2004). Recently a few researchers have addressed the use of fingerprint for gender recognition and classification.

Studies have been made by several researchers in different parts of the world to see whether any significant differences in the fingerprint features of male and female. According to Acree's (1999) study, Caucasian and African American women tend to have a significantly higher ridge density than their men. The results of the study of Gungadin (2007) shown that within the population of Indian origin, females have significantly greater number of ridges than males. Rastogi and Pillai (2010) observed that there is an association between distribution of fingerprint patterns and gender. Their study was carried out among medical students of Kasturba Medical College, Mangalore, India. Nayak et al. (2010a) in their study on population of Indian origin viewed that the mean ridge count is more in female than in male. Nayak et al. (2010b) made similar observation on populations of Chinese and Malaysian origins. Singh's (2012) studies realized significant differences in epidermal ridge density between males and females in two Northern Indian populations of Chandigarh Region (Khatri and Bania), confirming higher mean ridge density for females compared to males. Agnihotri, Jowaheer and Allock (2012) conducted study on 200 healthy medical students (100 men and 100 women) in the Indo-Mauritian population in the Department of Forensic Medicine, SSR Medical College, Mauritius. They observed that the maximum mean ridge density over all fingers in male falls below the minimum mean ridge density over all fingers in female. The studies performed by Dhungana and Sahu (2013) revealed significant mean difference in the finger loop ridge counts between males and females from Utterpradesh in India. According to them, a ridge count of < 13 ridges/25 mm^2 is

more likely to be of male origin and that of > 14 ridges/25 mm^2 is likely to be of female origin. From the fingerprint features of Egyptian population, Eshak, Zaher, Hasan and Ewis (2013) recognized that females have more ridge count and higher ridge density. All these findings encourage the effort of gender classification based on fingerprint features as in this present work.

Badawi, Mahfouz, Tadross and Jantz (2006) used Fuzzy-C Means (FCM), Linear Discriminant Analysis (LDA) and NN classifiers for gender classification. NN classifier based on feature vectors such as ridge count, Ridge Thickness to Valley Thickness Ratio (RTVTR), white lines count, ridge count asymmetry and pattern type concordance with a fingerprint database of 10 fingerprint images of 1100 males and 1100 females was used. They got 80.39%, 86.5%, and 88.5% correct classification using FCM, LDA, and NN, respectively.

Verma and Agarwal (2009) combined the fingerprint features such as ridge width, ridge density and RTVTR to implement gender classification algorithm using SVM classifier. As a preprocessing step, the images were normalized to standardize intensity values. The database contained fingerprints of 200 males and 200 females. They could achieve 53% correct classification for ridge density, 59.5% for RTVTR and 68% for ridge width and a combined classification accuracy of 88%.

Purohit, Imam and Beg (2011) presented an efficient and simple method showing the usefulness of PCA in recognizing gender from fingerprints. They evaluated eigen matrix from the test fingerprints to recognize the gender. As observed by them, gender recognition systems give better results as the size of the database is increased.

Gnanasivam and Muttan (2012) used frequency domain feature vectors formed by 19 DWT subband energies from all the subbands of six-level DWT and spatial domain feature vectors formed by 260 SVD components of fingerprints. The system was experimented with an internal database of 1980 male and 1590 female fingerprints. A KNN classifier was employed. They achieved 91.67% and 84.69% classification accuracy for male and female persons respectively. The overall classification accuracy was reported as 88.28%.

Omidiora, Ojo, Yekini and Tubi (2012) performed gender classification based on RTVTR and ridge count in fingerprints. The database contained 10 fingerprint images for 100 males and 100 females. They attained 80% classification using BPNN classifier.

The work done by Kaur, Mazumdar and Bhonsle (2012) employed feature vectors from FFT, DCT and Power Spectral Density (PSD) operations on fingerprints. An internal fingerprint database of 110 males and 110 females was used. The frequency domain calculations were compared with predetermined manual analysis threshold and gender was judged. As reported, 79.07% male and 90% female were correctly classified.

Chand and Sarangi (2013) employed frequency domain feature vectors comprising of 19 DWT subband energy from six-level DWT and spatial domain feature vectors comprising of 512 SVD components to classify male-female from a fingerprint database of 50 males and 50 females. Both the SVD and DWT outputs were combined to shape the final feature vector. They achieved more than 80% correct classification using KNN classifier.

Gornale, Geetha andKruthi (2013) proposed an algorithm for fingerprint based gender identification by using combined features like FFT, eccentricity and major axis length of fingerprint image. The database was composed of good quality left thumb impressions of 450 male samples and 550 female samples. Optimal threshold values were set for each feature type. Their experiment resulted in producing accurate decision of 80% of male and 78% of female.

Tom and Arulkumaran (2013) employed a frequency domain technique and pattern recognition technique such as 2D DWT and PCA to classify gender from fingerprints. The database contained 547 individual fingerprints of males and females. The fingerprints were preprocessed by resizing to 512 x 512 pixels size and enhanced. The DWT feature vectors were formed by 19 subband energies from all the six-level DWT. The PCA feature vectors composed of 512 principal components. Feature vectors made up of 531 components formed by combining DWT and PCA feature vectors were used for classification of 200 males and 200 females. The

classification was performed using minimum distance classifier and obtained 70% overall classification.

2.6 Present Issues and Remedies

Based on the detailed study of the published works, it is realized that wavelets have stimulated a big deal of importance in fingerprint image compression. The well-known and widely accepted FBI fingerprint standard WSQ, and the general image compression standard JPEG 2000 use the cdf 9/7 (bior 4.4) biorthogonal wavelet for lossy compression. The classical cdf 9/7 wavelet is composed of sixteen coefficients for forward transform and another sixteen for inverse transform and the conventional WT techniques used in applications including fingerprint compression employ frequency domain approach. In frequency domain, convolution method is used for finding WT coefficients. More number of wavelet coefficients consumes more time in transforming the image into wavelet domain. The convolution operation itself is time consuming as it contains large number of addition and multiplication arithmetic operations. By reducing the number of arithmetic operations, particularly the multiplication operations can lead to perform wavelet transformation faster.

The main requirement of an image compression system is to reduce the size of the compressed image as much as possible without compromising the image quality. In other words, a good image compression system is one which gives compressed images with maximum quality at any particular CR. Quality of the compressed image is usually measured in terms of PSNR. As seen in the literature survey, several research works employing various techniques have been done to realize fingerprint image compression systems that could offer better PSNR values. Optimization of classical wavelets for better fingerprint image compression is a noteworthy approach in this direction. Recently many research works have been done by using evolutionary algorithms for optimizing wavelet coefficients. Promising results using GA for evolving optimized classical wavelet coefficients for fingerprint image compression have been reported. Since the classical wavelet filter length is large the computational complexity is also large, which in turn takes tens of hours for

GA evolution. So, to meet the huge computational requirements researchers have been forced to use supercomputers.

Thus, the issues related to the huge amount of computational requirements involved in GA evolution for optimizing cdf 9/7 wavelet coefficients for fingerprint image compression to get best quality (with best PSNR) compressed image still remains unsolved. It is a problem open to all the researchers working in the area of fingerprint image compression. So, the first phase of this thesis work attempts to solve the problem by employing many novel techniques that will be dealt with in the subsequent chapters.

The literature survey of gender classification based on fingerprint images reveals that there is scope for further improvement in the classification system. Though many classification systems reviewed offer satisfactory classification accuracy, the issues related to the speed of the classifier and its performance still remain to be attended to as the previous works need further improvements in both aspects and there is scope for the same. For example, NN classifiers employing components of transforms like DWT, SVD, PCA, etc. as feature vectors to produce outputs with reasonable accuracy consume large amount of time owing to the use of full set of transform components. Also, the initial seed value for the NN changes randomly for different runs of the algorithm causing inconsistent and non-optimal solutions. This gives room for further investigation to device new improved techniques to realize better fingerprint based gender classification systems. Thus, the second phase of this thesis work proceeds in such a way intending to optimize the cdf 9/7 wavelets and the initial seed values of feed forward BPNN classifiers and also to use minimum numbers of components in feature vectors for faster gender classification with better classification accuracy.

Chapter 3

Image Compression and Gender Classification: Materials and Tools

In digital image processing it is required to handle a large quantity of data. Large storage space is required to store the image data for future use. Similarly image data transmission needs wide channel bandwidth. Image compression techniques are usually employed to reduce the above requirements. Automated gender classification is a major research area. Gender classification using fingerprints is a useful preprocessing step for easy search of an individual in many forensic and non-forensic applications. WT is the state-of-the-art technique used in image processing including image compression and feature extraction for gender classification. SVD and PCA are also very much accepted as feature extraction tools. So, this chapter presents the concepts of WT, SVD and PCA along with the popular NN that are used in this thesis work for image compression and gender classification.

3.1 Wavelet Transforms (WT)

WT (Meyer, 1992; Chui, 1992; Daubechies, 1992) or wavelet analysis is an area of applied mathematics, which has been found to be best suited for analyzing signals of aperiodic, intermittent, noisy or transient nature. It was developed to overcome the shortcomings of the Fourier Transform (FT) (Bochner & Chandrasekharan, 1949). In signal analysis, it is often desirable to know the strength of each frequency component in the signal as well as the time at which the frequency components occur. This is called time-frequency localization. As far as stationary signals (signals whose statistical properties are invariant over time) are concerned the FT provides information about both time and frequency, since the frequency content of such signals do not change in time. In this case, it is meaningless to know the time of occurrence of frequency components since all frequency components present at all times. However, most practical signals like speech, biomedical measurement, communications etc. are extremely non-stationary. The major problem with Fourier transform is that it is not suitable for analyzing non-stationary signals as it provides only frequency information, but no time information.

The Short Time Fourier Transform (STFT) or Windowed Fourier Transform (WFT) was developed then with non-stationary signal analysis in mind. In STFT, the signal is sliced into small portions so that these portions can be assumed to be stationary. Such small portions are selected by multiplying the signal with a small window function ‘w’ and then FT of that portion (assumed to be stationary) is computed. The STFT is obtained from the FT of all such portions formed by moving the window function along the entire signal duration. The problem with STFT is that it gives a fixed resolution at all times due to its fixed window function, irrespective of the frequency components in the signal. Usually high frequency signals are of short duration whereas low frequency signals lasts for more time. So, the efficient analysis of such signals demanded for a transform giving variable resolution at different times for different frequencies.

The limitation of STFT has been overcome by WT. The following section gives some basic ideas about wavelets and WT.

3.1.1 Wavelets

A wavelet is a “small wave” with its energy confined to a finite duration to provide a means for the analysis of transient, non-stationary or time-varying events (Young, 1993; Rao & Bopadikar, 1998). In finding WT of a signal, the wavelets act as the basis functions. Then, like any other transform, WT of the signal is obtained by computing its inner product with the wavelets. The following detailed discussions on wavelets and WT have reference to the research papers and text books (Mallat, 1989a; Vetterli & Herley, 1992; Daubechies, 1992; Kaiser, 1994; Sheng, 1996; Burrus, Gopinath & Guo, 1998) and similar materials. There are varieties of wavelets that can be used for analyzing the signal depending upon the type of the applications.

3.1.2 Properties of Wavelets

Wavelet behaves like a window function similar to that in STFT (Goswami & Chan, 1999). A real or complex-value continuous-time function $\psi(t)$ qualifies as a wavelet if it satisfies the following conditions.

The function integrates to zero:

$$\int_{-\infty}^{\infty} \psi(t)dt = 0 \tag{3.1}$$

which indicates that the function is oscillatory.

The function is square integrable:

$$\int_{-\infty}^{\infty} |\psi(t)|^2 \, dt < \infty \tag{3.2}$$

which indicates that the function has finite energy.

It satisfies the admissibility condition:

$$C_\psi = \int_{-\infty}^{\infty} \frac{|\psi(\omega)|^2}{|\omega|} \, d\omega < \infty \tag{3.3}$$

the condition to be satisfied for finding the inverse WT. Here, C_ψ is called the admissibility constant whose value depends on the chosen wavelet (Addison, 2002).

The function $\psi(t)$ is called a mother wavelet. The mother wavelet acts as a prototype for generating the other window functions used for transforming the other segments of the signal. It is the main function from which the other functions (windows) with different region of support that are employed in the transformation procedure are derived. The different wavelet basis functions or windows are generated by performing two operations, viz. translation and scaling.

The term translation relates to the location of the window, as it shifts the window along the signal to locate different segments and hence captures the time information. The term scale relates to the support in time of the window. The mother wavelet is scaled down (contraction) or scaled up (expansion) to capture the high frequency or low frequency information of the signal. From the single mother wavelet function $\psi(t)$ a family of functions could be derived, that form the basis functions corresponding to the particular $\psi(t)$ represented as:

$$\psi_{a,b}(t) = \frac{1}{\sqrt{a}}\,\psi\left(\frac{t-b}{a}\right) \qquad a \in \boldsymbol{R}^+, b \in \boldsymbol{R} \tag{3.4}$$

where *b* is the translation parameter and *a*, the scale parameter.

The scale parameter *a* is defined as $|1/frequency|$. Scaling either dilates (expands) or compresses (contracts) a signal. Large scales (low frequencies) dilate the signal to give global information buried in the signal, while small scales (high frequencies) contract the signal to offer detailed information about the signal (Graps, 1995; Polikar, 1996).

3.1.3 Continuous Wavelet Transform (CWT)

CWT is a powerful mathematical tool, equipped for giving both time and frequency information of the signal simultaneously. It provides especially the time-frequency representation of non-stationary and fast transient signals. For a square integrable function *f*(*t*), the CWT with respect to a wavelet $\psi(t)$ is given as,

$$W(a,b) = \int_{-\infty}^{\infty} f(t)\psi_{a,b}^{*}(t)\,dt$$

$$= \int_{-\infty}^{\infty} f(t)\frac{1}{\sqrt{|a|}}\psi^{*}\left(\frac{t-b}{a}\right)dt \qquad (3.5)$$

where * stands for complex conjugation.

The term $1/\sqrt{|a|}$ is the normalizing factor maintaining the same energy for all wavelet basis functions obtained by the scaling and translation of the mother wavelet. The CWT of a function is essentially a collection of inner products of the function with the translated (shifted) and scaled (dilated) wavelet $\psi_{a,b}(t)$ for all a and b. The CWT can be interpreted as a set of Linear Time Invariant (LTI) filters whose impulse responses are dilations of the mother wavelet reflected about the time axis. The scale and frequency are inversely proportional. So the CWT provides better frequency resolution (but poorer time resolution) at low frequencies and better time resolution (but poorer frequency resolution) at high frequencies of the signal. This is what required as naturally the time period of low frequency signal is larger and that of high frequency signal is smaller.

The inverse CWT exists if the mother wavelet satisfies the admissibility condition given in equation (3.3).

Then the inverse CWT is mathematically represented as,

$$f(t) = \frac{1}{C}\int_{a=-\infty}^{\infty}\int_{b=-\infty}^{\infty}\frac{1}{|a|^2}\,W(a,b)\psi_{a,b}(t)\,da\,db \qquad (3.6)$$

3.1.4 Wavelet Families

Wavelets are classified as orthogonal and biorthogonal wavelets according to the type of basis functions they use. The orthogonal wavelets use orthogonal bases and biorthogonal wavelets employ biorthogonal bases. In each class, there is a variety of wavelet families, the qualities of their elements depend upon the length of the support of the mother wavelet, the number of vanishing moments, symmetry, regularity, etc.

3.1.4.1 Support of the Mother Wavelet

Length of the support of the mother wavelet quantifies the width of the wavelet function, which obviously differ for different wavelet families. For example, daub'N' (N represents the order of the wavelet filter) has a support equal to 2N - 1. Wavelets having small support (narrow) such as the daub2 (support = 3) are able to be computed quickly. However, the small support in time implies a very large width in frequency. On the other hand, the wavelets with large support (wide) like daub20 (support = 39) have very large width in time and the frequency resolution is higher.

3.1.4.2 Vanishing Moments

The vanishing moment is a criterion on how a wavelet decays toward infinity. A wavelet $\psi(t)$ has *m* vanishing moments if,

$$\int_{-\infty}^{\infty} t^k \, \psi(t) \, dt = 0 \quad for \; k = 0, \dots, m \tag{3.7}$$

The number of vanishing moments measures the oscillation of a wavelet and the interval where it takes values significantly different from zero evaluates its localization. The wavelets should have higher vanishing moments. A wavelet with more vanishing moments has better capacity of compression of the basis. If a wavelet with *m* number of vanishing moments is used to analyze a polynomial with a degree less than *m*, then all detail coefficients will be zero, which give good compression. With more number of vanishing moments the wavelets turn out to be smoother or more regular and more complex functions can be represented with a sparser set of wavelet coefficients (Michel, Yves, Oppenheim & Poggi, 2007; Chun-Lin, 2010).

3.1.4.3 Symmetry of the Wavelet

Symmetric or anti-symmetric wavelets lead to filters with linear phase, a desired parameter ensuring that the transformed output signal is not distorted. Daubechies has shown that, except for the Haar wavelet, there exist no orthogonal compactly supported wavelet which is either symmetric or anti-symmetric (Daubechies, 1998).

3.1.4.4 Regularity of the Wavelet

The regularity provides an approximate measure of the number of times a function can be differentiated at any given point. Regularity of a wavelet function gives a measure of its smoothness. Higher regularity gives a smoother wavelet. The regularity of wavelets is closely related to the number of vanishing moments. The more the number of vanishing moments, the smoother the wavelet is. For example, the Haar wavelet has only the "zeroth" vanishing moment and hence its wavelet function is discontinuous. The regularity property is usually applied to the wavelets so as to have the wavelet transform coefficients to decrease fast with diminishing values of the scale, *a*. So, it is desirable to have wavelets which possess higher regularity.

Examples of wavelet families include Daubechies, Symmlet, Meyer, Morlet, Haar, Coiflet, Cohen daubechies feauveau (cdf), etc. Each wavelet family contains sub-families of wavelets discerned by the number of wavelet coefficients and the properties discussed above (Mallat, 1999; Stolojescu, Railean, Moga & Isar, 2010).

3.1.4.5 Orthogonal Wavelets

Orthogonal expansion is an important tool for analyzing a signal. In orthogonal decomposition of a signal, the computation of the coefficients of expansion which represent the magnitudes of the decomposed basis function components is done in a simple and efficient manner. Thus, by using orthogonal wavelets as basis functions it is straightforward to transform, decompose or analyze the signal by computing the inner product of the signal with each basis function. Also, WT obtained using orthogonal wavelet basis functions is energy preserving.

The Haar wavelet is an example of orthogonal wavelet, which was proposed in 1909 by Alfréd Haar. It qualifies as the simplest wavelet and has the shortest support among all wavelets. The Haar wavelet is not a good choice for approximating smooth signals as it is non-continuous and has only one vanishing moment. However,

this property makes it useful for the analysis of abrupt changes or time localized information in the signal.

Daubechies, Coiflet, Symmlet etc. are examples of other wavelet families which belong to the orthogonal class. The Daubechies wavelets discovered by Ingrid Daubechies is a family of orthonormal and compactly supported wavelet functions having the highest regularity for a given support length. Symmlets is a family of nearly symmetric wavelets proposed by Daubechies. Their construction is similar to that of Daubechies wavelets and properties other than symmetry are similar for both wavelet families. Coiflets represent another family of orthogonal wavelets developed by Daubechies, as requested by Ronald Coifman, to have vanishing moments for both wavelet and scaling functions. This wavelet is more symmetric than the Daubechies wavelets.

3.1.4.6 Biorthogonal Wavelets

As far as orthogonal wavelets are concerned, the analysis and synthesis wavelet functions are the same with same vanishing moments. In contrast, the biorthogonal wavelets have different analysis and synthesis wavelet functions and the *m* vanishing moments correspond to synthesis wavelet only. In biorthogonal case, construction of symmetric wavelets is possible allowing the linear phase property, which is required for distortion-less signal reconstruction. Thus, it permits more degree of freedom in design compared to orthogonal wavelet. In fact, orthogonal wavelets constitute a special class of biorthogonal wavelets. Reverse biorthogonal wavelet family, which is derived from the biorthogonal wavelet family, also falls in the class of biorthogonal wavelets.

3.1.5 Multiresolution Analysis

Multiresolution Analysis (MRA) is a technique by which a signal can be analyzed at different frequencies with different resolutions. Mallat in his work in 1989 described the wavelet approach to multiresolution decompositions. He explained that by decomposing a function into a wavelet orthonormal basis, the variation in information among the approximations of a function at different resolutions could be computed

(Mallat, 1989b). WT is capable of performing multiresolution signal analysis with the varying scale factor, *a*. The fundamental technique of MRA is that of successive approximation of the signal by adding detail information to the current coarse approximation signal to get a subsequent finer approximation signal.

An MRA of the space $L^2(R)$ of finite energy signals $f(t)$ is a chain of nested closed subspaces $\{V_i\}_{i\in Z}$, represented as

$$... \subset V_2 \subset V_1 \subset V_0 \subset V_{-1} \subset V_{-2} \subset V_{-3} \subset \cdots \subset L^2(R) \tag{3.8}$$

The intersection of the subspaces reduces to $\{0\}$ and their union is dense in $L^2(R)$. All the subspaces can be derived from the fundamental space V_0 (for $i = 0$) by contracting ($i < 0$) or expanding or dilating ($i > 0$). That is,

$$f(t) \in V_i \;\Leftrightarrow\; f(2t) \in V_{i-1}; \qquad i \in Z \tag{3.9}$$

Let W_i be the orthogonal compliment of V_i in V_{i-1} and this is represented in mathematical form as,

$$\begin{aligned} V_{i-1} &= W_i \oplus V_i \\ &= W_i \oplus W_{i+1} \oplus V_{i+1} \\ &\vdots \\ &= W_i \oplus W_{i+1} \oplus W_{i+2} \oplus W_{i+3} \oplus \cdots \end{aligned} \tag{3.10}$$

This shows that the W_i space holds the detail information required to go from V_i space to V_{i-1} space. Thus, in MRA technique, a signal with higher resolution can be obtained by adding a sum of details to the signal with lower resolution. Apart from the wavelet function, ψ a second function called the scaling or dilation function, ϕ is also associated with the MRA. The wavelet function, ψ spans the detailed or wavelet space W_i and the scaling function, ϕ spans the coarse or approximation space V_i.

To make the idea more clear, assume $f_0(t)$ be an approximation of the function $f(t)$ corresponding to V_0. The $f_0(t)$ is actually the weighted sum of scaling function and its translates at scale = 0. Now, a finer approximation $f_1(t)$ of $f(t)$ can be obtained by adding the details corresponding to W_0. The detail or

wavelet space W_0 is the weighted sum of wavelet function and its translates at that scale, obtained by projecting $f(t)$ to W_0. This technique is iterated so as to successively approximate the signal at finer and finer scales by adding weighted sum of wavelets corresponding to each scale (Rioul & Vetterli, 1991; Michel et al., 2007).

3.1.6 Discrete Wavelet Transform

The CWT contains a large amount of redundant information when analyzing a signal and hence takes a substantial amount of computation time and resources. Alternatively, the DWT offers considerable reduction in the computation while eliminating the redundancy and providing adequate information needed for analysis and synthesis of the signal. This facilitates easier implementation of the DWT.

The DWT uses wavelets with discretized scale and translation parameters. Usually scale and translation parameters are chosen based on powers of 2 called dyadic scales and translation, such as $a = 2^{-j}$ and $b = k2^{-j}$, where $j, k \in Z$ represent discrete scale and translation parameters respectively (Soman & Ramachandran, 2006). Then the DWT coefficients of a signal x(n) are obtained as,

$$W_{\phi}(j_0, k) = 2^{\frac{j}{2}} \sum_{n} x(n)\ \phi_{j_{0,k}}(n) \tag{3.11}$$

$$W_{\psi}(j_0, k) = 2^{\frac{j}{2}} \sum_{n} x(n)\ \psi_{j,k}(n) \tag{3.12}$$

where $j \geq j_0$. The input $x(n)$, ϕ and ψ (scaling and wavelet functions respectively) are discrete variable functions.

3.1.7 Subband Coding

Subband coding is a method in which the channels of a filter bank are employed for coding signals. It is a multiresolution signal processing approach that was originated from speech compression application. In subband coding scheme the signals are considered in spectral bands for analysis as well as compression purposes. In fact, besides providing means for deriving wavelet bases, the multiresolution approach

finds very much importance in conceptualizing problems connected to wavelet and subband decompositions of signals.

Subband coding works on the fundamental concept of successive approximation. A signal is decomposed to coarse and detail approximations. The detail part is the difference between the original signal and the coarse approximation. Typically, the coarse approximation is a lowpass filtered, subsampled (downsampled) version of the original signal whereas the detail is a highpass, subsampled version. The procedure can be repeated on the coarse signal. The original signal is reconstructed from the coarse and the detail signals simply by adding them together. This approach carries out a multiresolution analysis identical to the wavelet decomposition of the signal (Vetterli & Kovacevic, 1995).

In DWT or subband coding, the signal $x(n)$ is passed through a succession of low pass and high pass filters to analyze the low frequencies and high frequencies respectively. The two sets of basis functions in DWT namely, the scaling functions and wavelet functions are associated with lowpass (h) and highpass (g) filters, respectively. The filtering processes change the resolution (a measure of the amount of detail information) of the signal and the downsampling and upsampling (used in reconstruction phase) operations change the scale.

In the analysis or decomposition phase, the signal $x(n)$ is filtered by a half band lowpass filter with impulse response $\tilde{h}(n)$. It filters out all frequency components that are above half of the highest frequency in the signal and thus the resolution of the resulting coarse (lowpass) signal is half that of $x(n)$. Half the number of samples in the filtered output signal is redundant; hence they are removed by downsampling by two, causing an increase in the scale by two. The whole operation results in half the time resolution and double the frequency resolution. The same process is done with a highpass filter $\tilde{g}(n)$ (replacing the lowpass filter) to separate the high frequency components. The synthesis (reconstruction) process performs the inverse operation of the analysis process.

A schematic diagram of the subband algorithm is shown in Figure 3.1, in which $\tilde{h}(n)$ and $\tilde{g}(n)$ represent the lowpass and highpass analysis filters, while $h(n)$ and $g(n)$ represent the lowpass and highpass synthesis filters, respectively. The reconstructed signal is represented by $x_0(n)$.

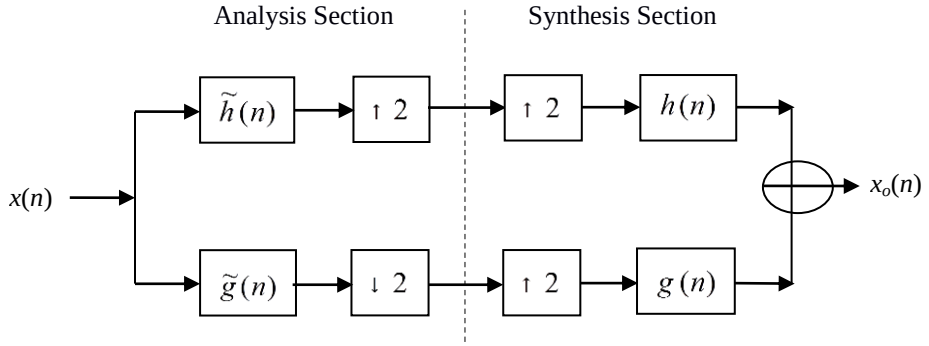

Figure 3.1 Schematic diagram of the subband algorithm to realize analysis and synthesis sections of the DWT.

The subband coding technique for realizing DWT is slow. A method called 'lifting scheme' can be used to perform faster implementation of the DWT.

3.2 Wavelet Lifting Scheme

The traditional wavelets, which are translates and dilates of one mother function, are often referred to as the first generation wavelets. Lifting scheme (Sweldens, 1996; Sweldens & Schröder 1996; Sweldens, 1997; Daubechies & Sweldens, 1998) is a new tool to construct the so called second generation wavelets. The traditional methods of constructing wavelet bases employ FT to achieve the time-frequency localization. In contrast to the traditional methods, which is done in frequency domain, LS can be used to design wavelets in spatial domain.

There are several advantages of LS in employing for the construction of wavelets. Transformation of signals of an arbitrary size with proper treatment of the boundaries is possible with transforms employing wavelet lifting. LS permits faster implementation of the WT, thereby making the computational time optimal. Fully in-

place computation of the WT, without any auxiliary memory to store the interim results, can be done. Since the LS works on the spatial domain, it is suitable for those interested in applications rather than complex mathematical expressions. The inverse WT for signal reconstruction can easily be computed by undoing the steps performed in the forward transform.

The LS begins with a traditional wavelet filter set and the properties of the corresponding WT are improved (lifted) using lifting steps. The lifting steps are of two types: the primal lifting step and the dual lifting step. Several such lifting steps are cascaded in alternate order to achieve desired properties of a WT (Soman & Ramachandran, 2006). Daubechies and Swelden (1998) further proved that any orthogonal and biorthogonal wavelet decompositions can be made into lifting steps by factorizing the associated polyphase matrix.

3.2.1 Basic Ideas of LS

Let *a* and *b* be two adjacent samples of a sequence. Now, *a* and *b* can be replaced by their average *s* and difference d by performing a simple transformation:

$$s = \frac{a+b}{2} \tag{3.13}$$

$$d = b - a \tag{3.14}$$

For well correlated samples *a* and *b*, the difference d is small and hence require only fewer bits for its representation. From *s* and *d*, the original samples *a* and *b* can simply be regained as,

$$a = s - \frac{d}{2} \tag{3.15}$$

$$b = s + \frac{d}{2} \tag{3.16}$$

To generalize this, assume a signal s_n of length 2^n with sample values $s_{n,l}$:

$$s_n = \{s_{n,l} \,|0 \leq l < 2^n\} \tag{3.17}$$

The average and difference transform of each sample pair $a = s_{n,2l}$ and $b = s_{n,2l+1}$ are obtained as,

$$s_{n-1,l} = \frac{s_{n,2l} + s_{n,2l+1}}{2}, \quad l = 0, \ldots\ldots, 2^{n-1} \tag{3.18}$$

$$d_{n-1,l} = s_{n,2l+1} - s_{n,2l}, \quad l = 0, \ldots\ldots, 2^{n-1} \tag{3.19}$$

Thus, s_n is split into an average (coarse) signal s_{n-1} and a difference (detail) signal d_{n-1} with samples represented as $s_{n-1,l}$ and $d_{n-1,l}$ respectively, both having length 2^{n-1}. Now, the original signal s_n can easily be reconstructed by merging s_{n-1} and d_{n-1}.

The above operation can be iterated on the coarse signal s_{n-1} to get a coarser signal s_{n-2} and a detail signal d_{n-2}, both having length of 2^{n-2} samples. This can be performed n number of times till no more samples remain. This is a simple example of the Haar case (Sweldens & Schröder,1996; Soman & Ramachandran, 2006). Figures 3.2 and 3.3 show the structure of the forward and inverse WTs.

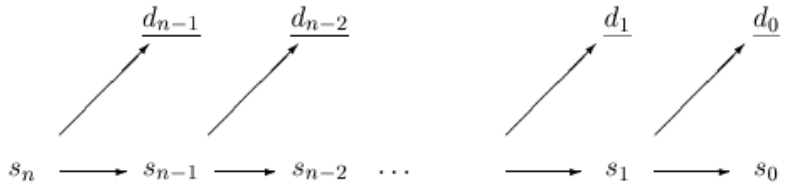

Figure 3.2 Structure of the forward WT (lifting).

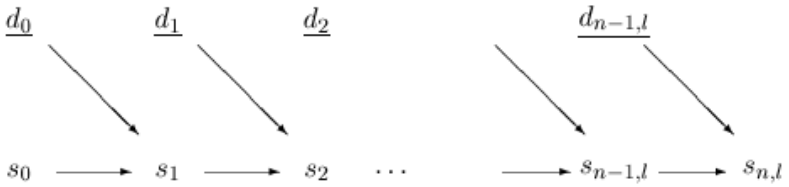

Figure 3.3 Structure of the inverse WT (lifting).

3.2.2 The Lifting Steps

The construction of a typical WT via lifting involves three steps: split, predict and update.

3.2.2.1 Split

This is the first step in lifting, by which the signal is split into two disjoint sets of samples such as the one containing even indexed samples s_{2l} and the other containing odd indexed samples s_{2l+1}. Obviously, the length of each set of samples will be half that of the original signal. The splitting into sets of even and odd samples is called the *Lazy wavelet transform.* The split operator is:

$$\left(even_{j-1}, odd_{j-1}\right) = Split\left(s_j\right) \tag{3.20}$$

3.2.2.2 Predict

Being closely correlated sets of samples, if one of the sets (e.g., the odd) is known, the other (i.e., even) can be predicted by using a predictor operator, say *P*. In the simple LS (i.e., Haar case), the odd samples are predicted from the difference (or detail) of the neighbouring even samples as shown below.

$$d_{j-1,l} = s_{j,2l+1} - s_{j,2l} \tag{3.21}$$

In general,

$$d_{j-1} = odd_{j-1} - P\left(even_{j-1}\right) \tag{3.22}$$

3.2.2.3 Update

The running average of the $even_{j-1}$ samples (i,e., coarser signal) will be different from that of the original samples. The update step preserves the same average value for both coarser and original signals by replacing the $even_{j-1}$ samples with smoothed s_{j-1} values with the help of an update operator, *U* such that,

$$s_{j-1} = even_{j-1} + U\left(d_{j-1}\right) \tag{3.23}$$

In the case of Haar , $U = 1/2$ and therefore

$$s_{j-1,l} = s_{j,2l} + d_{j-1,l}\,/2 \tag{3.24}$$

3.2.3 Inverse Lifting Transform

Reversing the order of the operations and flipping the signs give the inverse transform, as below.

Inverse Update:

$$even_{j-1} = s_{j-1} - U(d_{j-1}) \tag{3.25}$$

In the case of Haar,

$$s_{j,2l} = s_{j-1,l} - d_{j-1,l}/2 \tag{3.26}$$

Inverse Predict:

$$odd_{j-1} = d_{j-1} + P(even_{j-1}) \tag{3.27}$$

In the case of Haar,

$$s_{j,2l+1} = d_{j-1,l} + s_{j,2l} \tag{3.28}$$

Merge:

$$s_j = Merge(even_{j-1}, odd_{j-1}) \tag{3.29}$$

Figure 3.4 shows the forward and inverse transform using LS.

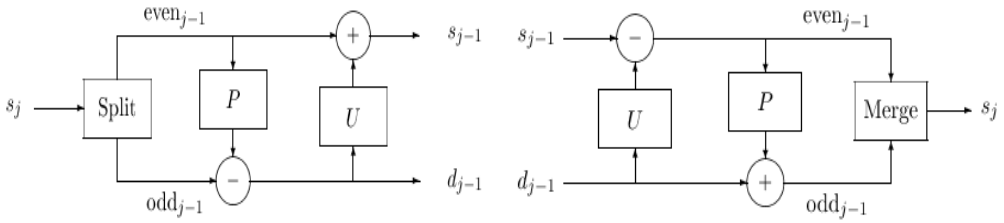

(a) (b)

Figure 3.4 (a) Forward, and (b) inverse transform using LS. The outputs s_{j-1} is the coarse and d_{j-1}, the detail signal.

3.3 Optimization

Optimization is the process used for finding better solution to a problem. It adjusts the inputs of a problem or a process to get the maximum or minimum output as per the requirement.

In Merriam-Webster dictionary, a subsidiary of Encyclopaedia Britannica Inc., optimization is defined as "an act, process, or methodology of making something (as a design, system, or decision) as fully perfect, functional, or effective as possible; *specifically* **:** the mathematical procedures (as finding the maximum of a

function) involved in this". Usually, the mathematical procedures involved can be either finding the maximum or minimum of the process or function.

Optimization tries to vary initial inputs to a process to gain improvement in the result. The inputs are represented by variables and the function or process is termed as the fitness function. In optimization terminology the fitness function is also known as objective function or cost function. The output of the process is called the fitness or cost. For a problem having only one input variable, the optimization is one-dimensional. Multidimensional optimization involves two or more variables. Optimization becomes more complex when the number of variables or dimensions is increased. The main operation in a minimum-seeking optimization algorithm is searching the cost surface for the minimum cost, where the cost surface is formed by all possible values of the function. In general, a cost surface is characterized by several peaks and valleys. The deepest valley corresponds to the minimum cost or the global minimum and the other valleys represent local minima. Similarly, the highest peak corresponds to the maximum cost or the global maximum and the other peaks represent local maxima.

Optimization involves certain kind of searching for the best solution from among the set of all feasible solutions. Various non-classical algorithms can be used in optimization problems that could not be solved by the classical procedures. These non-classical algorithms are broadly classified into deterministic and stochastic searches. Deterministic search algorithms use techniques like steepest gradient methods. Stochastic search algorithms employ random variables. Both these algorithms employ a transition rule to have better reliability or possibility to get near optimum results. The different kinds of transition rules result in different optimization algorithms (Rajasekaran & Vijayalakshmi, 2012).

3.3.1 Natural Optimization Algorithms (NOA)

The conventional optimization algorithms like Gradient-Based Local Optimization Method, Stochastic Hill Climbing etc. show the possibility to get stuck in certain local optimum points in the space of all feasible solutions. Therefore, these

algorithms cannot guarantee ‘best’ or ‘near best’ solution. There are many optimization algorithms that models natural processes. The popular algorithms that come under this category are (Randy & Sue, 2004) Ant Colony Optimization (ACO), Simulated Annealing (SA), Particle Swarm Optimization (PSO), Genetic Programming (GP), Evolutionary Strategies (ES), Genetic Algorithm (GA), etc.

Ant Colony Optimization (Dorigo & Gambardella, 1997) provides an optimal solution for the search tasks using the social behavior of real ant colonies. Real ants can find shortest path between a source of food and their colony even in the absence of any visual indications. If any obstruction is found in the current path they can find a new shortest path, which means that they can adjust with the variations in the surrounding situations. ACO mimics this behavior where a number of software agents called artificial ants construct solutions to the optimization problem (Sivanandan & Deepa, 2008).

Simulated Annealing (Kirkpatrick, Gelatt & Vecchi, 1983) mimics the physical cooling phenomenon which results in the formation of crystals in solids. In the process of annealing, when a substance is heated beyond its melting point and slowly cooled thereafter produce the crystalline structure. This exemplifies the natural process of finding an optimal structure or solution.

Particle Swarm Optimization (Eberhart & Kennedy, 1995) is a stochastic optimization technique. The idea behind the algorithm was taken from the social behaviour of animals like bird flocking, fish schooling or swarm of insects. For example, the swarm of insects can rapidly follow the insect which finds a suitable way to proceed for food, shelter etc. In PSO, each particle in the swarm possesses some ability to perform independent exploration of the search space.

Genetic Programming (Koza, 1992; Willis, Hiden, Marenbach, McKay & Montague, 1997) is a technique used for the automatic creation of computer programs. The GP technique can be used to build computers which perform what one needs, without telling them how to perform the same. It is similar to GA, but the input variables are formed by the programming constructs and the output is a measure of the performance of the program in attaining its objectives.

Evolutionary Strategies (Rechenberg, 1973) are well-known techniques in the field of evolutionary computation, employing the theory of natural genetics and natural selection as in GA and GP. The ($\mu + \lambda$) evolution strategy and (μ,λ) evolution strategy make a few examples of ES.

Genetic Algorithm (Holland, 1975) is the most popular evolutionary computation technique. GA is a general search algorithm based on natural genetics and natural selection rules. In this thesis work, GA is employed as the searching algorithm for optimizing wavelet coefficients and seed values in neural network for image processing applications such as image compression and gender classification.

The following section introduces the concept of GA and various terms associated with GA in detail.

3.3.2 Genetic Algorithm (GA)

Since early 1960s, the researchers got interested in imitating the natural evolution process in species to solve difficult optimization problems. An EA is an iterative and stochastic method that simulates the natural evolutionary process of human being. EA can do better than the conventional optimization techniques while dealing with complex real-world optimization problems (Back,1996). EA works on a population of individuals. GA (Coley, 1999; Goldberg, 2004; Randy & Sue, 2004; Sivanandan & Deepa, 2008; Rajasekharan & Vijayalakshmi, 2012) is perhaps the most popular method that belongs to the EAs.

According to Goldberg (2004), "Genetic Algorithms are rich-rich in applications across a large and growing number of disciplines". The popular applications of GA include sequence scheduling, signal processing, vehicle routing and scheduling, evolving computer programs, engineering design, machine learning, robotic route planning and many others. Prof. John Holland of Michigan University brought the idea of GA in 1960's. The concept of GA was later developed by him and published in his book written in 1975 (Holland, 1975).

According to Rajasekharan and Vijayalakshmi (2012), "Genetic Algorithms are good at taking larger, potentially huge, search spaces and navigating them looking

for optimal combinations of things and solutions which we might not find in a life time". Conventional optimization techniques have a single point approach, whereas GA uses a multi-point approach with a population of solutions at a time. Thus, in GA simultaneous searching in a wide search space is possible and the possibility to get stuck in local minima (or false valley) is reduced. There are several other important things that make GA different from the conventional algorithms. GA uses a coding of the parameter set and not the parameters themselves. They use objective function rather than any auxiliary information. They employ probabilistic transition rules in contrast to deterministic rules.

3.3.2.1 Biological Background of GA

The theory of GA is directly related to natural evolution. This section discusses the relation between the GA operations and the terms in natural evolution (Goldberg, 2004; Rajasekharan & Vijayalakshmi, 2012).

Chromosomes

Every living organism consists of cells. Each cell contains a set of chromosomes. All the genetic information is stored in the chromosomes. Chromosomes are strings of Deoxyribonucleic Acid (DNA) that behaves as a model representation for the complete organism. The chromosomes are composed of genes, which code the individual's characteristics. There is one gene for one characteristic; for example, colour of the eyes. The various possibilities of the genes for a particular characteristic are termed as allele. The possible alleles in this particular example of eyes colour can be black, brown, blue, etc. Thus, one gene can have different alleles. Each gene holds its specific location in the chromosome called locus. The arrangements of one or more chromosomes shape the overall genetic information needed for the creation and functioning of some organism. The complete genetic package for an individual is called the genotype. The interaction of the genotype with environment results in the formation of the organism called the phenotype. Figure 3.5 summarizes the correspondence between biological and GA terminology.

Biological term	Genetic algorithm term
Chromosomes	Strings (often binary)
Genes	Features
Alleles	Feature values
Locus	A particular (bit) position on string
Genotype	Encoded string (or structure)
Phenotype	Parameter set (or decoded structure)

Figure 3.5 Correspondence between biological and GA terminology

Search Space

For a particular problem, the set of all feasible solutions is called its search space. Each point in the search space corresponds to one possible solution and each possible solution is characterized by its fitness value, depending upon the problem under consideration. GA searches the search space for the best solution represented by a point in that space. The best solution means either minimum or maximum depending upon the definition of that particular problem. At the starting point of the search one knows only a few points in the search space. In the ongoing process of seeking the best solution, GA generates other points which represent other possible solutions.

Population

In GA terminology, a group of individuals or chromosomes being evaluated for fitness value is called a population. The size of the population is dependent on the complexity of the problem at hand. Usually the population is initialized randomly. For binary GA having binary coded chromosomes it is common to set the initial bits to a random zero or one. Initialization of population with chromosomes corresponding to good solutions that are already known is also common.

Gene Encoding

In GA, individual genes are represented as codes. Gene encoding can be done using bits, numbers, trees, arrays, lists or any other objects, depending on the problem. The most popular approach of encoding uses binary string. Holland (1975) mainly used binary strings in his works. Figure 3.6 shows an example of binary coded chromosomes in a population of four individuals (chromosomes) where a binary

string of 8 bits represents each chromosome. Each bit (gene) in the string (chromosome) typifies some characteristics of the solution. Obviously, depending upon the problem, one may use other options like vector of integers or real numbers for encoding. Here, each number represents a single parameter of the function.

Population	Chromosome 1	1 0 1 1 0 0 1 0
	Chromosome 2	1 1 0 1 0 1 0 1
	Chromosome 3	0 0 1 1 0 1 1 0
	Chromosome 4	1 0 0 1 1 0 1 0

Figure 3.6 Example of binary coded chromosomes in a population.

3.3.2.2 Operators of GA

In contrast to the conventional optimization methods, the GA begins by creating an initial set of random individuals or random solutions called initial population. An individual representing a solution to the particular problem is called a chromosome. A chromosome is formed by a string of symbols called genes. The consecutive iterations of the GA are called generations. In each generation, the fitness of each individual is evaluated to find the best individual. The subsequent generations are formed by creating new individuals called offspring.

The three main operators used in simple GA are reproduction, crossover and mutation. They are also called inheritance operators.

Reproduction

Reproduction is an operation by which individual strings are created based on their objective function or fitness values. According to the Darwin's theory of evolution and survival of the fittest, the strings in the current generation with higher fitness values have higher probability to offer better individuals in the subsequent generation. So, such strings are copied to form one or more offspring in the mating pool to form the subsequent generation. Reproduction operator is sometimes called the selection operator.

Selection

Selection is the process of picking two or more parent chromosomes from the population according to their evaluation function for mating (reproduction) in creating the next generation. The selection process aims at reproducing more copies of individuals with higher fitness values to create new offspring for the next generation. Generally, selection shrinks the search region within the population by removing poor solutions. Roulette wheel, tournament, Boltzmann etc. are a few examples of methods for selecting chromosome from parents.

***Roulette Wheel Selection*:** Roulette wheel selection is one among the common GA selection methods. In this approach, the probability of selection from the mating pool is proportional to the fitness of individuals. That is, an individual parent with higher fitness holds higher probability to be selected.

Proportional selection is called roulette wheel selection as its mechanism is reminiscent of the working of a roulette wheel (Andina & Pham, 2007). In this analogy, the entire population corresponds to a roulette wheel and the size of an individual's slot in the wheel is proportional to its fitness. In the selection operation, the roulette wheel is spun randomly to choose an individual for the subsequent generation. Then, the individuals with higher fitness values have larger slots in the wheel to possess higher chances to be selected. A typical roulette wheel selection for reproduction is shown in Figure 3.7. In this example, chromosome 1 has 10% of the total fitness while chromosome 2 has 25% of the total fitness. Obviously, chromosome 2 has greater probability of selection compared to chromosome 1.

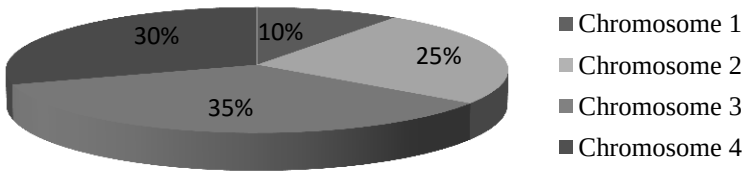

Figure 3.7 Roulette wheel selection for a population of four individuals.

Roulette wheel selection method is implemented as follows:

1. Sum the fitness of all individuals in the population. Let this be *TF* (Total Fitness).
2. Select a random number *r* between 0 and *TF*.
3. Add the fitness of the individuals one by one till the sum becomes equal to or greater than *r*. The individual whose fitness value causes the sum above or equal to *r* is selected.
4. The above steps are repeated *N* times, *N* being the number of individuals in the population.

***Crossover (Recombination)*:** Crossover is a recombination operator that permits individual solutions to exchange information by mimicking what is done by natural organism during sexual reproduction. It produces two fresh individuals (children or offspring) from two individuals (parents) chosen from the current population through selection (reproduction) process. Reproduction produces replicas of better individuals in the new population. It is not responsible for creating new individuals. Better (new) individuals (offspring) are created by crossover operator from the existing individuals in the mating pool.

Single point crossover is the simplest crossover operation. It is the one usually used by the conventional GA. A crossover point is chosen randomly along the length of the mated parent individuals and they are cut one time at corresponding points. The sections formed in the two parents by the cutting operation are swapped to form two children (offspring). Better children can be created if proper crossover point is selected. An illustration of single point crossover is given in Figure 3.8, where the crossover point is denoted by the symbol '|'.

Before crossover	Parent 1	**1 0 1** | **1 0 0 1 0**
	Parent 2	1 1 0 | 1 0 1 0 1
After crossover	Child 1	**1 0 1** | 1 0 1 0 1
	Child 2	1 1 0 | **1 0 0 1 0**

Figure 3.8 Illustration of single point crossover.

***Mutation*:** A mutation operator prevents irreversible loss of genetic diversity in the population by recovering the lost materials. It establishes new genetic structures in the population by altering some individual bits in the strings at random. In mutation, bit values are reversed (flipped) within the individual strings according to a given rate. Mutation helps the GA to get out of the trap of local minima and thus prevent premature convergence of the algorithm. It forces the GA to explore new search areas. As already discussed, crossover utilizes the current population to create better strings, but mutation facilitates exploration of the complete search space.

***Elitism*:** Selection of strings based on their proportional fitness does not ensure the selection of even the fittest one. Thus the best fit individual obtained so far cannot be copied to the new population. It is quite natural to see that search speed can be significantly enhanced by keeping the best (elite) individual among generations. Guaranteeing the transmission of the elite individual from one generation to the next is termed as elitism. An additional requirement is that the elite member(s) copied should not become altered by crossover or mutation. In elitist selection the best individual (or a few best individuals) is propagated to the new population, ensuring that the quality of the population is not degraded in the next generation.

3.3.2.3 Parameters of GA

There are certain control parameters that are carefully chosen for the effective working of GA. The choice of parameters can have considerable effect on the performance of the GA. The parameter values are dependent on the particular optimization problem at hand. The parameters of a simple GA include the (*i*) population size (*ii*) crossover rate (*iii*) mutation rate and (*iv*) convergence criteria.

***Population Size* (P_{size}):** As mentioned in the previous sections, P_{size} represents the number of individuals in a population. Usually, P_{size} depends on the problem's complexity. The effectiveness of GA in finding global optimum greatly depends on the P_{size}. If the P_{size} is small, only a small portion of search space is explored since the chance to carryout crossover is less. On the other side, a large population has higher computational cost and memory requirements and eventually the GA slows down. In

fact, it is undesirable to increase the population beyond certain limit determined by the particular problem because it will not provide a faster solution compared to populations with moderate sizes. Typical population size in the simple GA ranges from few tens to thousands.

***Crossover Rate* (P_c):** P_c determines the number of pairs of chromosomes to be crossed in each generation. It is computed as the ratio of the number of chromosome pairs to be crossed to the P_{size}. With a higher P_c a large area of the search space can be explored. However, it takes more computational time for the exploration of the parts of search space where the solutions are not so promising. On the other hand, a low P_c causes reduction in the speed of convergence of GA. Typical value of P_c in the simple GA for a P_{size} of 30 to 200 ranges from 0.5 to 1 (Rajasekharan & Vijayalakshmi, 2012).

***Mutation Rate* (P_m):** P_m is defined as the percentage of the total number of bits mutated in the population. Too high mutation rate may cause the children lose their similarity to the parents, thus it is unable to learn from the previous search information. If the rate is very low, many useful changes in bit states of strings will not be tried out. Typical range of values of P_m is from 0.001 to 0.5 (Rajasekharan & Vijayalakshmi, 2012).

***Convergence*:** There is no clear cut rule for the convergence criteria in GA. In one approach, it can be presumed that the GA met convergence when a particular percentage of individuals in the population turned out to become the same. According to another observation, the convergence can be attained when the average fitness of the population comes very near to the best individual's fitness. Then there will be little variation between the average and the best individual's fitness. The necessary condition for convergence in GA in terms of schemata is discussed in Goldberg's (2004) book on GA.

A self-explanatory flowchart of simple GA (Randy & Sue, 2004) is shown in Figure 3.9. GA approach for optimization is helpful and efficient for search in large, less understood or complex search spaces. It is also suitable when mathematical

analysis of the problem is unavailable and also with problems having limited domain knowledge.

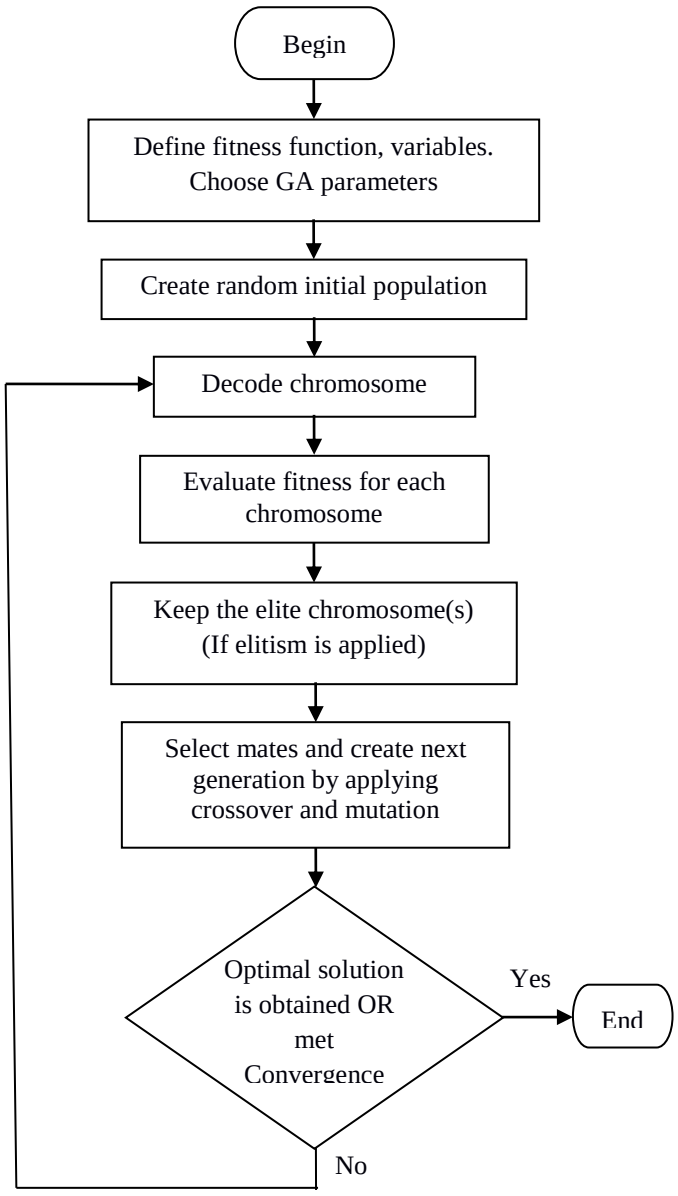

Figure 3.9 Flowchart of simple GA.

3.4 Feature Extraction

In the proposed work of gender classification, the popular tools such as WT, SVD and PCA are employed for feature extraction.

3.4.1 Wavelet Transform

Wavelets appear to be effective for feature extraction from signals. The DWT coefficients of the fingerprint images are used to reveal features related to the different gender classes. A detailed description on wavelets and WTs has been already given in section 3.1.

3.4.2 Singular Value Decomposition (SVD)

SVD (Strang, 1988; Ientilucci, 2003; Garcia, 2006; Fieguth, 2011; Baker, 2013) is a popular method that can be used to decompose (or factorize) a matrix into a number of component matrices. By SVD method, correlated variables are transformed into a set of uncorrelated ones to give better idea about the correlations among the input data. It identifies and organizes the dimensions along which data points hold the most variation. Then, by using fewer dimensions a better approximation of the original data can be obtained. Thus, the SVD can reduce a high dimensional, highly variable data set to a lower dimensional space, revealing the substructure of the data more evidently and organizing it starting from most variation to the least. By ignoring the variation under a specific threshold, data reduction is achieved. Hence, the SVD can be viewed as a data reduction technique. In the course of dimensionality reduction, SVD makes similar items to become more similar to each other and the dissimilar items more dissimilar.

SVD makes use of a theorem from linear algebra, according to which a matrix X of dimension $m \times n$ can be decomposed into the product of an $m \times m$ orthogonal matrix U, an $m \times n$ diagonal matrix D, and the transpose of an $n \times n$ orthogonal matrix V. Mathematically this is expressed as:

$$X = UDV^T \tag{3.30}$$

where $UU^T = I, VV^T = I$. The eigenvectors of XX^T and X^TX are known as the “left" singular vectors (*U*) and the “right” singular vectors (*V*), respectively. The expression UDV^T is known as the SVD of *X*. It can be constructed by keeping the nonzero eigenvalues.

The square roots of eigenvalues from *U* or *V* arranged in descending order form the diagonal elements of *D*, i.e.,the diagonal elements σ_1 to σ_n obey the relation:

$$\sigma_1 \geq \sigma_2 \geq \sigma_3 \geq \cdots\cdots \geq \sigma_n \geq 0 \tag{3.31}$$

The σ ’s give the singular values of *X*, and hence the SVD. For any matrix *X*, the sequence of singular values are unique. If the singular values are all different, then the sequence of singular vectors is also unique.

3.4.3 Principal Component Analysis (PCA)

PCA (Jolliffe, 1986; Madsen, Hansen & Winther, 2004; Strang, 2009) is a standard mathematical tool which finds application in areas like image analysis, pattern recognition, feature extraction, data compression, etc. It is also known as Karhunen-Loeve transform (Rao & Yip, 2001), a very useful tool for dimensionality reduction of multivariate data. PCA transforms a matrix of correlated variables to a new coordinate system that contains uncorrelated variables of lesser size with greater meaning and without loss of information. These uncorrelated variables are the principal components. They are orthogonal and are ordered in terms of the variability they have. The first principal component has the maximum amount of variability and each of the following orthogonal components comprises as much of the residual variability as possible. For a data set with already uncorrelated variables, PCA is of no significance (Semmlow, 2004).

Basically, the PCA transforms a set of data samples $Y = \{y_1, y_2, \ldots, y_n\}$ into another set $Z = \{z_1, z_2, \ldots, z_n\}$ with most of the information content stored in the first few dimensions, which enables the PCA to reduce the dimension of the data set without much loss in information. The PCA transformation relies on the assumption that high information corresponds to high variance. The matrix operation represents

$$Z = A \cdot Y \tag{3.32}$$

a transformation, by which a set of input dimensions *Y* can be reduced to a single dimension *Z*. The matrix *A* is chosen such that *Z*, known as the first principal component, bears the maximum variance possible for the given data set. Thus, the first principal component is an axis in the direction of the largest variance, which minimizes the sum of squares distance between the data points and their projections on the axis. Now, to find *A* it is required to calculate the sample covariance matrix *C* first. The covariance matrix is given by

$$C = \frac{1}{n-1}\sum_{i-1}^{n}(y_i - \bar{y})^T\,(y_i - \bar{y}) \tag{3.33}$$

where $\bar{y}$ is the sample mean vector. Further, the eigenvalues of the covariance matrix *C* for the input data set are computed and then the eigenvectors related to the *m* largest eigenvalues of *C* characterize *m*-dimensional space with uncorrelated features. The eigenvectors are ranked based on the quantity of variation in the input data that they correspond to. These eigenvectors act as the principal components. Generally, the first few principal components correspond to most of the variations in the data set so that there is a possibility of discarding the insignificant ones (Novakovic & Rankov, 2011).

3.5 Classification

In a classification problem the first and the most significant step is feature extraction. The next step is the actual classification, where the features extracted are assigned to the individual classes. In our problem of gender classification, the features extracted from the fingerprint images (i.e., the input data to be classified) are assigned to either male or female classes. Being a widely used practice, NN classifiers are used for gender classification work, proposed in this thesis. A theoretical understanding of NNs is provided in the following sections.

3.5.1 Neural Network (NN)

NN (Michie, Spiegelhalter & Taylor, 1994; Bishop, 1995; Rojas, 1996) is a mechanism that is embedded in many disciplines like neurosciences, mathematics, physics, computer science, engineering, etc. They can learn from input data with or without a teacher; the key property which makes them important in applications like classification, modeling, time series analysis, pattern recognition, signal processing, control, etc. (Haykin, 1999). Inspired from the functioning of human brains, they include new processing models that make use of features from the brain's physiology. NNs are more accurately known as Artificial Neural Networks (ANN) or Artificial Neural Systems (ANS). The power of ANN technique lies in its ability to find its own solution to particular problems provided only examples of the desired behaviour of the problem are known (Freeman & Skapura, 1991).

Human brain contains biological neurons (nerve cells) as basic units, who get nerve impulses from other neurons via a host of short branched tree like fine structures called dendrites, which act as input channels. The output channels are provided to the neurons by nerve fibers called axons that carry away information in the form of spikes of electrical activity to other neurons. The axon is connected with the dendritic associated to another neuron with specialized structure known as synapse or synaptic junction and it is assumed that synapse can impose excitation or inhibition on the connected neuron. The synapse is characterized by its own weight or strength. If the weight associated is positive then the synapse is excitatory and if it is negative the synapse is inhibitory. The neuron, on getting an adequately large excitatory input compared to its inhibitory input sends an impulse of electrical activity to its axon. The influence of one neuron on other changes as learning takes place due to change in the effectiveness of the synapses.

ANNs are based on the parallel structural design of the human brain and can imitate certain processing skills of the brain. It acquires knowledge through a learning process. Similar to the brain, the NNs are also composed of processing units (artificial neurons) or Processing Elements (PE) and connections linking them. The acquired knowledge is stored by the interneuron connection strengths called synaptic weights.

The values stored in these weights enable these networks to have the ability to learn, memorize, and create relationships between data. Since the NNs learn by examples, they can be trained using examples of a problem that are already known and the knowledge gained by such training can be efficiently employed for solving unknown instances of the problem. This attribute provides NNs very attractive in application areas where the knowledge about the problem to be solved is inadequate, but data for training the network are on hand.

3.5.1.1 Fundamental Concepts of NN

ANNs are parallel distributed models with a set of key distinguishing aspects:

- a set of processing units;
- an activation state for each unit, which is equivalent to its output;
- connections between the units defined by a weight w_{ij} which resolves the effect that the signal of unit i has on unit j;
- the effective input of the unit from its external inputs is determined by a propagation rule;
- an activation function decides the new activation level based on the effective input and the present activation;
- an external input for each unit, which is also known as bias or offset;
- a learning rule that provides a method for information gathering;
- An operating environment for the system supplying input signals and, if needed, error signals.

Example of a simple ANN is shown in Figure 3.10.

3.5.1.2 Processing Unit

The information processing unit is fundamental to the functioning of a NN. An ANN consists of a group of simple processing units that communicate signals to each other through a large number of weighted connections. ANN is able to do parallel processing, as it can carry out computation cycles of many units concurrently. The processing unit, also known as neuron or node processes the input received from the

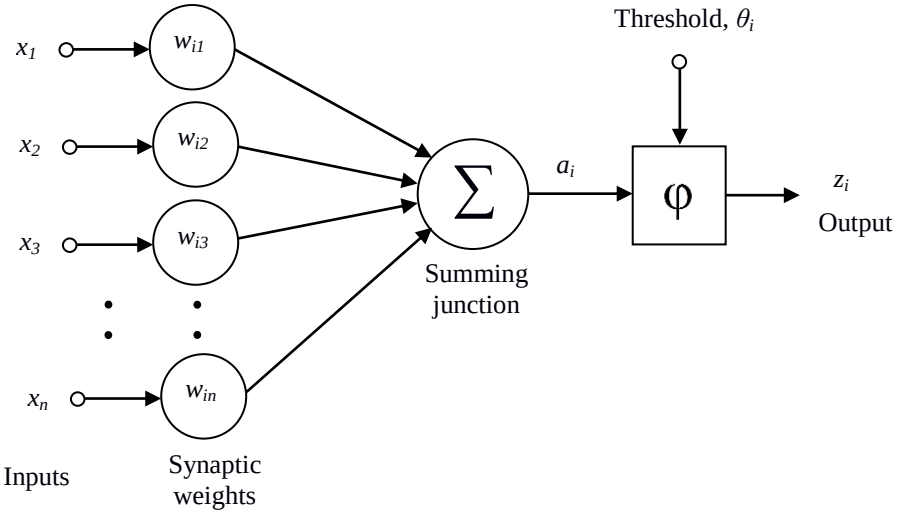

Figure 3.10 Example of a simple ANN.

neighbouring units or external sources to produce the output signal, which is transported to other units. Another job performed by the processing unit is the adjustment of the weights. Neural systems are composed of three types of units:

- the Input Units to accept signals from external sources of the network;
- the Output Units that function as the ANN endpoints to send data outside the net;
- the Hidden Units where the input and output signals are internal to the network.

A processing unit i can have inputs x_1, x_2, …, x_n, and one output z_i. Input signal can be external or internally produced, i.e., the output of another unit or its own output.

3.5.1.3 Summation Function

For the input vector X and corresponding weights W with a set of n components represented as $X = \{x_1, x_2, \dots, x_n\}$ and $W = \{w_1, w_2, \dots, w_n\}$ respectively, the product of each input x_j and its corresponding weight w_j, j=1,..,n are added up to produce the cumulative weighted combination a_i as,

$$a_i = \sum_{j=1}^{n} w_{ij}\, x_j \tag{3.34}$$

Depending upon the chosen network architecture there can be more complex summation functions that combine the inputs and weights in many other ways.

3.5.1.4 Activation Function

The summed output a_i is applied to an activation function or transfer function or squashing function, φ to produce the output signal z_i. It transforms the summed output to a value that is limited within a range. Typical value ranges between 0 and 1 or -1 and 1. The activated value of z_i can function as input to neighbouring neurons or as output of the network.

The threshold value, θ_i for the neuron *i*is the magnitude offset which provides the baseline input to the neuron in the dearth of other inputs. In fact, neurons normally produce an output only when their total input goes beyond a threshold value. Thus the total input to a neuron i is given by the weighted sum of the individual outputs from the connected units plus a threshold or bias, θ_i as (Prasad and Prasanna, 2008)

$$a_i = \sum_{j=1}^{n} w_{ij}\, x_j + \theta_i \tag{3.35}$$

Some cases use more complex rules for combining inputs.

The Sigmoid functions (the plots of which are S-shaped) (Fausett, 1994) have particular advantage for use in backpropagation networks because of the easy relationship of the function with its derivative at a point, which reduces the computational load for training. It is given by,

$$g(x) = \frac{1}{1 + e^{-ax}} \tag{3.36}$$

The parameter σ determines the steepness of the S-shaped curve. This function often finds application in neural networks whose desired output values range between 0 and 1.

3.5.2 NN Architectures

There are many types of NNs, classified based on their learning mechanisms. Feedforward and Recurrent networks are two fundamental classes (Kröse & Smagt, 1996; Rajasekaran & Vijayalakshmi, 2012).

3.5.2.1 Single Layer Feedforward Network

This class of network has only two layers: the input layer and the output layer. In a feedforward network there are no feedback connections from output units to input units and obviously the input to output data flow is feedforward.

3.5.2.2 Multilayer Feedforward Network

Besides the input and output layers this network has one or more intermediate layers known as hidden layers, which perform intermediary computations before passing the input to the output layer. The hidden layer has the computational units called hidden neurons or hidden units (y_k). The weights on the connections between input layer to hidden layer is called input-hidden layer weights (v_{ij}), whereas that between the hidden layer to output layer is called hidden-output layer weights (w_{jk}). A multilayer feedforward network with a configuration having m input units (x_j), n_1 and n_2 units respectively in the first and second hidden layers and o output units (z_{kl}) is represented as m - n_1 - n_2 - o. A multilayer feedforward network having a configuration m - n- o is shown in Figure 3.11.

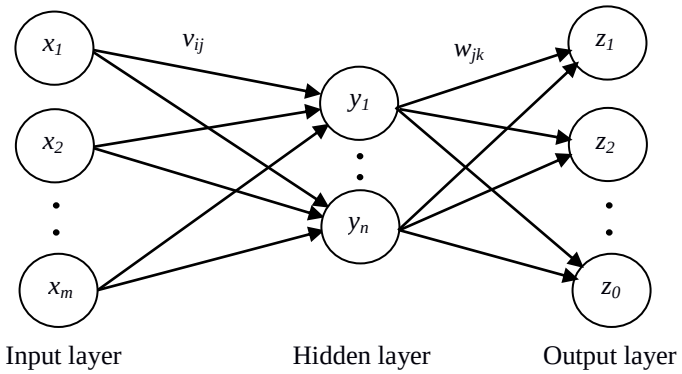

Figure 3.11 A multilayer feedforward network with single hidden layer.

3.5.2.3 Recurrent Network

This network is similar to feedforward network with at least one feedback connection. There can be self-feedback connections with the output of a unit fed backs into it to become an input.

3.5.3 Neural Network Learning Techniques

Learning or *training* is a process in which the synapses weights are adjusted so that the network learns the relationship between the inputs and targets (i.e., the desired output values). Supervised and unsupervised methods are the most popular categories of learning techniques that are being used to find the optimum values for the weights.

3.5.3.1 Supervised Learning

The inputs and the expected outputs are given to the network for its training. In Supervised learning, it is assumed that the learning process is done under the supervision of a teacher. An error signal is derived from the difference between the actual output and the expected output, which helps in finding the optimum weights. Figure 3.12 shows a model of the supervised learning (Hajek, 2005).

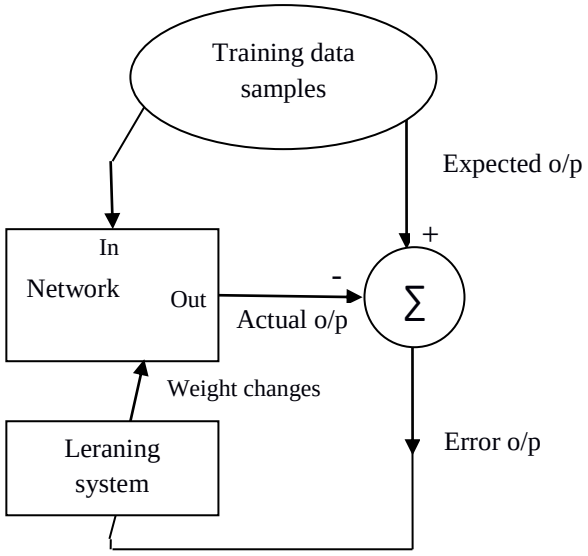

Figure 3.12 Supervised learning model.

3.5.3.2 Unsupervised Learning (Self-Organized Learning)

In this class of learning there is no feedback from the environment. There is no teacher to supervise the learning process, or there are no specific samples of the function to be trained by the network. By discovering and tuning with the structural features in the input patterns, the network does self-learning.

3.5.4 Backpropagation Networks

Backpropagation (BP) is the most common method used for training multilayer feedforward networks having differentiable activation functions. BP (more accurately, Error BP as it is based on error-correction learning rule) algorithm is powerful and efficient in solving difficult problems by training them in a supervised approach. This method was popularized by Rumelhart, Hinton & Williams (1986). Ever since its introduction it has been one of the most studied and utilized algorithms for NNs training and the network using this technique is called a BPNN.

The learning process in most networks is based on an appropriate error function, which is to be minimized with regard to the weights and offset values. For a network with differential activation functions, the derivative of the error with regard to the weights and offset values can easily be found out. By employing the gradient descent or other optimization methods and using these derivatives the weights that minimize the error can be determined. During the learning process the error function propagates in backward direction through the network and hence the name “error backpropagation”.

3.6 Chapter Summary

The main objective of this chapter is to introduce the fundamental theoretical concepts of the materials and tools involved in image compression and gender classification algorithms. The state-of-the-art WT that forms the core of fingerprint image compression and also feature extraction for gender classification were presented in this chapter. The concepts of MRA, subband coding, wavelet LS (which allows faster implementation of WT) were explained.

GA, being the technique used for the optimization of wavelet coefficients and the initial seeds of the classifiers are well discussed. Apart from WT, the other methods such as SVD and PCA used for feature extraction are explored. The chapter finally provides an insight into the well-known NNs as the classifier used for gender classification in this work.

Chapter 4

Fingerprint Image Compression using GA Optimized Wavelet Lifting Coefficients under Quantization: A Multi-Objective Approach

---

This chapter presents the GA evolution of optimized coefficients from the cdf 9/7 wavelet for fingerprint image compression and reconstruction in the context of quantization, exploiting the specific characteristics of fingerprint images. Instead of using cdf 9/7 classical wavelet, its equivalent lifting coefficients are evolved more rapidly using GA. The Fingerprint compression under quantization conditions is a dual-objective problem. It requires the maximization of PSNR and minimization of file size (or maximization of CR) simultaneously. Image IE gives a precise calculation of the compressed file size. Since the computation of IE is very fast when compared to file size calculation, instead of minimizing the file size, the IE is minimized in this work. Thus the computational complexity of fitness evaluation during GA evolution is reduced to a greater extent.

The first few sections of this chapter explain the concepts of cdf 9/7 wavelet LS, its implementation, general idea of optimization of wavelet coefficients, basic concepts of IE, Multi-Objective Optimization (MOO), etc. The succeeding section provides a detailed discussion on optimizing wavelet under quantization for single-level and three-level DWT.

4.1 Introduction

In fingerprints, the ridges appear smoothly organized in a parallel form except in some regions having different shapes distinguished by curvature, ridge terminations, etc. These regions are known as singularities or singular regions, which are generally classified into categories such as loop, delta, and whorl. Based on singularity, almost all fingerprints occupy one of the categories with (i) arch having no singularity (ii) tented arch and loop having one core and one delta and (iii) whorl and double loop having two cores and two deltas (Wei, 2008). The orientation fields (i.e., the ridge flow) of fingerprints have specific characteristics that can distinguish them from other kinds of images (Yoon& Jain,2013). Orientation field for arch, tented arch, left loop, right loop, whorl and double loop type fingerprints are shown Figure 4.1. Figure 4.2 shows the plot when the same program is run on other types of images like natural and texture images. From this, it is confirmed that the fingerprints form a specific class of images having distinct characteristics.

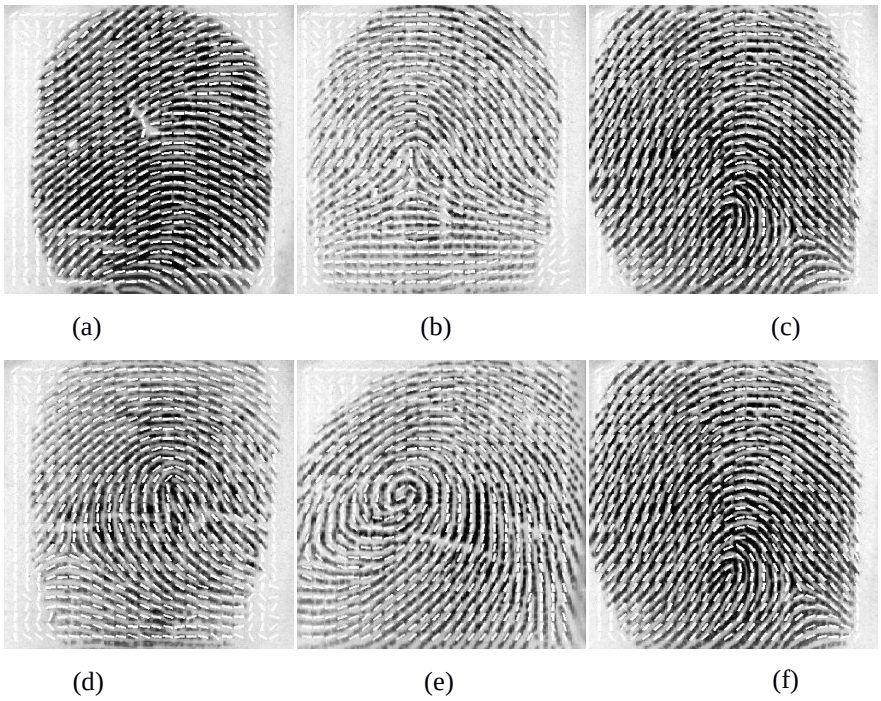

Figure 4.1 Orientation field for (a) arch, (b) tented arch, (c) left loop, (d) right loop, (e) whorl and (f) double loop type fingerprints.

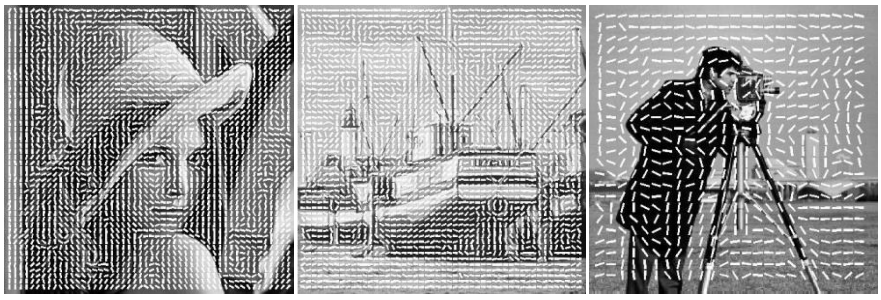

(a)

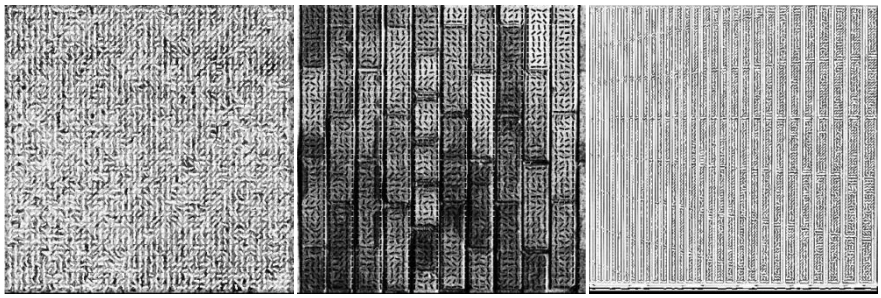

(b)

Figure 4.2 Orientation field for (a) natural images (b) texture images.

For easy archiving of fingerprint images and to overcome the long delay involved in transmitting them over band limited communication channels, the FBI fingerprint identification division has adopted WSQ as standard for Fingerprint Image Compression (FIC) (Maltoni et al., 2009). Wavelet based image compression (Daubechies, 1992; Lewis & Knowles, 1992; Suresh, Sudha & Sukanesh, 2009) is very promising, since it examines the image signal at different resolutions. DWT (Daubechies, 1992) decomposes the original image to horizontal, vertical and diagonal components. Biorthogonal wavelet (Taubman & Marcellin, 2002) has both symmetry and compact support. Many wavelets and techniques have been reported in literature till date (Mallat, 1989a; Daubechies, 1992; Shapiro, 1993; Sweldens, 1996; Said & Pearlman, 1996; Mallat, 1999). The hand-designed classical cdf 9/7 biorthogonal wavelet introduced in 1992 by Cohen, Daubechies, and Feauveau (cdf) (Cohen, Daubechies & Feauveau, 1992) is used by the FBI fingerprint compression

standard (Bradley et al.,1993; Babb, 2007). The classical cdf 9/7 (or Bior 4.4) wavelet is represented by four sets of coefficients as shown below.

Lo_D = [0.03783, -0.02385, -0.11062, 0.37740, 0.85270, 0.37740, -0.11062, -0.02385, 0.03783]

Hi_D = [0.06454, -0.04069, -0.41809, 0.78849, -0.41809, -0.04069, 0.06454]

Lo_R = [-0.06454, -0.04069, 0.41809, 0.78849, 0.41809, -0.04069, -0.06454]

Hi_R = [0.03783, 0.02385, -0.11062, -0.37740, 0.85270,-0.37740, -0.11062, 0.02385, 0.03783]

Here, Lo_D is the low pass decomposition (analysis) filter coefficients, Hi_D, the high pass decomposition (analysis) filter coefficients, Lo_R, the low pass reconstruction (synthesis) filter coefficients and Hi_R is the high pass reconstruction (synthesis) filter coefficients. In fact, the cdf 9/7 classical wavelet is represented by 16 coefficients of Lo_D and Hi_D filter sets. The other filter coefficients sets, Lo_R and Hi_R can be derived from these filter coefficients.

PSNR, RMSE and CR (Annadurai & Shanmughalakshmi, 2007) are the measures of image compression performance used in this work.

4.2 Cdf 9/7 Wavelet LS

The classical Wavelet or Subband transform employed for image compression makes use of two decomposition (analysis) filters: a low pass filter ($\tilde{h}$) and a high pass filter ($\tilde{g}$). These filters decompose the image into low and high frequency data respectively, and subsampling by two is performed subsequently to get the final transformed data. In the reconstruction phase, the transformed data is first upsampled by two, followed by filtering using two reconstruction (synthesis) filters: a low pass (h) and a high pass (g) filter. The upsampling and filtering operations finally provide the reconstructed image.

Figure 4.3 shows the decomposition and reconstruction structures of the DWT. Here s_{j+1} is the original image data, whereas s_j and d_j are the low pass filtered (approximation) coefficients and high pass filtered (detail) coefficients respectively.

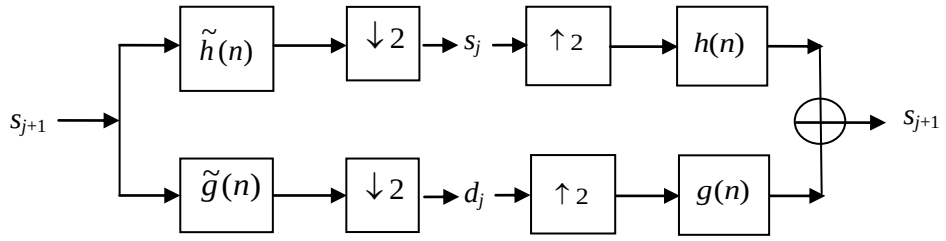

(a) (b)

Figure 4.3 DWT (or subband transform): (a) the forward (decomposition) transform, (b) the inverse (reconstruction) transform.

In the case of classical cdf 9/7, the low-pass forward and inverse transform filters are:

$$\begin{aligned}\tilde{h} = \quad & 0.602949018236 + 0.266864118443\,(Z^1 + Z^{-1}) \\ & - 0.078223266529\,(Z^2 + Z^{-2}) - 0.016864118443\,(Z^3 + Z^{-3}) \\ & + 0.026748757411\,(Z^4 + Z^{-4}) \end{aligned} \tag{4.1}$$

and

$$\begin{aligned} h = \quad & 0.557543526229 + 0.295635881557\,(Z^1 + Z^{-1}) \\ & - 0.028771763114\,(Z^2 + Z^{-2}) - 0.045635881557\,(Z^4 + Z^{-4}) \end{aligned} \tag{4.2}$$

As mentioned earlier, to produce every pair of subband samples using classical cdf 9/7 wavelet, 16 multiplications are needed. This may be cut down to 9 multiplications if the symmetry property of the filter coefficients is taken into consideration. But, the computational complexity in implementing classical cdf 9/7 WT is still high (Taubman & Marcellin, 2002).

4.2.1 Implementation of Cdf 9/7 Wavelet LS

LS (Sweldens, 1996; Daubechies & Sweldens, 1998) is an efficient way to represent hand-designed classical wavelets with fewer coefficients. This was done by

factorizing the polyphase matrix of the wavelet into elementary matrices. LS has particular significance in image compression applications. Many factorizations of cdf 9/7 wavelet do exist. The symmetric LS is used in this work. In symmetric LS, the cdf 9/7 wavelet is represented by just four coefficients. Using LS and lesser number of lifting filter coefficients, the speed with which the image decomposition or reconstruction is performed increases considerably. The four lifting coefficients that represent the cdf 9/7 wavelet are as given below:

$$\begin{aligned} \alpha &= -1.586134342060 \\ \beta &= -0.052980118573 \\ \gamma &= \ \ 0.882911075531 \\ \delta &= \ \ 0.443506852044 \end{aligned} \tag{4.3}$$

with scale factors $K_s = \zeta$ and $K_d = {}^{1}/_{\zeta}$ where ζ = 1.149 604398860. The filters for cdf 9/7 wavelet LS implementation are:

$$\begin{aligned} p_1(z) &= \alpha\left(1+z\right) \\ u_1(z) &= \beta\left(1+z^{-1}\right) \\ p_2(z) &= \gamma\left(1+z\right) \\ u_2(z) &= \delta\left(1+z^{-1}\right) \end{aligned} \tag{4.4}$$

The symmetric factorization of cdf 9/7 wavelet leads to the forward (decomposition) implementation as shown in Figure 4.4. The inverse (reconstruction)

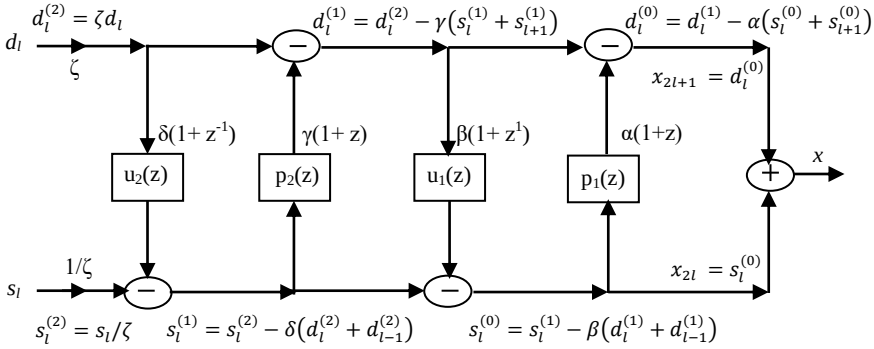

Figure 4.4 Implementation of Cdf 9/7 LS forward transform.

implementation is shown in Figure 4.5 (Barua, Kotteri, Bell & Carletta, 2004; Taubman & Marcellin, 2002; Daubechies & Sweldens, 1998).

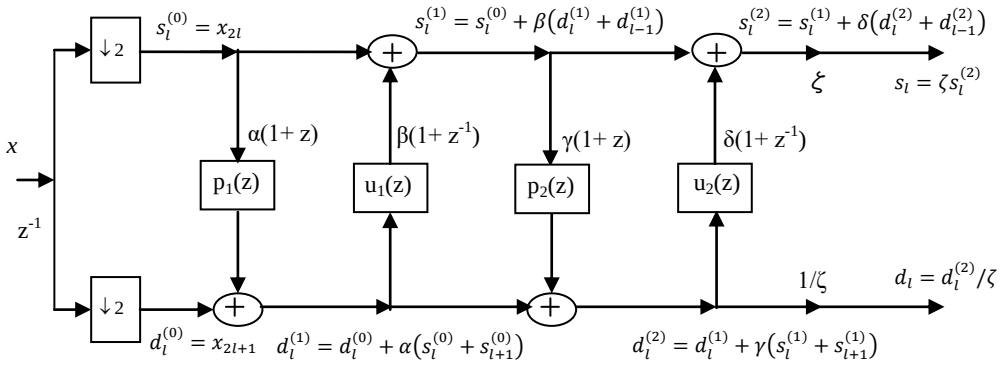

Figure 4.5 Implementation of Cdf 9/7 LS inverse transform.

The lifting steps of cdf 9/7 (with symmetric factorization) with the input data 'x' are:

$$
\begin{aligned}
& s_l^{(0)} = x_{2l} && d_l^{(2)} = \zeta d_l \\
& d_l^{(0)} = x_{2l+1} && s_l^{(2)} = s_l/\zeta \\
& d_l^{(1)} = d_l^{(0)} + \alpha\left(s_l^{(0)} + s_{l+1}^{(0)}\right) && s_l^{(1)} = s_l^{(2)} - \delta\left(d_l^{(2)} + d_{l-1}^{(2)}\right) \\
& s_l^{(1)} = s_l^{(0)} + \beta\left(d_l^{(1)} + d_{l-1}^{(1)}\right) && d_l^{(1)} = d_l^{(2)} - \gamma\left(s_l^{(1)} + s_{l+1}^{(1)}\right) \\
& d_l^{(2)} = d_l^{(1)} + \gamma\left(s_l^{(1)} + s_{l+1}^{(1)}\right) && s_l^{(0)} = s_l^{(1)} - \beta\left(d_l^{(1)} + d_{l-1}^{(1)}\right) \\
& s_l^{(2)} = s_l^{(1)} + \delta\left(d_l^{(2)} + d_{l-1}^{(2)}\right) && d_l^{(0)} = d_l^{(1)} - \alpha\left(s_l^{(0)} + s_{l+1}^{(0)}\right) \\
& s_l = \zeta s_l^{(2)} && x_{2l+1} = d_l^{(0)} \\
& d_l = d_l^{(2)}/\zeta && x_{2l} = s_l^{(0)} \qquad (4.5) \\
& \text{(Decomposition)} && \text{(Reconstruction)}
\end{aligned}
$$

Now, it can be seen that, to produce every pair of subband samples using cdf 9/7 wavelet symmetric LS only 4 multiplications are enough. Thus, the computational complexity is reduced to a great extent, which in turn increases the speed of the image decomposition and reconstruction.

4.3 Optimization of Wavelet Coefficients under Quantization

Works done by a number of researchers to evolve wavelet coefficients for image compression under conditions subject to quantization have been reported over the past few years. In almost all these works, wavelet coefficients similar to classical wavelets, were evolved using GA. They evolved classical wavelet coefficients for image compression using single photographic and satellite images for training. SQ with step sizes, q = 64 and 32 were used in their works. Improvements in PSNR were reported for single-level transform and three-level transform with single set of coefficients and different sets of coefficients for each level. One of the major issues with these works is the computational complexity as the classical wavelets are comprised of large number of coefficients. As the number of coefficients to be optimized becomes more, the time taken for the evolution of the coefficients becomes larger. Due to the computational complexity, the researchers used computers with higher specifications supporting high speed operations in their works. For example, Babb et al. (2007) executed their algorithm on ARSC platforms for evolving wavelet coefficients for image compression.

4.3.1 Optimization of Wavelet Coefficients

Quantization is the procedure where each of the sampled values of signals is mapped against a lesser range of possible values. By quantization the entire data range is divided into equal intervals of length q, known as quantization interval or quantization step size. For example, a quantization step of 16:1 maps an 8-bit signal to a 4-bit binary value. Quantization trims down the precision of each sampled value, but allows more compression on the signal. It causes distortion in images reconstructed by wavelets. This distortion increases in proportion to increase in quantization step size.

Under quantization, quality of the reconstructed image is maintained precisely to a large extent by causing less compression. That is, for higher quality of the reconstructed image, the file size may be higher. This issue is addressed by

incorporating file size into the fitness function for GA evolution. So, image compression and reconstruction under quantization requires the minimization of MSE (or maximization of PSNR) and file size simultaneously. But, the file size calculation is time-consuming. As the population size increases the GA evolution of wavelet coefficients takes more time due the calculation of file size corresponding to each candidate wavelet in the population.

The CR depends on the information content of the image. The compressibility of image and its information content are inversely proportional to each other (Fidler, Skaleric & Likar, 2006). Image IE is a good estimate of the amount of information content available in the image (Khalid, 2006). So, IE gives a precise calculation of the size of the compressed file. Larger compressed files have higher values of IE. Computation of IE is very fast compared to file size calculation. Thus the computational complexity of fitness evaluation during GA evolution could be reduced to a greater extent. This idea has been successfully utilized by Babb et al. (2007) in their work evolving transforms for image compression and reconstruction under quantization using classical cdf 9/7 wavelet.

4.3.2 Information and Entropy

Entropy of the data is the average information content per symbol of the source (Acharya & Tsai, 2005). The concept of entropy was formalized in the original work of Shannon (1948). The entropy is a measure of the average number of bits needed to represent the source output. It also puts a lower bound on the average number of bits needed to code the output. The entropy $H(Y)$ of a discrete random variable Y having k values with probabilities P_j, is defined as

$$H(Y) = -\sum_{j=1}^{k} P_j \ log_2 P_j \tag{4.6}$$

For a gray scale image, P_j contains its histogram counts. For maximum entropy, the image data has maximum information content and hence further compression is not possible without loss of information. Thus, as the entropy reaches its maximum, the image data redundancy approaches to zero.

4.3.3 Multi-Objective Optimization (MOO)

The present work aims at the optimization of cdf 9/7 wavelet coefficients for maximum PSNR value and minimum file size. As discussed in section 4.3.1, in order to minimize the time taken for file size calculation, IE value is computed. So, PSNR and IE qualify as the cost functions for GA evolution of wavelet coefficients. It is obvious that the multi-objectives, PSNR and IE are conflicting. It is not possible to improve PSNR objective, without making the IE objective worse or vice versa. In MOO there are a number of optimal solutions with respect to all solutions. Each solution is not a single point in the fitness landscape, but with a one dimensional vector for each objective (Coley, 1999).

4.3.4 Pareto Optimal Solutions

The set of optimal solutions in a MOO is known as Pareto optimal solutions or non-dominated solutions. Pareto optimal front or Pareto Front (PF) is the set of points that bounds the bottom area of feasible of solutions. PF depicts the tradeoff among PSNR (or MSE) and IE and hence the file size in the solution space of evolved transform coefficients.

GA is an effective tool for solving problems involving MOO. With the use of GA the optimization is known as evolutionary MOO or genetic MOO (Sivanandan & Deepa, 2008). GA works on a whole population of solutions rather than a single solution. It performs multi-directional global searches for solutions. From one generation to the next generation, it retains a population of prospective solutions. Populations with finer sets of potential solutions would be maintained in subsequent generations, which help in the formation of Pareto optimal solutions. Thus, it is straightforward to explore the Pareto optimal set of solutions using GA. A solution is Pareto optimal when it is dominated by no other solutions.

4.3.5 Pareto Optimal Front or Pareto Front (PF)

An MOO problem has a set of solutions. The idea of Pareto optimality states that the solutions corresponding to the multiple objective functions cannot be improved all at

the same time. In MOOs the components of the vector produced by evaluating the set of solutions make compromise in objective space.

Pareto concepts and associated terms are explained by Fonseca and Fleming (1995) and Coello, Lamont and Veldhuizen (2007) as follows:

An MOO solution minimizes the components $f_l,\ l = 1, \cdots\cdots, m$ of a vector function $\boldsymbol{f}(\boldsymbol{x})$ where $\boldsymbol{x}$ is an *m*-dimensional decision vector variable from a universe $\boldsymbol{S}$. Here,

$$\boldsymbol{f}(\boldsymbol{x}) = \left(f_1(\boldsymbol{x}), \cdots\cdots, f_m(\boldsymbol{x})\right) \tag{4.7}$$

Now, a solution $\boldsymbol{x} \in \boldsymbol{S}$ is said to be Pareto-optimal if and only if there is no $\boldsymbol{x}' \in \boldsymbol{S}$ for which $\boldsymbol{v} = \boldsymbol{f}(\boldsymbol{x}') = \left(f_1(\boldsymbol{x}'), \cdots\cdots, f_m(\boldsymbol{x}')\right)$ dominates $\boldsymbol{u} = \boldsymbol{f}(\boldsymbol{x}) = \left(f_1(\boldsymbol{x}), \cdots\cdots, f_m(\boldsymbol{x})\right)$ (*represented as* $\boldsymbol{v} \leq \boldsymbol{u}$).

The family of all Pareto-optimal decision vectors is known as Pareto-optimal (*P*), admissible, or efficient set of the MOO. Collection of the related set of objective vectors forms the non-dominated set, which is known as PF. From the PF a single compromise solution is chosen according to certain preference criteria. In an MOO problem dealing with minimizing functions, the minima will lie in the boundary of the design area.

4.4 Methodology

4.4.1 Structure of the GA for Optimizing Wavelet under Quantization

The algorithm for MOO of wavelet under quantization for fingerprint image compression is given below.

Algorithm:

Step 1: Initialize value of maximum generation, G_{max}.

Step 2: Set the current generation as G_1=1.

Step 3: Initialize population of [α, β, γ, δ], the lifting coefficients as $w_1, w_2, \cdots, w_n$.

Step 4: Obtain the standard training images $I_1, I_2, \cdots, I_n$.

Step 5: *Do wavelet decomposition of* $I_1, I_2, \cdots, I_n$ *with* $w_1, w_2, \cdots, w_n$ *to get wavelet transforms,* $W_1, W_2, \cdots, W_n$.

Step 6: *Do 64:1 quantization on* $W_1, W_2 \cdots, W_n$ *to get quantized transforms,* $Q_1, Q_2 \cdots, Q_n$.

Step7: *Do 64:1 de-quantization on* $Q_1, Q_2 \cdots, Q_n$ *to get quantized transforms,* $W_1^{'}, W_2^{'}, \cdots, W_n^{'}$.

Step 8: *Using* $w_1, w_2, \cdots, w_n$ *do wavelet reconstruction of the images from* $W_1^{'}, W_2^{'}, \cdots, W_n^{'}$ *to get* $I_1^{'}, I_2^{'}, \cdots, I_n^{'}$.

Step 9: *Compare* $I_1, I_2, \cdots, I_n$ *with* $I_1^{'}, I_2^{'}, \cdots, I_n^{'}$ *to get fitness values (PSNR & IE) as* $P_1, P_2, \cdots, P_n$ *and* $e_1, e_2, \cdots, e_n$.

Step 10: *Check for the condition, current generation >* G_{max}.

Step 11: *If no, obtain a new population of lifting coefficients from the fitness values using GA and repeat Steps 5 to 10.*

Step 12: *Else, optimum coefficients = best set of coefficients in the population.*

Step 13: *Stop.*

Figure 4.6 shows the structure of the GA for optimizing wavelet lifting coefficients under conditions subject to quantization. Step size, q for quantization as well as de-quantization is selected as 64. The symmetric lifting scheme of cdf 9/7 wavelet requires the optimization of only four coefficients and hence it ensures faster evolution of the coefficients.

The wavelet decomposition block transforms the training images into the wavelet domain using the initial population of chromosomes comprised of randomly mutated copies of lifting coefficient sets. The transformed coefficients of the training images are subjected to uniform SQ to achieve compression. The wavelet coefficients used for decomposition are utilized for reconstruction as well. The quantization is undone using scalar de-quantization operation. Quality of the reconstructed image/s is measured in terms of PSNR and IE. Both the PSNR and IE provide the fitness functions of the multi-objective GA optimization. The associated chromosomes are ranked according to their fitness. Then, only the best are selected to continue for reproduction. Crossover and mutation operations are performed on the

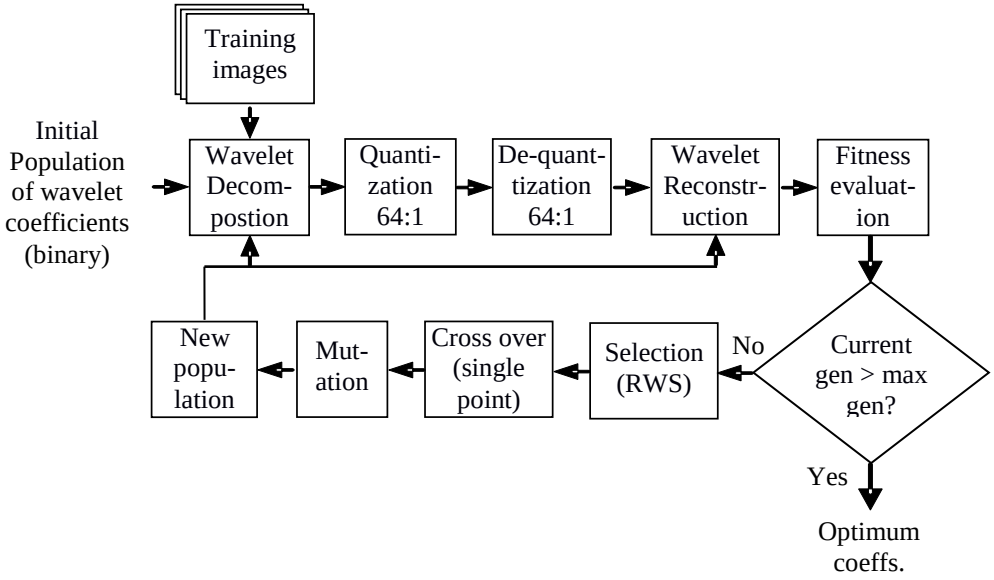

Figure 4.6 Structure of the GA for optimizing wavelet lifting coefficients under quantization.

selected chromosomes to produce new set of chromosomes. The above operations are repeated for several generations with the new populations to obtain a Pareto optimal set of solutions to the optimization problem. The wavelet optimization is performed for single-level and three-level wavelet decompositions.

4.4.1.1 GA Parameters

Each set of 4 lifting coefficients is represented by a 68 bit binary chromosome. Each coefficient has a length of 17 bits, out of which the first bit represents sign and the other 16 bits represent the coefficient value. The P_{size} for GA evolution is fixed as 250 and the number of generations is 1000. The algorithm uses single point crossover. Crossover rate, P_c = 0.7 and mutation rate, P_m = 0.0075. The other parameters are kept as the default values.

4.4.1.2 Image Database for Training and Testing

Fingerprint images from the image set B of the DB1 database in Fingerprint Verification Competition (FVC) 2000 database (Fingerprint Verification Competition, 2000) is used for training and testing in this work. The image set B contains 80 fingerprint images. Each image has a size 300 x 300 pixels and a

resolution of 500 dpi. Images from NIST fingerprint database having 605 x 589 pixels size are also used for testing. Typical fingerprint images from these image sets are shown in Figure 4.7.

(a) (b)

Figure 4.7 Typical fingerprint images (a) DB1_B of FVC2000 (300 x 300 pixels), (b) NIST (605 x 589 pixels).

4.5 Results and Discussion

4.5.1 Wavelet Optimization for Single-Level MRA with Single Training Image

With a single training image 101_1.tif of database DB1_B of FVC 2000 and choosing quantization step size, q = 64, the optimized coefficients evolved for single-level MRA offered improvements in PSNR and percentage IE compared to classical cdf 9/7 wavelet. The optimized coefficients evolved are given below in Table 4.1.

Figure 4.8 shows the 101_1.tif image reconstructed using the classical as well as the optimized wavelets. The improvements in average PSNR over 80 fingerprint images of DB1_B database using the same optimized coefficients for various quantization levels are shown in Table 4.2. For q = 128 and 64 the average PSNR using optimized wavelet is far better than that obtained with classical wavelet. For q = 32, increase in percentage IE is too large (i.e., 1.3672%). Hence the value of PSNR (i.e., 0.852 dB) improvement is not realistic. It has been

observed that this is due to the use of a single representative image for training and more realistic results can be obtained using multiple training images.

Table 4.1 Optimized coefficients evolved for the multi-objective problem (with q = 64, single-level decomposition, single training image).

Optimized lifting coefficients	
Notation	**Value**
α	- 0.055197483503182
β	0.578897678639738
γ	- 0.219117379643640
δ	0.209552907878616

(a) (b)

Figure 4.8 101_1.tif image reconstructed (with single-level, single training image, q = 64) using (a) classical (PSNR = 28.7516 dB, IE = 0.8114) , and (b) optimized (PSNR = 31.9427 dB, IE = 0.8117) wavelets.

Table 4.2 Improvement in average PSNR and % IE (with q = 64, single-level decomposition, single training image).

Test Image	**q**	**Level**	**Classical**		**Optimized**		**% Increase in IE**	**PSNR Improvement**
			PSNR	**IE**	**PSNR**	**IE**		
DB1_B (80 Images)	128	1	22.1387	0.8113	27.6912	0.8113	**0**	**5.5525**
	64	1	28.7063	0.8113	32.0038	0.8116	**0.0370**	**3.2975**
	32	1	33.9074	0.8119	34.7598	0.8230	**1.3672**	**0.8524**

4.5.2 Wavelet Optimization for Single-Level MRA with Four Training Images

The optimized coefficients evolved for single-level DWT with q = 64 and four training images (i.e., 101_1.tif, 102_1.tif, 103_1.tif and 104_1.tif) are listed in Table 4.3.

Table 4.3 Optimized coefficients evolved for the multi-objective problem (with q = 64, single-level MRA, four training images).

Optimized lifting coefficients	
Notation	**Value**
α	- 0.094490422
β	0.668710181
γ	- 0.194919819
δ	- 0.327635548

Average improvements in PSNR using optimized coefficients for single-level MRA with four training images and q = 64 are shown in Table 4.4. With four images in the training set, the algorithm provided better results. The 101_1.tif image reconstructed using the classical and the optimized wavelets are shown in Figure 4.9.

It can be observed from Table 4.4 that for q = 128 and 64 the average PSNR using optimized WTs the classical wavelet and the result is better when compared to the single training image case. As in the previous case when q = 32, there is little improvement in PSNR. Babb et al. (2009a) reported that at 64:1 quantization, the evolved transform reduced the average PSNR in reconstructed fingerprints by 3.00 dB in comparison to cdf 9/7, allowing 4.36% increase in the average IE of compressed images. In this work, the evolved transform reduced the average PSNR by 3.4058 dB in comparison to the classical cdf 9/7 wavelet, while the percentage increase in the average IE of compressed images is only 0.0315%, which is close to zero. This result is much better than the previous results. The evolved coefficients tender improvements in PSNR for quantization levels 128 and 32 too. The PSNRs offered by coefficients evolved at q = 64 are poor at quantization levels below 32.

(a) (b)

Figure 4.9 101_1.tif image reconstructed (with single-level, four training images, q = 64) using (a) classical (PSNR = 28.7516 dB, IE = 0.8114) , and (b) optimized (PSNR = 32.0488 dB, IE = 0.8116) wavelets.

Table 4.4 Improvement in average PSNR and % IE (with q = 64, single-level decomposition, four training images).

Test Image	**q**	**Level**	**Classical**		**Optimized**		**% Incr-ease in IE**	**PSNR Impro-vement**
			PSNR	**IE**	**PSNR**	**IE**		
DB1_B (80 Images)	128	1	22.1387	0.8113	27.9735	0.8113	**0**	**5.8348**
	64	1	28.7063	0.8113	32.1121	0.8116	**0.0315**	**3.4058**
	32	1	33.9074	0.8119	34.8361	0.8214	**1.1701**	**0.9287**

Figure 4.10 shows the error images obtained by taking the difference between the original fingerprint and the resultant image, after compression and reconstruction by the classical 9/7 wavelet and the optimized coefficients for single-level under q = 64. It compares and discloses the extent to which the evolved transform surpasses the classical wavelet. The error images were built from the absolute value of the difference among the grey-scale intensity value of each pixel from the original and the reconstructed images, making all values less than 10 to zero to have an easier view of the differences. The evolved coefficients are unacceptable as they provide unsatisfactory results for higher-level MRAs, for example, PSNR and IE obtained for three-level MRA are 30.94 dB and 0.3582 respectively. So, in the subsequent work, it has been attempted to optimize wavelets for three-level MRA.

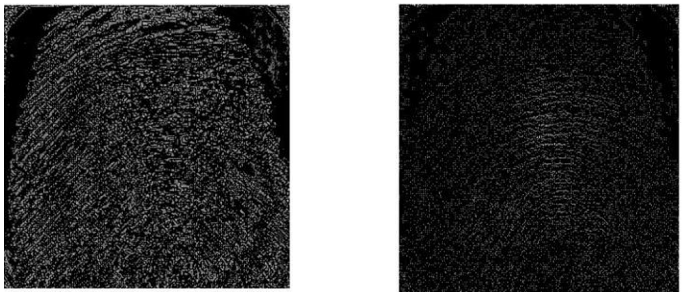

(a) (b)

Figure 4.10 Error images showing the difference between the original fingerprint and the resultant image after compression and reconstruction for single-level, q = 64 by (a) classical 9/7 wavelet and (b) optimized coefficients.

4.5.3 Wavelet Optimization for Three-Level MRA

In this work, lifting coefficients of cdf 9/7 wavelet was optimized for three-level MRA using multiple numbers of training images. The GA evolved coefficients are shown in Table 4.5. The average PSNR improvement for fingerprints for three-level transform, reported in the previous work (Babb et al., 2009b), is less than 0.54 dB. In the proposed work with three training images, an average PSNR improvement of 2.0810 dB was obtained along with 23.6152% increment in IE compared to the classical wavelet. This large value of IE means that the images compressed by

Table 4.5 Optimized coefficients evolved for the multi-objective problem (with q = 64, three-level MRA, three training images).

Optimized lifting coefficients	
Notation	**Value**
α	- 0.792932335
β	- 0.635398005
γ	0.167903023
δ	1.479168923

optimized wavelet are of larger size and hence the CR provided by the optimized wavelet is poorer when compared to the classical wavelet. This makes the comparison between the optimized and classical wavelets difficult. In order to have a fair

comparison a Pareto optimal front was constructed from PSNR and percentage IE values.

Figure 4.11 shows the PF obtained for three-level MRA with three fingerprint images subject to quantization step size, q = 64. Table 4.6 shows the results corresponding to two best solutions (points) in the Pareto front. The first solution corresponds to 0.81 dB improvement in PSNR at the expense of a small increment of 0.1% in IE (i.e., by compromising CR). The second solution corresponds to decrease

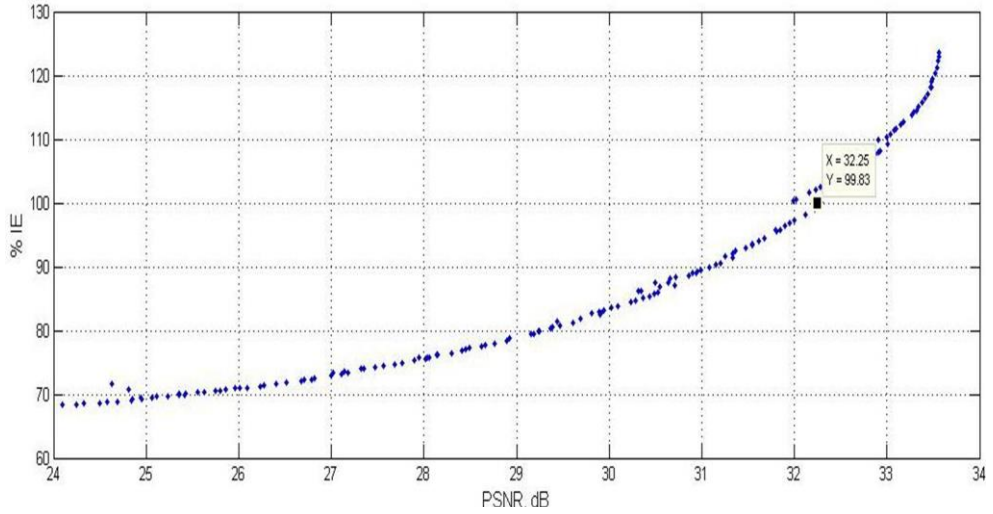

Figure 4.11 Pareto optimal front for average PSNR for three-level transform subject to q = 64.

Table 4.6 Improvement in average PSNR over 80 fingerprint images.

Image set	**q**	**Level**	**PSNR (dB)**		**% increase in IE**	**PSNR (dB) Impro-vement**
			Classical	**Evolved**		
DB1_B (80 Images)	64	3	31.48	32.29	**0.1**	**0.81**
			31.48	32.25	**- 0.19**	**0.77**

in IE by 0.19%, giving better CR and improvement of 0.77 dB in PSNR. This confirms that the oiptimized coefficients perform better than the classical wavelet.

Table 4.7 shows the coefficients evolved corresponding to 0.77 dB PSNR improvement that has been mentioned in Table 4.6. Figure 4.12 shows the fingerprint

image 101_1.tif after three-level transform, quantized with a quantization step size, q = 64, de-quantized, and reconstructed by classical cdf 9/7 wavelet and evolved coefficients.

Table 4.7 Optimized coefficients evolved for the multi-objective problem (with q = 64, three-level MRA, three training images) corresponding to the results in Table 4.6.

Optimized lifting coefficients	
Notation	**Value**
α	- 0.649805356
β	- 0.633952891
γ	0.106524991
δ	1.261697919

(a) (b)

Figure 4.12 101_1.tif image reconstructed (with three-level MRA, three training images, q = 64) using (a) classical (PSNR = 31.6369 dB, IE = 0.2082) , and (b) optimized (PSNR = 32.1426 dB, IE = 0.2150) coefficients.

Table 4.8 shows the improvement in average PSNR using the optimized coefficients for various quantization levels. Even with reduced percentage IE and hence reduced file size, the evolved coefficients outperformed the classical wavelet for various quantization levels. No improvement in PSNR was seen below quantization level 32.

Figure 4.13 shows the difference between the original fingerprint and the corresponding image after compression and reconstruction by the classical 9/7 wavelet and the evolved coefficients for three-level transform under q = 64.

Table 4.8 Improvement in average PSNR over 80 fingerprint images using coefficients evolved for three-level transform with three fingerprint images subject to quantization size = 64.

Test Image	q	Level	Classical		Optimized		% Increase in IE	PSNR Improvement
			PSNR	IE	PSNR	IE		
DB1_B (80 Images)	128	3	27.8499	0.1659	29.0125	0.1555	**- 6.2688**	**1.1626**
	64	3	31.4812	0.2058	32.2530	0.2054	**- 0.1944**	**0.7718**
	32	3	35.1451	0.2753	35.2948	0.2709	**- 1.5983**	**0.1497**

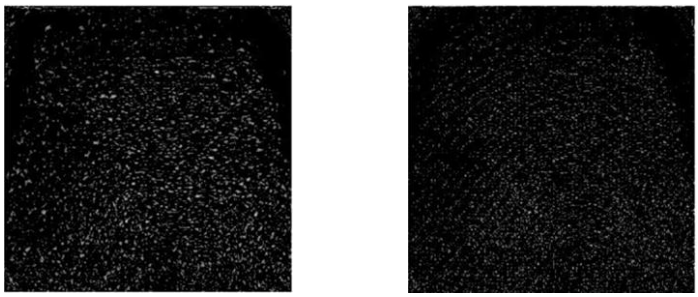

(a) (b)

Figure 4.13 Difference between the original fingerprint and the resultant image after compression and reconstruction for three-level transform under q = 64 by (a) classical 9/7 wavelet, and (b) evolved coefficients.

Emmanuel et al. (2014) explained techniques that used a fingerprint test suit of 30 images from NIST database, giving an average PSNR of 27.36 dB, whereas the optimized wavelets in the present work offered a better average PSNR of 27.4 dB. Table 4.9 shows the comparison of PSNRs at CR = 20:1 for NIST database. Comparison of the results with the previous works is shown in Table 4.10.

4.6 Chapter Summary

The orientation field of fingerprints has specific characteristics that differentiate the fingerprint images from other kinds of images such as natural, texture, photographic and other types of images. So, the fingerprint images can be treated as a specific class of images having distinct characteristics. This chapter dealt with a GA based evolution method developed for optimizing the cdf 9/7 wavelet

Table 4.9 PSNR values obtained for CR = 20:1.

Source Images	Size of original image	Size of quantized image	PSNR (dB)	
			Emmanuel *et al.* (2014)	Proposed method
Cmp00001.pgm	356360	17818	22.9	22.96
Cmp00002.pgm	638991	31949	29.1	28.53
Cmp00003.pgm	638991	31949	32.9	34.33
Cmp00004.pgm	612895	30645	33.3	33.47
Cmp00005.pgm	638991	31949	35.5	34.03
Cmp00006.pgm	638991	31949	28	27.45
Cmp00007.pgm	347725	17386	25.6	25.17
Cmp00008.pgm	600015	30001	28.8	29.58
Cmp00009.pgm	347151	17358	25.1	25.99
Cmp00010.pgm	197265	9863	25.4	26.33
Cmp00011.pgm	440253	22012	25.4	25.41
Cmp00012.pgm	369471	18473	24.9	25.03
Cmp00013.pgm	350904	17545	24.9	26.58
Cmp00014.pgm	269363	13468	25.7	27.75
Cmp00015.pgm	292135	14606	30.4	32.53
Cmp00016.pgm	504843	25242	31.7	31.83
Cmp00017.pgm	347001	17350	26	26.55
a001.pgm	1520081	76004	27.1	26.62
a002.pgm	1460729	73036	25.5	24.95
a018.pgm	1534580	76729	30.1	29.44
a039.pgm	458175	22908	24.9	24.37
a070.pgm	1605297	80264	26.5	26.03
a076.pgm	612848	30642	27.6	27.1
a089.pgm	1574914	78745	24.1	23.38
a107.pgm	1862081	93104	27.1	26.73
a129.pgm	365777	18288	27.1	26.61
a165.pgm	387047	19352	26.3	25.92
b124.pgm	1510456	75522	25.5	25.06
b157.pgm	1572731	78636	26.3	25.68
b186.pgm	371349	18567	27.1	26.57
Average PSNR			**27.36**	**27.40**

coefficients for fingerprint compression and reconstruction in the context of quantization. The GA based technique utilizes the specific characteristics of fingerprint images that make them belong to a particular class. The techniques used in

Table 4.10 Comparison of the results with the previous works (test image: fingerprints).

Reference	**Evolutionary Algorithm**	**Conditions**	**Training Image**	**MSE reduction %**	**PSNR improve-ment (dB)**
Aldridge, et. al (2010)	GA	Single-level MRA 64:1 Quantizn.	Fingerprint images	12.36	-
Proposed work	GA	Single-level MRA 64:1 Quantizn.	Fingerprint images	21.12	1.02
Babb, et. al (2009b)	CMA-ES	Three-level MRA 64:1 Quantizn.	Satellite images	-	0.54
Proposed work	GA	Three-level MRA 64:1 Quantizn.	Fingerprint images	-	0.77

the previous works in literature for optimizing wavelet coefficients for image compression in the context of quantization were computationally complex and hence slow. The amount of time consumption in evolving coefficients, similar to symmetric lifting coefficients of cdf 9/7 wavelet, was reduced and the optimum values of coefficients were obtained.

Image compression and reconstruction under quantization necessitates the simultaneous minimization of MSE (or maximization of PSNR) and file size. It has been established that the image IE provides a precise calculation of the size of the compressed file. Since the computation of IE is very fast when compared to file size calculation, the MOO algorithm employs two conflicting objectives, PSNR and IE. The optimization demands high PSNR with low IE value for the compressed image.

In the work proposed in this chapter, initially the process of wavelet optimization was done for a single-level DWT with a single training image and a quantization step size, q = 64. An average PSNR improvement of 3.2975 dB (with only 0.0370% increment in IE) over the 80 fingerprint images in the DB1_B of FVC 2000 database was obtained, which is better than that offered by the previous work. Secondly, four training images were used with single-level transform and q = 64. The results (3.4058 dB PSNR and 0.0315% IE increments) are much promising as the

optimized coefficients gave better performance than the one using single training image. Finally, optimization was done for three-level MRA that outperformed the previous work, offering 0.7718 dB PSNR increment with 0.1944% decrease in IE. These optimized wavelets offered a better average PSNR over Coiflet wavelet based compression, employing NIST fingerprint database.

Chapter 5

Optimization of Wavelet Filter Coefficients for Fingerprint Image Compression using GA: A Single-Objective Approach

In the dual-objective problem discussed in the previous chapter the PSNR and the IE were conflicting, i.e., when the PSNR was improved, the IE also increased. An exact measure of the improvement in the PSNR could be obtained only if the IE can be kept unchanged. So, the proposed work in this chapter concentrates on evolving optimized coefficients from the lifting coefficients of cdf 9/7 wavelet at CR = 16:1 using PSNR as the single-objective of GA. Optimized coefficients are evolved for various levels of MRA using single and multiple training images. In addition, techniques have been presented for the optimization of wavelet lifting coefficients for faster and better fingerprint image compression. Generally, full-size images are being used for evolving wavelet coefficients, which is time consuming. To overcome this, in this work, wavelets are optimized with resized, cropped, resized-average and cropped-average images to give better PSNR at various CRs. It is shown that there is improvement in PSNR even in the case of degraded as well as noisy fingerprint images. The technique also gives better PSNR for various bit rates with SPIHT coder. The coefficients optimized with single-objective approach give better average PSNR and IE even under quantization conditions as discussed in the previous chapter. These coefficients perform well with other fingerprint databases as well.

5.1 Introduction

The dual-objective approach to optimize wavelet coefficients for fingerprint image compression under quantization provided a set of solutions. The task intended was to improve the PSNR of the compressed image along with reduction in IE or at least keeping a constant IE to maintain a constant CR. PSNR and IE are two conflicting objectives, i.e., when the PSNR was improved the IE (a measure of file size) was also increased. In this MOO problem, keeping IE constant was a difficult task. So, due to the conflicting nature of the two measures a compromise between them should be agreed upon. An exact measure of the improvement in PSNR could be possible only if the file size and hence IE is kept unchanged or the CR is maintained to a constant value. As a result, the exact evaluation and understanding on the change in the image quality after compression is difficult in the dual-objective approach described in the previous chapter.

The CR of the compressed image can be held constant (i.e., k:1) by employing a common technique in wavelet based image processing by retaining the largest 1/k transformed image coefficients and making the remaining values zero. This technique has been used by a few researchers in their related works (Grasemann & Mikkulainen, 2005; Babb, 2007). Another advantage of employing this technique is that by retaining only a small fraction of transformed coefficients, the computational complexity in evolving optimized wavelet coefficients could be reduced considerably.

For general compression purposes, the coefficients optimized for single-level through four-level MRAs using single training images are not suitable. This problem can be tackled by using multiple training images in GA evolution. The complexity of the EA is another issue of great concern. Due to the huge amount of computational complexity involved, Babb (2007) used even supercomputers for evolving optimized coefficients for fingerprint image compression. The size of the training images can do something in this context. Generally, full-size multiple images are being used for evolving wavelet coefficients, which is time consuming. To overcome this, in this

work, wavelet coefficient optimization has been tried with resized, cropped, resized-average and cropped-average images and compared.

5.2 Methodology

In this work the largest 6.25% (i.e., $1/k^{th}$, where k = 16) of the transformed image coefficients are retained and the remaining values are set to zero to have a CR = 16:1. This provides the possibility for maximum comparability of the test results with the results of other published works where 16:1 ratio has been used. The structure of the GA for optimizing wavelet by this technique is similar to the structure presented in chapter 4 with a few modifications.

5.2.1 The Single-Objective GA Structure for Optimizing Wavelet

The algorithm for single-objective optimization of wavelet coefficients for fingerprint image compression is given below.

Algorithm:

Step 1: Initialize value of maximum generation, G_{max}.

Step 2: Set the current generation as G_1=1.

Step 3: Initialize population of [α, β, γ, δ], the lifting coefficients as $w_1, w_2, \cdots, w_n$.

Step 4: Obtain the standard training images $I_1, I_2, \cdots, I_n$.

Step 5: Do wavelet decomposition of $I_1, I_2, \cdots, I_n$ with $w_1, w_2, \cdots, w_n$ to get wavelet transforms, $W_1, W_2, \cdots, W_n$.

Step 6: Discard smallest 93.75% of $W_1, W_2 \cdots, W_n$ coefficients to get thresholded transforms, $T_1, T_2 \cdots, T_n$.

Step 7: Using $w_1, w_2, \cdots, w_n$ do wavelet reconstruction of the images from $T_1, T_2 \cdots, T_n$ to get $I_1', I_2', \cdots, I_n'$.

Step 8: Compare $I_1, I_2, \cdots, I_n$ with $I_1', I_2', \cdots, I_n'$ to get fitness values (PSNR) as $P_1, P_2, \cdots, P_n$.

Step 9: Check for the condition, current generation > G_{max}.

Step 10: If no, obtain a new population of lifting coefficients from the fitness values using GA and repeat Steps 5 to 9.

Step 11: Else, optimum coefficients = best set of coefficients in the population.
Step 12: Stop

The block diagram of a single-objective GA structure that uses only the largest 6.25% of the image transform samples for optimizing cdf 9/7 wavelet coefficients for fingerprint image compression is shown in Figure 5.1.

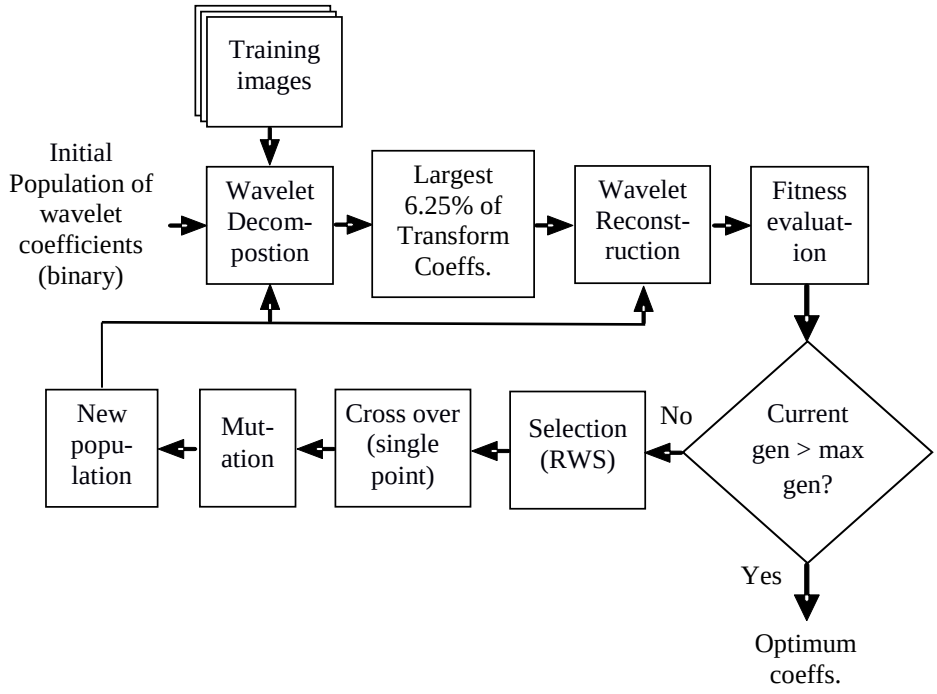

Figure 5.1 Block diagram of the single-objective GA for optimizing cdf9/7 lifting coefficients for fingerprint image compression.

As in the case of dual-objective optimization problem discussed in the earlier chapter, the wavelet decomposition block decomposes the training images into transform coefficients using the initial population of chromosomes generated by randomly mutating the copies of cdf 9/7 lifting coefficients. Generating initial population in this way enables the GA to search around the solution space containing the original lifting coefficients so that early convergence of the search process is possible. In the first generation of GA, the input image is decomposed using each coefficient in the initial population, giving same number of transform coefficients as

that of the original image. In the next stage, 6.25% of the most significant transform coefficients are retained and the remaining coefficients are set to zero. For this, firstly, the transform coefficients are ordered according to their significance (i.e., magnitude) in descending fashion. Then the first 6.25% of the ordered transform coefficients are kept as such and the rest are discarded. Finally, the retained transform coefficients are placed in their original positions. Then, in the resultant transformed image the retained significant transform coefficients occupy their original place with zero valued coefficients elsewhere. This operation is known as "thresholding" in the literature (Aldridge, Babb, Moore & Peterson, 2010).

In the next stage, the transformed image after thresholding, is subjected to wavelet reconstruction, using the same lifting coefficients that were used for the decomposition. The PSNR, being the performance measure of compression, is evaluated next and this forms the fitness function for GA evolution. The GA operators, such as selection, crossover, mutation and elitism are applied on the initial population of the chromosomes that represent the lifting coefficients and based on the fitness function a new and better population of chromosomes is created. This new population of chromosomes is used in the next generation of GA. The whole process is repeated till the current generation becomes equal to the maximum generation, whose value is set to a particular value depending upon the specific optimization problem at hand.

In the single-objective optimization problem described here, both single and multilevel WTs with single and multiple training images using the optimized lifting coefficients in each case are carried out and their performance is compared with that of the corresponding classical wavelets. The algorithm is run several times to get the best results in each case.

5.2.1.1 GA Parameters

As in the case of the dual-objective optimization, the algorithm proposed in this chapter also uses binary GA, parameters such as $P_c = 0.7$, $P_m = 0.0075$, roulette wheel selection, single-point crossover and the same chromosome structure already

discussed in chapter 4. P_{size} and number of generations vary for different works described in the coming sections.

5.2.1.2 Fingerprint Database

For training purpose, fingerprint images from the database DB1_B of FVC 2000 are used. There are 80 images each having a size of 300 x 300 pixels. The images from this database are used for testing too. Fingerprint images from databases DB2_B (80 images of size: 364 x 256 pixels), DB3_B (80 images of size: 478 x 448 pixels), DB4_B (80 images of size: 320 x 240 pixels) and images collected using NITGEN USB Fingkey Hamster (HFDU 01) fingerprint scanner (200 images of size: 292 x 248 pixels) also are used for testing purpose.

5.3 Results and Discussion

5.3.1 Optimization for Single-Level MRA using Single Training Image

Optimized wavelet coefficients from cdf 9/7 lifting filter coefficients for single-level MRA and a single training image for fingerprint image compression are evolved using GA. As mentioned earlier, the CR is fixed at 16:1, which means out of 90000 transform coefficients 84375 coefficients of less significance are discarded and the remaining 5625 transform coefficients retained. The image 101_1.tif (300 x 300 pixels) of DB1_B database is used for evolving the coefficients. P_{size} and number of generations are chosen as 50 and 200 respectively. Table 5.1 shows the optimized values of the coefficients obtained after many runs of the algorithm.

Table 5.1 Optimized coefficients evolved using a single training image for single-level transform.

Optimized lifting coefficients	
Notation	**Value**
α	- 0.3436
β	- 1.9621
γ	0.4935
δ	- 1.1299

The average PSNR improvements over 80 images of DB1_B database for different levels of MRA at CR = 16:1 are given in Table 5.2, which show that the optimized coefficients, evolved using single-level transform, degrade PSNRs when used for higher level transforms. Therefore, these optimized coefficients cannot be used in general. Moreover, the PSNR with classical wavelet coefficients for five levels is less than or equal to that for four levels. So, transformation up to four levels is sufficient.

Table 5.2 The average PSNR over 80 images of DB1_B database for different levels of transform at CR = 16:1 (using coefficients evolved by single-level transform).

Test image	**Level**	**PSNR (dB)**		**PSNR improvement (dB)**
		Classical	**Evolved**	
DB1_B (80 images of size: 300 x 300 pixels)	1	3.8266	6.7749	2.9483
	4	35.9119	- 30.6301	Nil
	5	35.8677	- 37.9602	Nil

Figure 5.2 provides a visual comparison of the difference between the original fingerprint and the resultant image after compression and reconstruction for single-level with CR = 6:1 using classical 9/7 wavelet and optimized coefficients . It shows that the error in the reconstructed image is less with optimized coefficients.

(a) (b)

Figure 5.2 Difference between the original fingerprint and the resultant image after compression and reconstruction for single-level (with CR = 6:1)
(a) classical 9/7 wavelet, and (b) optimized coefficients.

5.3.2 Optimization for Two-Level MRA using Single Training Image

It has been noted that for proper convergence of the algorithm at higher MRA levels, the P_{size} and the number of generations should be increased. P_{size} and number of generations are taken as 100 and 500 respectively. The values of the optimized coefficients obtained after many runs of the algorithm are shown in Table 5.3.

Table 5.3 Optimized coefficients evolved using a single training image for two-level MRA.

Optimized lifting coefficients	
Notation	**Value**
α	- 1.724539933
β	- 0.113406781
γ	0.787377544
δ	0.705374310

The average PSNR over 80 images of DB1_B database for different levels of transform depicted in Table 5.4 reveals that the optimized coefficients, evolved using two-level transform, provide improved PSNRs, compared to single-level coefficients when used for higher level transforms. However, as there is no improvement for single-level, the coefficients are generally not acceptable.

Table 5.4 The average PSNR over 80 images of DB1_B database for different levels of transform at CR = 16:1 (using coefficients evolved by two-level transform).

Image database	**level**	**PSNR (dB)**		
		Classical	**Evolved**	**Improvement**
DB1_B (80 images of size: 300 x 300 pixels)	1	3.8266	3.6499	Nil
	4	35.9119	36.4414	0.5295

The reconstructed images after two-level transform are shown in Figure 5.3. The error images, showing the difference between the original fingerprint and the resultant image after compression and reconstruction for two-level using classical wavelet and optimized coefficients, vide Figure 5.4, prove that the optimized coefficients reconstruct the image with less error than the classical wavelet.

(a) (b)

Figure 5.3 Reconstructed images after two-level transforms using (a) classical PSNR = 16.9083 dB) (b) optimized coefficients (PSNR = 33.7334 dB), at CR = 16:1.

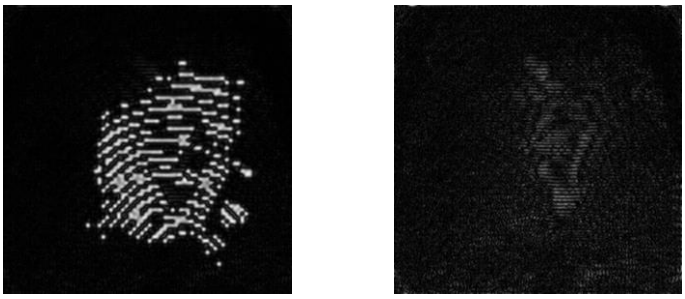

(a) (b)

Figure 5.4 Error image for two-level transform (with CR = 6:1) using (a) classical 9/7 wavelet, and (b) optimized coefficients.

5.3.3 Optimization for Three-Level MRA using Single Training Image

Since three-level transform is used in this experiment, it requires a large population size and generations to ensure proper convergence of the algorithm. P_{size} and number of generations are chosen as 150 and 800 respectively. After several runs of the algorithm, the values of the optimized coefficients obtained are shown in Table 5.5. Table 5.6 depicts the average PSNR over 80 images of DB1_B database for other levels of transforms. It tells that the optimized coefficients evolved using three-level transforms provide better PSNRs compared to two-level coefficients when used for higher level transforms. But, the PSNR obtained with optimized coefficients for single-level MRA is still below that obtained with classical wavelet. So, the optimized coefficients are generally not acceptable.

Table 5.5 Optimized coefficients evolved using a single training image for three-level transform.

Optimized lifting coefficients	
Notation	**Value**
α	- 1.561326944792020
β	- 0.101870784630879
γ	0.741142002624592
δ	0.641163365581225

Table 5.6 The average PSNR over 80 images of DB1_B database for different levels of transform at CR = 16:1 (using coefficients evolved by three-level transform).

Test Image	**level**	**PSNR (dB)**		
		Classical	**Evolved**	**Improvement**
DB1_B (80 images of size: 300 x 300 pixels)	1	3.8266	3.7968	Nil
	4	35.9119	36.7001	0.7882

Figure 5.5 shows the reconstructed images after three-level transform. The error images for compression with three-level transform using classical wavelet and optimized coefficients shown in Figure 5.6 verify that the optimized coefficients reconstruct the image with better PSNR than the classical wavelet.

(a) Classical, CR=16:1, PSNR=35.6781 dB

(b) Evolved, CR=16:1, PSNR=36.7027 dB

Figure 5.5 Reconstructed images after three-level transforms using (a) classical (b) optimized coefficients, at CR = 16:1.

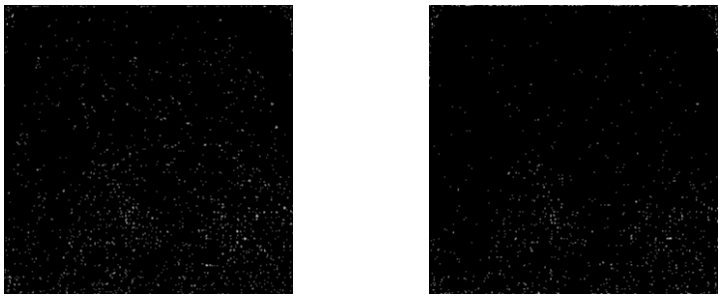

(a) (b)

Figure 5.6 Error image for three-level transform (with CR = 6:1) using (a) classical 9/7 wavelet, and (b) optimized coefficients.

5.3.4 Optimization for Four-Level MRA using Single Training Image

P_{size} and number of generations used in the optimization for four-level MRA are 150 and 1000 respectively. Table 5.7 depicts the values of the optimized coefficients obtained. The average PSNR over 80 images of DB1_B database for other levels of transforms are depicted in Table 5.8. It says that the optimized coefficients, evolved for four-level MRA, offer better PSNRs compared to four-level coefficients. However, still it exhibit degradation in PSNR for single-level. Figure 5.7 shows the compressed images reconstructed after four-level transform. Figure 5.8 displays the corresponding error images using classical wavelet and optimized coefficients.

Table 5.7 Optimized coefficients evolved using a single training image for four-level MRA.

Optimized lifting coefficients	
Notation	**Value**
α	- 1.69194616534928
β	- 0.08127079073458
γ	0.859309671315653
δ	0.593218787194433

All the experiments previously discussed in this chapter use single image for training the GA. The coefficients evolved for four-level transform provide the best average PSNR for the reconstructed images in the database. The same evolved

(a) Classical, CR = 16:1, PSNR = 35.9082 dB

(b) Evolved, CR = 16:1, PSNR = 36.9561 dB

Figure 5.7 Reconstructed images after four-level transforms using (a) classical (b) optimized coefficients, at CR = 16:1

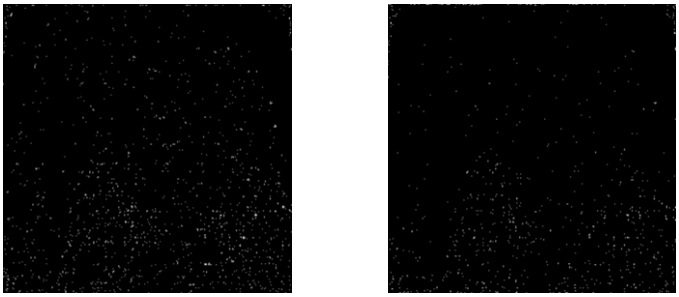

(a) (b)

Figure 5.8 Error image for four-level transform (with CR = 6:1) using (a) classical 9/7 wavelet, and (b) optimized coefficients.

coefficients exhibit degradation in PSNR for single-level. This means that the above optimized coefficients are poorer than classical wavelets, at least for single-level transform. So, they cannot have a general acceptance in compressing fingerprint images.

5.4 Optimization for Four-Level MRA using Multiple Training Images

5.4.1 Parameters

In order to have a fair comparison, the parameters used in the previous works are used in this work too. The group of 4 lifting coefficients is represented by a 68 bit

binary chromosome with each coefficient having a length of 17 bits, out of which the first bit represents sign and the other 16 bits for the coefficient value. The initial GA population is created by randomly mutated copies of the symmetrical lifting coefficients of cdf 9/7 wavelet. The P_{size} for GA evolution is fixed as 250 and the number of generations is 1000. Roulette wheel selection, single point crossover with crossover rate P_c = 0.7, mutation rate P_m = 0.0075 and elitism = 1 are used in the algorithm.

5.4.2 Development of an Optimum Training Image Set

The training image data set is derived from the image set B of the DB1 dataset in FVC2000 gray scale fingerprint database. Each image has a size 300 x 300 pixels and a resolution of 500 dpi. A typical fingerprint image was shown in Figure 4.7(a) of chapter 4. In the earlier work (Grasemann & Mikkulainen,2005; Babb, 2007) training image set was comprised of four numbers of full size (300 x 300 pixels) representative fingerprint images. In the proposed work, to start with, a Training Image Set (TIS) with only one image of full size (300 x 300 pixels) was used for GA evolution. Images were added in the image data set one by one up to 10. Average improvement in PSNR (dB) over hand-designed classical wavelet (Villasenor, Belzer & Lia,1995; Davis & Nosratinia,1999) for various numbers of training images were observed and plotted in Figure 5.9. A maximum improvement of 1.012 dB in average PSNR above the hand-designed classical cdf 9/7 wavelet over the 80 fingerprint

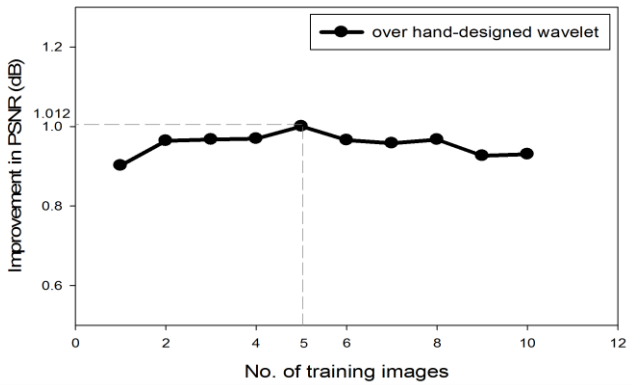

Figure 5.9 Improvement in PSNR (dB) over classical wavelet for various nos. of training images.

images in the database was obtained. The training set was comprised of 5 full size fingerprint images (TIS_300). The algorithm was able to evolve the coefficients in 11.29 hours on an Intel Xeon 3.00 GHz Processor with 6 GB memory. With one image in the training set, it took 2.26 hours for evolution. With 10 images, the time taken was 23.03 hrs. For 2 to 4 and 6 to 8 numbers of training images, improvement in average PSNR was slightly less. For 1, 9 and 10 numbers of training images, improvement in average PSNR was even less. The optimized coefficients for TIS_300 are shown in Table 5.8. Plot of PSNR for classical wavelet and coefficients evolved from the training set TIS_300 for CR = 16:1 is shown in Figure 5.10. For all the 80 images in the database, the performance of the evolved wavelet was much

Table 5.8 Optimized coefficients evolved for TIS_300.

Optimized lifting coefficients	
Notation	**Value**
α	- 1.99801629688406
β	- 0.04632709738456
γ	1.17267372661519
δ	0.488906521805475

.

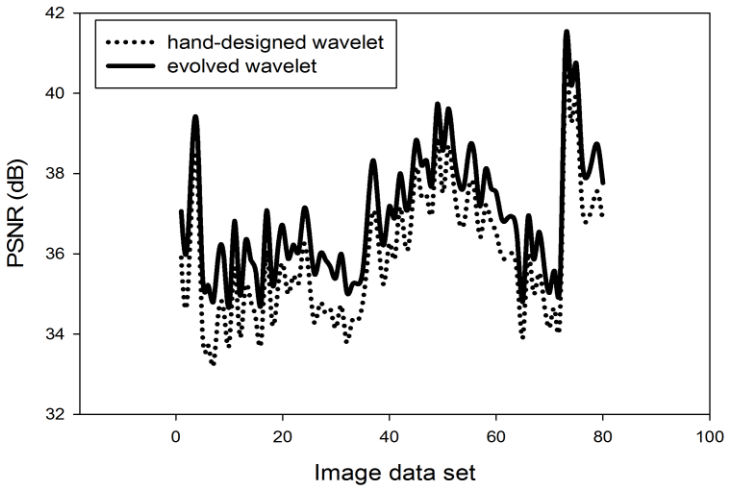

Figure 5.10 PSNR for hand-designed wavelet and wavelet coeffs. evolved from five full size (300 x 300 pixels) fingerprint images for CR = 16:1.

better than that of the hand-designed classical wavelet. It shows a maximum PSNR improvement of 1.599 dB for the image 101_7.tif and minimum of 0.681 dB for the image 106_5.tif. Table 5.9 shows the average PSNR over 80 images of DB1_B database for different levels of transform at CR = 16:1 (using coefficients evolved for TS_300, four-level MRA). The PSNR for single-level has become better than that obtained using classical wavelet.

Table 5.9 The average PSNR over 80 images of DB1_B database for different levels of transform at CR = 16:1 (using coefficients evolved for TS_300, four-level MRA).

Test Image	**level**	**PSNR (dB)**		
		Classical	**Evolved**	**Improvement**
DB1_B (80 images of size: 300 x 300 pixels)	1	3.8266	3.8974	0.0708
	4	35.9119	36.9239	1.0120

To further study the effects of the training image sets on the speed and quality of coefficients, the fingerprint images were modified to build different training image sets. Coefficients were evolved using each set and the corresponding PSNR and computational speed were observed. In this work, four training image sets comprising of various numbers of fingerprint images with different sizes, resolution etc. were derived as described below.

Figure 5.11 shows the convergence plot of a typical GA evolution of lifting coefficients. As shown, by generation around 700 the algorithm converges to the maximum value of the fitness function (i.e., PSNR). So, the optimum lifting coefficients can be obtained within a lesser number of generations than we used.

5.4.3 Training Image Set 1 (TIS1)

As mentioned earlier, maximum average PSNR was obtained with the training set comprising of 5 full size fingerprint images (TIS_300). So, this image data set consists of five images with their size reduced by cropping at the centre. The cropped

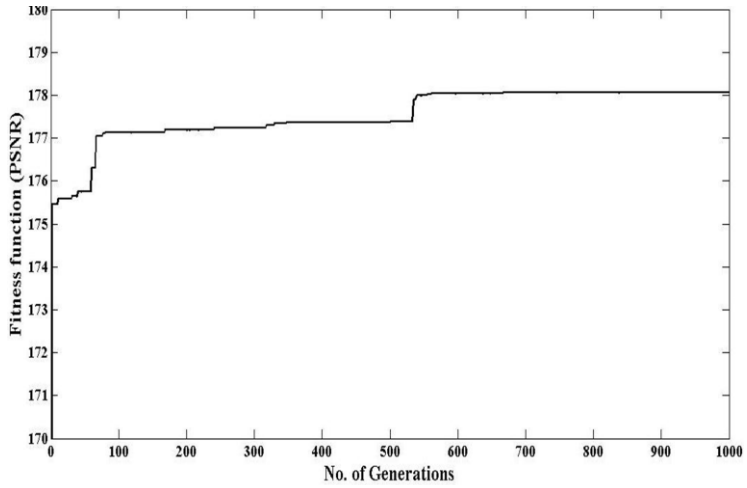

Figure 5.11 Convergence plot of a typical GA evolution of lifting coefficients.

training image sets TIS1_256, TIS1_128, TIS1_64, TIS1_32 of sizes 256 x 256, 128 x 128, 64 x 64, 32 x 32 pixels respectiveley were used for evolution. Figure 5.12 represents a cropped image of size 128 x 128 pixels (TIS1_128).

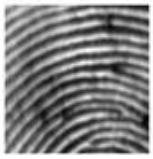

Figure 5.12 A cropped fingerprint image of size 128 x 128 pixels (TIS1_128).

5.4.4 Training Image Set 2 (TIS2)

Similar to TIS1, five images are present in this image set as well. Here, the image data sets TIS2_256, TIS2_128, TIS2_64, and TIS2_32 were derived by resizing the five individual images to 256 x 256, 128 x 128, 64 x 64, 32 x 32 pixels sizes respectively. Figure 5.13 depicts a resized image of size 128 x 128 pixels (TIS2_128). In this way the whole fingerprint image is considered.

Figure 5.13 A resized fingerprint image of size 128 x 128 pixels (TIS2_128).

5.4.5 Training Image Set 3 (TIS3)

This set contains only one image which is obtained by averaging the component images. To begin with, average of two images was used for GA evolution. Subsequently, images were appended in the data set one by one up to 10. Maximum PSNR was obtained from the average of 4 images. So, TIS3_256, TIS3_128, TIS3_64, TIS3_32 were derived by averaging four component images cropped to 256 x 256, 128 x 128, 64 x 64, 32 x 32 pixel sizes respectively. TIS3 with the average of 4 full size images and that of 4 images cropped to a size of 128 x 128 pixels (TIS3_128) are shown in Figure 5.14.

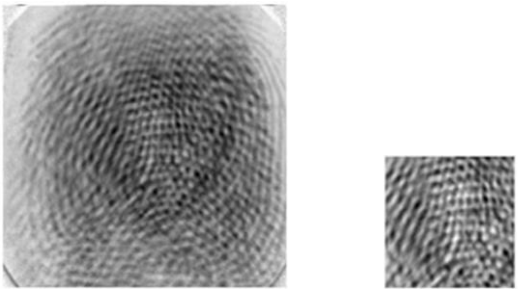

(a) (b)

Figure 5.14 Average of 4 fingerprint images (a) full size (300 x 300 pixels) (b) cropped to 128 x 128 pixels (TIS3_128).

5.4.6 Training Image Set 4 (TIS4)

Similar to TIS3, only one image is present in this image set too. Training image sets, TIS4_256, TIS4_128, TIS4_64, and TIS4_32 were obtained from the average of four individual images resized to 256 x 256, 128 x 128, 64 x 64, 32 x 32 pixel sizes respectively. Figure 5.15 represents the average of four resized images of size 128 x 128 pixels (TIS4_128).

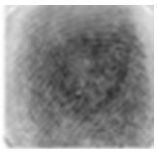

Figure 5.15 Average of 4 resized fingerprint images of size 128x128 pixels (TIS4_128).

It was observed that evolved coefficients yielded reduced PSNR compared to the classical wavelets when resized / cropped images with sizes below 32 x 32 were used.

The training image sets TIS1 to TIS4 were applied to the EA. The algorithm was run several times. The optimum lifting coefficients evolved were employed for finding the average improvement in PSNR for CR = 16:1 over 80 fingerprint images in the database. These coefficients were used to compute the average improvement in PSNR for other CRs too. Besides this, the performances of the coefficients on degraded images were also studied. To perform this, the quality of the input image was degraded to various amounts by setting certain percentages of lower pixel values to zero. Percentage degradation was calculated as,

$$Degradation = \frac{No.\ of\ pixels\ set\ to\ zero}{Total\ no.of\ pixels} \times 100\ \% \qquad (5.1)$$

The evolved wavelet coefficients were used with SPIHT (Said & Pearlman, 1996; Set Partitioning In Hierarchical Trees, n.d.) algorithm without arithmetic coder to observe their performance. In addition to the above, the performance of these coefficients was tested on other fingerprint image databases too.

5.4.7 Results and Discussion

5.4.7.1 Improvement in PSNR for Various Training Image Sets

The different data sets TIS1, TIS2, TIS3 and TIS4 with suitable number of images to give Maximum PSNR were constructed as mentioned in the previous section. They were used to evolve optimum wavelet lifting coefficients giving maximum PSNR for CR = 16:1. These evolved coefficients were employed to find the average improvement in PSNR over 80 fingerprint images. The results are compared with the result of the image set TIS_300 which contains full size images for validation purposes. Figure 5.16 shows the average improvement in PSNR for each image size in all the above image data sets. As illustrated in the figure, performance of TIS1 & TIS3 with cropped images is better than the TIS2 & TIS4 with resized images. It can

also be seen that TIS3_256 with cropped average images performs better compared to other image sets except TIS_300. The average PSNR improvement of 1.012 dB corresponding to TIS_300 is shown as a single point in Figure 5.16. PSNR improvement of 1.009 dB was achieved from TIS3_256. The evolution took only 1.692 hours. So, at the expense of just 0.003 dB (a negligibly small value), 81.35% improvement in the speed of evolution could be achieved. The evolution time and PSNR are better than the previous results. The optimized coefficients for TIS3_256

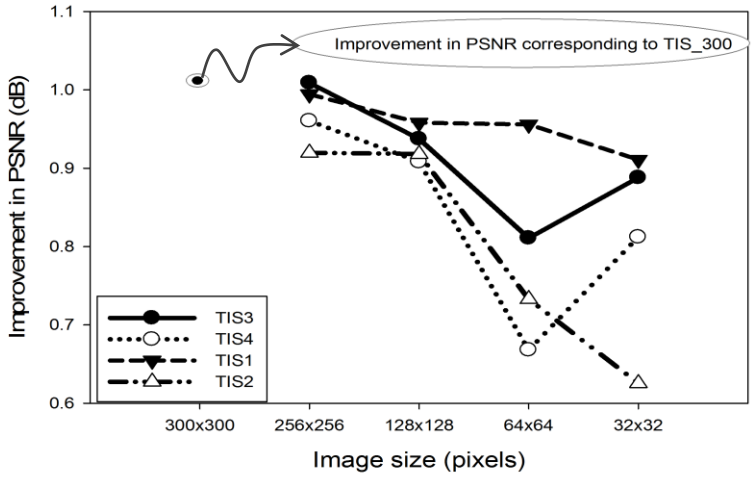

Figure 5.16 Comparison of average PSNR improvement for TIS1, TIS2, TIS3 and TIS4.

are shown in Table 5.10. Plot of average evolution time taken with image sets TIS1 to TIS4 is shown in Figure 5.17. It is obvious that the images with reduced size caused faster evolution of wavelets with little compromise in PSNR improvement.

Table 5.10 Optimized coefficients evolved for TIS3_256.

Optimized lifting coefficients	
Notation	**Value**
α	- 1.97521897030549
β	- 0.05389568773461
γ	1.119418927579580
δ	0.539170506912442

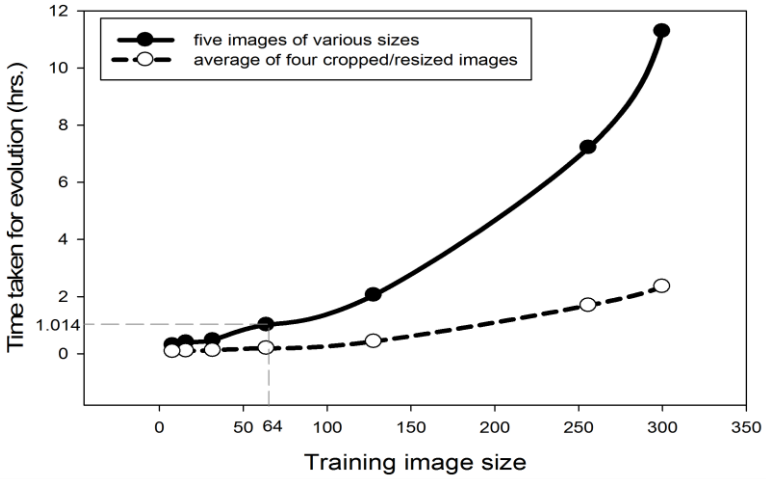

Figure 5.17 Plot of average evolution time vs. training image size.

For example, TIS1_64 took just 1.014 hours yielding 0.956 dB improvement in PSNR. Compared to TIS_300 improvement in PSNR differed by just 0.056 dB, which is too small. But, the speed of evolution was increased by 91.02%. In the case of averaged images, TIS3_32 & TIS4_32 surpassed TIS3_64 & TIS4_64 respectively with better PSNR and 39.51% increase in speed of evolution. Compared to the existing technique, TIS3_32 offered 98.7% increase in evolution speed only at the expense of 0.043 dB PSNR.

Among all these training image sets, the best PSNR improvements of 1.012 dB and 1.009 dB were tendered by TIS_300 and TIS3_256 respectively. So, the rest of this paper concentrates on the results related to these TISs. The original fingerprint image 101_1.tif and the reconstructed images corresponding to hand-designed classical cdf 9/7 wavelet, lifting coefficients evolved from TIS1_300 and the lifting coefficients evolved from TIS3_256 are shown in Figure 5.18.

5.4.7.2 Improvement in PSNR for Various Databases and CRs

The evolved wavelet coefficients exhibit improvement in PSNR for other CRs as well. Figure 5.19 compares the PSNRs of the evolved and hand-designed wavelets for various CRs. For all values of CRs, the evolved wavelets yielded better PSNR

over the classical wavelet. The wavelets evolved from the above two different training image sets (TIS_300 & TIS3_256) provided almost identical PSNRs.

(a) (b)

(c) (d)

Figure 5.18 101_1.tif fingerprint image (a) original, reconstructed image using (b) classical wavelet (PSNR = 35.908 dB) (c) evolved coefficients from TIS_300 (PSNR = 37.062 dB) (d) evolved coefficients from TIS3_256 (PSNR = 37.069 dB).

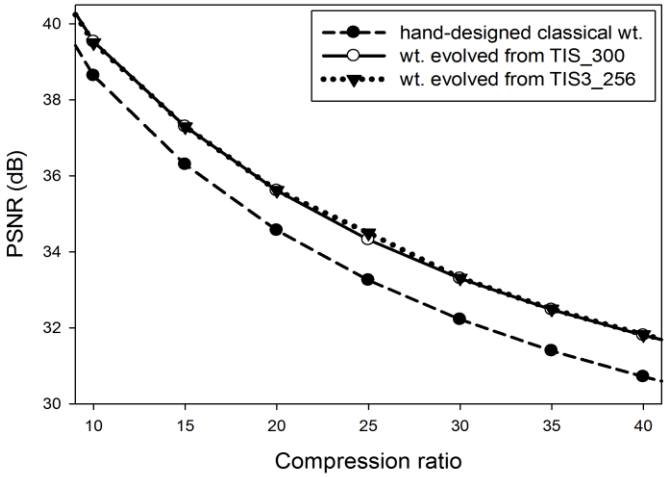

Figure 5.19 Plot of average PSNRs (dB) for classical wavelet, wavelet optimized from TIS_300 and wavelet evolved from TIS3_256.

5.4.7.3 PSNRs of Degraded Images

Figure 5.20 illustrates the comparison of average PSNRs of degraded images for CR = 10:1, computed from hand-designed wavelet and wavelet evolved from TIS3_256. Here, quality of the input images were degraded to various amounts by setting certain percentages of lower pixel values to zero. Percentage degradation was calculated using eqn. (6.1).

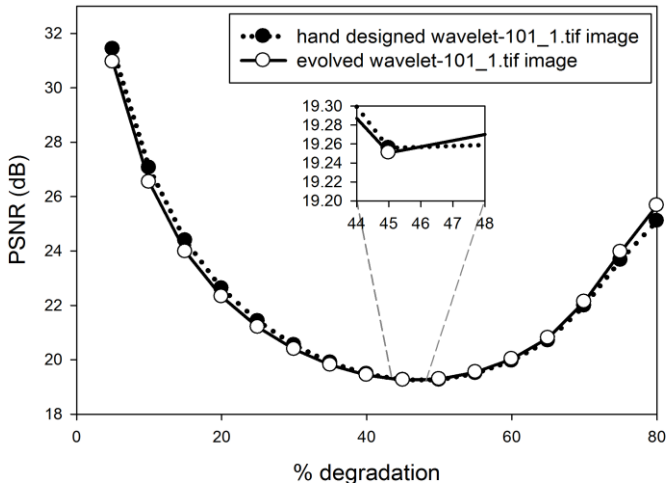

Figure 5.20 Comparison of average PSNRs of degraded images for CR = 10:1, computed from hand-designed wavelet and wavelet optimized from TIS3_256.

As shown in Figure 5.20, the PSNR corresponding to the classical wavelet was better than the evolved PSNR for lower values of degradation. The evolved PSNR became better beyond 46% of degradation. For lower CRs, evolved coefficients started to surpass the classical coefficients at higher degradation values. For example, with CR = 5:1, the evolved PSNR crossed the classical PSNR at 80% of degradation. For CRs above 20:1 evolved coefficients outperformed the classical wavelets for all degradation values. The results were similar in the case of lifting coefficients evolved from TIS_300. Figure 5.21 shows the 101_1.tif image with 15% degradation (i.e., 15% of lower pixel values were set to zero). The images reconstructed using classical as well as evolved coefficients for CR = 20:1 are also shown. The PSNR of the degraded image owing to evolved wavelets was slightly better.

(a) (b)

(c) (d)

Figure 5.21 101_1.tif image (a) 15% degraded, Reconstructed with (b) classical wavelet (PSNR = 22.982 dB) (c) optimized coefficients from TIS_300 (PSNR = 23.088 dB) (d) optimized coefficients from TIS3_256 (PSNR = 23.056 dB).

5.4.7.4 PSNR Improvement with SPIHT Coding

There was reasonable improvement in PSNR when evolved coefficients were used with SPIHT (Said & Pearlman, 1996; Set Partitioning In Hierarchical Trees, n.d.) algorithm without arithmetic coder. Figure 5.22 compares the average PSNR with SPIHT coder for various bits/pixel (bit rate) values for classical and optimized coefficients. It can be seen that the coefficients evolved from TIS3_256 outperformed the classical wavelet for all bit rates. The coefficients evolved from TIS_300 also confirmed the results.

5.4.7.5 Comparison of Histogram Differences

Direct visual inspection of the images would not probably give sufficient information for a fair judgment. Figure 5.23 compares the efficiency of the evolved wavelets in fingerprint image compression. Here the absolute difference between histogram values of 101_1.tif image and the images reconstructed with hand-designed classical

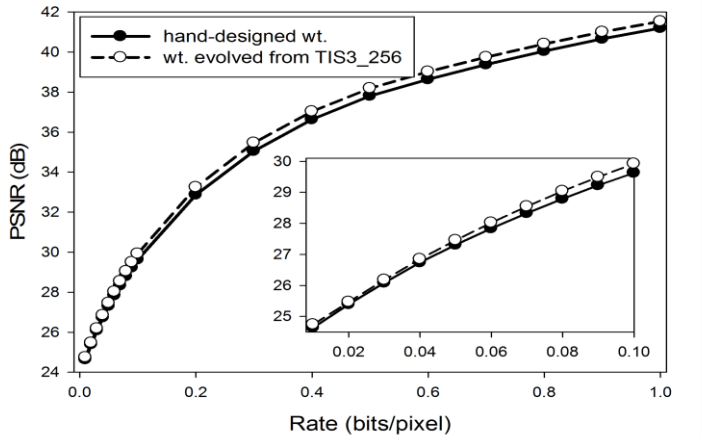

Figure 5.22 Comparison of average PSNR between classical and wavelet optimized from TIS3_256 used in SIPHT algorithm for various bit rates.

wavelet, wavelet optimized from TIS_300 and wavelet optimized from TIS3_256 are plotted. As illustrated in the figure, histogram differences of the images reconstructed from optimized wavelets are much less than that of the image reconstructed from hand-designed classical wavelet. It can also be seen that the minimum absolute histogram difference is offered by the wavelet optimized from TIS3_256 and hence it performs better than that optimized from TIS_300.

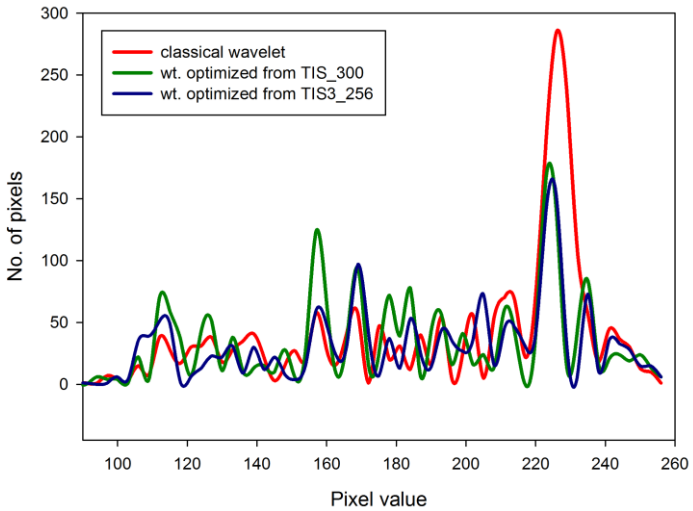

Figure 5.23 Absolute difference between histogram values of 101_1.tif image and the images reconstructed with classical wavelet, wavelet optimized fromTIS_300 and wavelet optimized from TIS3_256.

5.4.7.6 Improvement in PSNR under Quantization

The coefficients optimized for thresholding conditions (i.e., single-objective problem) for the database DB1_B of FVC 2000 were used for compression of fingerprint images under quantization conditions (dual-objective problem). They gave better average PSNR and better average IE for the database DB1_B of FVC 2000. Except in few cases there were improvements in average PSNR and IE for other fingerprint databases too. The results are tabulated in Table 5.11.

Table 5.11 Increment in PSNR obtained under quantization using 16:1 MRA (thresholding) coefficients evolved for TIS3_256.

Image database	q	Classical		Evolved	
		PSNR (dB)	IE	PSNR (dB)	IE
DB1_B (80 images of size: 300 x 300 pixels)	128	28.0399	0.0981	28.4921	0.0794
	64	31.4906	0.1533	31.8614	0.1337
	32	35.1382	0.2379	35.3617	0.2102
DB2_B (80 images of size: 364 x 256 pixels)	128	21.1692	0.2436	21.1825	0.2303
	64	25.0482	0.4532	24.8630	0.4473
	32	29.7082	0.6741	29.5714	0.6905
DB3_B (80 images of size: 478 x 448 pixels)	128	23.8897	0.1805	24.0275	0.1663
	64	27.1759	0.2946	27.2332	0.2784
	32	30.9675	0.4673	30.9448	0.4740
DB4_B (80 images of size: 320 x 240 pixels)	128	24.6726	0.1804	24.8423	0.1701
	64	28.5051	0.2622	28.7175	0.2694
	32	32.6717	0.3883	32.7363	0.4017

5.4.7.7 Improvement in PSNR of Noisy Images

Figure 5.24 illustrates the comparison of average PSNRs of noisy images for CR = 16:1, computed from classical and evolved coefficients for TIS3_256. Here, Gaussian white noise with mean 0 and variance 0.05 was added to the image. The noisy image (101_1.tif) and the images reconstructed with classical and evolved coefficients are shown in Figure 5.25. The PSNRs of the noisy image owing to evolved coefficients were better for higher CRs. For lower CRs PSNR values were

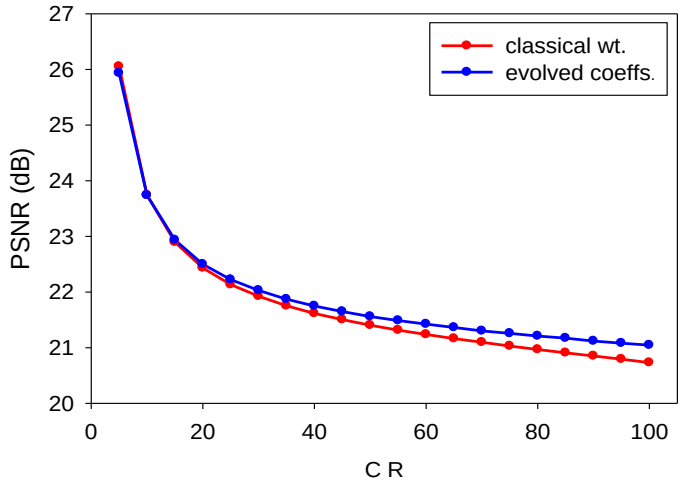

Figure 5.24 Comparison of average PSNRs of noisy images in DB1_B for various CRs.

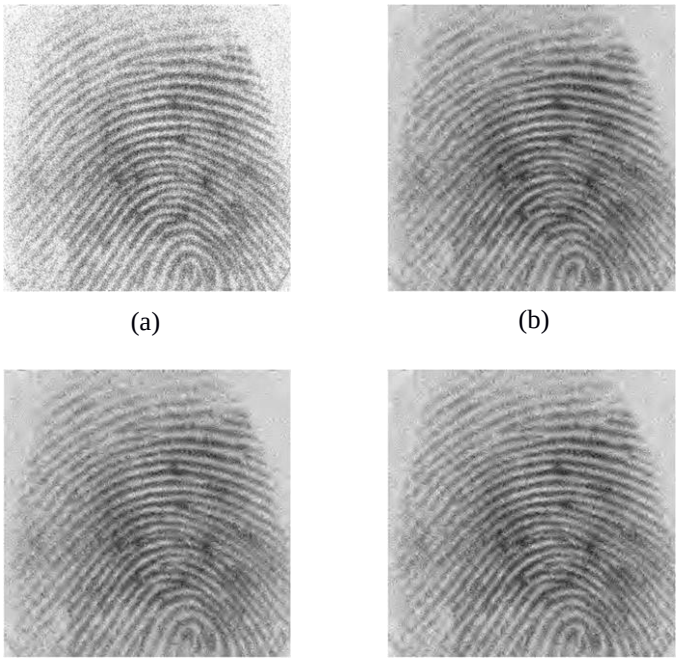

(a) (b)

(c) (d)

Figure 5.25 (a) Noisy 101_1.tif (GWN, $\mu = 0$, $\sigma = 0.05$) reconstructed image using (b) classical wavelet (21.30 dB), optimum coefficients using (c) TIS_300 (21.3927 dB) (d) TIS3_256 (21.3947 dB), for CR = 16:1.

almost equal. Figure 5.26 shows the comparison of PSNRs of noisy variants of 101_1.tif for different variances, at CR=16:1. For low variances the PSNR with

evolved coefficients is better than that with classical wavelets and for higher variances the values are almost same.

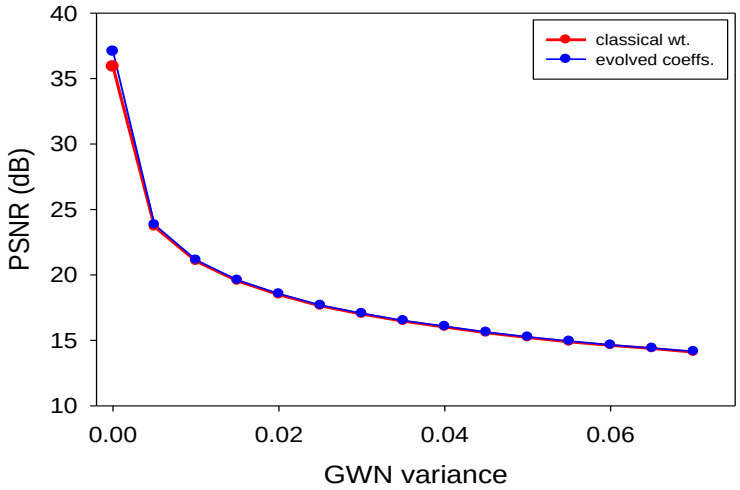

Figure 5.26 Comparison of PSNRs of noisy variants of 101_1.tif for different variances, at CR = 16:1.

5.4.7.8 Improvement in SSIM

The optimized coefficients offered significant improvements in SSIM between the original and compressed fingerprint images. Table 5.12 shows the comparison of average SSIM computed for DB1_B of FVC 2000 for various CRs in respect of the classical as well as optimized coefficients.

Table 5.12 Comparison of average SSIM index for various CRs in respect of the classical and the coefficients evolved for TIS3_256.

Image database	**CR**	**Structural similarity index Measure (SSIM)**		
		Classical	**Evolved**	**Improvement**
DB1_B (80 images of size: 300 x 300 pixels)	5	0.9778	0.9809	0.0031
	16	0.914	0.93	0.016
	20	0.8893	0.9102	0.0209
	25	0.8592	0.8857	0.0265
	30	0.8301	0.8623	0.0322
	35	0.8017	0.84	0.0383
	40	0.7748	0.8187	0.0439

5.4.7.9 PSNR improvement for other Fingerprint Databases

The coefficients evolved for the database DB1_B of FVC 2000 were applied to the other fingerprint databases of FVC 2000 (Fingerprint Verification Competition, 2000), FVC 2002 (Fingerprint Verification Competition, 2002), FVC 2004 (Fingerprint Verification Competition, 2004) and the database formed by the images collected using NITGEN USB Fingkey Hamster (HFDU 01) fingerprint scanner. Even though the images in these databases were of different sizes and clarity, except in few cases they gave better average PSNR. There were improvements in average PSNR except for the databases DB3_B (300 x 300 pixels) of FVC 2002 and DB1_B (480 x 460 pixels) of FVC 2004. Table 5.13 shows the optimization results showing the PSNRs obtained using coefficients for TIS3_256 for various fingerprint databases and CRs. Average PSNR improvement for DB1_B with CR=16:1 is 1.009 dB, which is better than that reported by Grasemann, et. al (2005) and Babb (2007), i.e., 0.75dB and 0.76 dB respectively. Comparison of the results with that of the previous works is shown in Table 5.14.

5.5 Chapter Summary

PSNR and IE are the two objectives in the dual-objective problem to optimize wavelet coefficients for fingerprint image compression under quantization. Due to their contradictory nature, the desirable increase in PSNR causes simultaneous increase in the IE (a measure of file size). However, by keeping the IE or the CR at a constant value, an exact measure of the improvement in PSNR could be obtained. Then, the dual-objective problem becomes a single-objective problem with PSNR as the objective to be maximized. So, the proposed works in this chapter focused on evolving optimized coefficients from the lifting coefficients of cdf 9/7 wavelet at CR = 16:1 (by retaining the largest 6.25% of the transformed image coefficients and the remaining values were set to zero) using GA. Optimized coefficients were evolved for various levels of MRA of wavelet image compression using single and multiple fingerprint training images. The improvements in average PSNRs offered by

the optimized coefficients over the whole fingerprints in various databases were noted.

For general compression purposes the coefficients optimized for single-level through four-level MRAs using single training images are not apt. This issue was circumvented by using multiple training images in GA evolution.

Table 5.13 The boost in average PSNR at various CRs in respect of different fingerprint databases (using optimized coeffs. for TIS3_256).

Image database	**CR**	**PSNR (dB)**		**PSNR improve-ment (dB)**
		Classical	**Evolved**	
DB1_B (80 images of size: 300 x 300 pixels)	20:1	34.5664	35.6175	1.05
	16:1	35.9119	36.9209	1.01
	10:1	38.6388	39.5017	0.86
	6:1	41.4887	42.1655	0.68
DB2_B (80 images of size: 364 x 256 pixels)	20:1	21.1166	21.3728	0.26
	16:1	21.8476	22.0404	0.19
	10:1	23.6800	23.7061	0.03
	6:1	26.3782	26.1275	-0.25
DB3_B (80 images of size: 478 x 448 pixels)	20:1	25.2746	25.6300	0.36
	16:1	26.2925	26.6325	0.34
	10:1	28.6065	28.9067	0.30
	6:1	31.563	31.7937	0.23
DB4_B (80 images of size: 320 x 240 pixels)	20:1	26.7049	27.0662	0.36
	16:1	28.2197	28.5433	0.32
	10:1	31.6747	31.9262	0.25
	6:1	36.191	36.1148	-0.08
200 images from NITGEN's scanner (size: 292 x 248 pixels)	20:1	21.8988	22.4699	0.57
	16:1	23.1583	23.6961	0.54
	10:1	25.9721	26.4263	0.45
	6:1	29.3423	29.5751	0.23

Table 5.14 Comparison of the results with that of the previous works (training and test images: fingerprints).

Reference	**Conditions**	**PSNR improve-ment (dB)**
Grasemann, et. al (2005)	4 level MRA 16:1 Thresholding	0.75
Babb (2007)	4 level MRA 16:1 Thresholding	0.76
Proposed work	4 level MRA 16:1 Thresholding	1.009

Usually, full size images are being used for evolving wavelet coefficients. This evolution process is too slow. To speed up this, in this work, wavelets were evolved with different image sets like resized, cropped, resized-average and cropped-average images. Comparing the PSNRs offered by the evolved wavelets, it was found that the cropped images outperformed the resized images and is at par with the results reported so far. Wavelet lifting coefficients, evolved from an average of four 256 x 256 centre cropped images, took less than $1/5^{th}$ the evolution time reported in literature. Besides increasing the computational speed by 81.35%, the evolved coefficients offered 1.009 dB improvements in average PSNR over 80 fingerprint images in the database. At the cost of very small amount of PSNR, additional reduction in evolution time could be achieved. The evolved wavelet coefficients exhibited improvement in PSNR for other compression ratios too. For higher compression ratios, evolved coefficients outperformed the classical wavelets in compressing degraded images. There was reasonable improvement in PSNR when evolved coefficients were used with SPIHT algorithm. The coefficients optimized for thresholding conditions (i.e., single-objective problem) gave better average PSNR and better average IE under quantization conditions (dual-objective problem) for the database DB1_B and for most of the other databases of FVC 2000. The optimized coefficients offered improvement in SSIM of the compressed images. Except in few cases, the coefficients evolved for the database DB1_B of FVC 2000 offered better average PSNR when applied to the other fingerprint databases of different sizes and

clarity. Image compression can be further improved by using application specific optimized wavelets for medical, satellite, and digital photography applications. One of the factors which improve the performance of the evolved wavelet is a properly designed training data set. Therefore, techniques can be developed to design an optimum training data set, which improves the compression performance.

Chapter 6

A Fingerprint Based Hybrid Gender Classification System using Genetic Algorithm

In this chapter, a multilevel hybrid approach which gives better accuracy for gender classification is presented. The first level uses DWT, SVD and PCA techniques to derive three independent sets of feature vectors for simultaneous gender classification by three independent neural networks. Optimum coefficients similar to cdf9/7 DWT lifting coefficients and optimum values of initial seeds for the classifiers are evolved using GA, for obtaining better feature vectors. Use of lifting coefficients causes faster evolution. In the second stage, the output is derived by decision formulated based on the outputs of the individual classifiers. With a database consisting of left thumb impressions of 100 males and 100 females, an overall success rate of 93.94% and an average improvement of 5.24% accuracy over the existing classifiers are achieved. It is observed that the use of feature vectors having lesser number of elements can enhance the speed of operation of the classifier as well.

6.1 Introduction

Fingerprints are the traces of impressions made by the tiny ridge formations or patterns seen on the fingertips. Permanence and individuality are the fundamental characteristics of fingerprints. The invariance and distinctiveness of fingerprints enable them as the tool for criminal identification. The forensics and law enforcement agencies across the world use AFIS. Many non-forensic applications find use of fingerprint technology for recognition of individuals because of national security issues, financial and identity cheatings. So, the scientific evidence behind fingerprint individuality makes it very useful in forensic and non-forensic applications. Fingerprint classification is a system that group fingerprints to one among the several predefined categories. Gender classification using fingerprint is a noteworthy step in forensic science, medical and anthropological studies to search an individual easily. By performing gender classification, the database for searching an individual can be narrowed as it requires searching either a female or male database alone. By this, to a great extent, it can facilitate reduction in time searching an individual in a huge database. Once an individual is identified as female or male, then some appropriate biometric characteristic can be employed for more specific classifications.

Studies made by several researchers in different parts of the world among various populations across different countries revealed that women have more ridges than men. Their observations encourage the efforts of gender classification based on fingerprint features as in this present work. In recent times, several research works have been done in the area of male-female gender classification using fingerprints.

In the proposed algorithm, attention is given to both the classification speed as well as the classification accuracy. Classification speed is improved by employing lesser number of feature components obtained from DWT, SVD and PCA. As mentioned in the earlier chapters, use of symmetrical lifting coefficients of cdf 9/7 wavelets results in faster computation of transform coefficients. This provides further improvement in classification speed. Optimizing wavelet coefficients and seed values of classifiers for gender classification using GA provides better classification accuracy.

6.2 Methodology

The gender classification is done by using a multilevel technique. The first level employs three different classifier modules using DWT, SVD and PCA transform techniques, to obtain three independent sets of fingerprint feature vectors. To speed up the classification process using DWT, wavelet LS is employed. SVD and PCA are powerful tools commonly used for multivariate data analysis (Semmlow, 2004), data representation by a lesser number of variables, and finding patterns in data. In gender classification system, the input fingerprint is preprocessed first and then the feature vector is extracted. The outputs of the feature extractors are fed to the classifiers to identify the gender. Optimum values of DWT coefficients and initial seeds for the three classifiers are evolved using GA, for better classification. The second level employs a decision module, which decides the resultant gender with better accuracy, based on the outputs of the individual classifiers. Block diagram of the resulting classifier is shown in Figure 6.1. The proposed algorithm is implemented in MATLAB installed in an Intel Xeon 3.00 GHz processor with 6 GB memory.

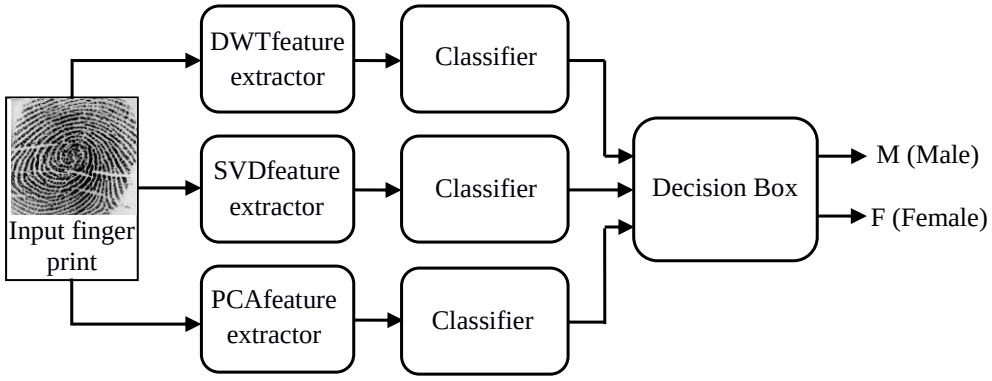

Figure 6.1 Block diagram of decision based gender classifier.

6.2.1 Database

The fingerprint databases used for compression, which were presented in earlier chapters, are not suitable for gender classification as they bear no gender information. Moreover, standard fingerprint databases suitable for gender classification were not

available in literature as well as from other sources. So, a database of fingerprints of size 248 (width) by 292 (height) pixels collected using NITGEN USB Fingkey Hamster (HFDU 01) fingerprint scanner was used. This database consists of fingerprints of left thumb of 200 persons (100 males and 100 females). Two-third of each category of fingerprints are used for training and the remaining one-third, for testing purpose. A typical fingerprint in the database is shown in Figure 6.2.

Figure 6.2 Typical fingerprint image from NITGEN USB Fingkey Hamster (HFDU 01).

6.2.2 Feature Extraction

The fingerprints are subjected to transformations such as DWT, SVD and PCA to extract features required at the classifiers' inputs. Prior to performing the transformations, the fingerprint images were preprocessed to have the standard image size of 256 × 256 pixels. Here, the top and bottom boundary regions of each image were cropped to reduce its height to 256 pixels. Zero padding was done at the other boundary regions to increase the image width to 256 pixels.

6.2.2.1 DWT Based Feature Extraction

WT is an effective tool in image processing and computer vision applications (Zhang, Zhang & Ge, 2004). The effectiveness of the DWT technique for the gender classification using fingerprint has been established by researchers who have successfully used wavelet features for applications such as fingerprint recognition and identification, gender identification, etc. In this work, LS of cdf 9/7 biorthogonal wavelet has been used. For faster computation of DWT coefficients for feature extraction and also for faster evolution of wavelet coefficients optimized for better feature extraction, symmetric LS (Daubechies & Sweldens, 1998; Taubman &

Marcellin, 2002) with only four coefficients has been used in this work. Refinement of the general purpose lifting filter coefficients using GA could be used to obtain optimum filter coefficients adapted to fingerprint feature extraction.

A single-level WT decomposes an image into four subband images known as Low-Low (LL), Low-High (LH), High-Low (HL) and High-High (HH) (Gnanasivam & Muttan, 2012). The energy in the decomposed image is mainly concentrated in the LL subband. Hence, the higher levels of decompositions were done only on the corresponding LL subband. An 'n' level DWT results in '3n + 1' subbands. In the proposed work, three levels of decomposition were done, which provided ten subbands. Using equation (6.1), energy of each subband was determined.

$$E_n = \frac{1}{M \cdot N} \sum_{k=1}^{M} \sum_{l=1}^{N} |x_n(k,l)| \tag{6.1}$$

Here, $x_n(k,l)$represent the pixel values of the n^{th} subband and the pixels are indexed by k, l. M is the width of the subband and N represents its height. Each image was decomposed into ten subbands. Corresponding to each subband there is one energy value. So, for each image, the DWT based feature was a ten element vector formed by the ten energy values corresponding to the ten subbands.

6.2.2.2 SVD and PCA Based Feature Extraction

SVD technique (Baker, 2013; Fieguth, 2011) transforms correlated variables into a set of uncorrelated ones that show the correlations among the input data in a better way. It recognizes and arranges the dimensions along which data points have the most variation. Then, a better approximation of the original data using fewer dimensions can be obtained. In the course of dimensionality reduction, SVD makes similar items to become more similar to each other and the dissimilar items more dissimilar. The singular values were stored in descending order to form the feature vector. The size of the feature vector for an input image of size 256 × 256 pixels is 1 × 256.

PCA is a mathematical method extensively used in investigative data analysis, signal processing, etc. (Jeong, Ziemkiewicz, Ribarsky & Chang, 2009).

Many researchers have used PCA technique for applications like face recognition (Turk & Pentland, 1991), motion analysis and synthesis (Safonova, Hodgins & Pollard, 2004), clustering (Koren & Carmel, 2003), dimension reduction (Huang, Ward & Rundensteiner, 2005; Theodoridis, Pikrakis, Koutroumbas & Cavouras, 2010), and especially the areas requiring the classification of the high-dimensional data (Prasad & Prasanna, 2008; Jolliffe, 1986), etc. It has been particularly used for gender classification by several researchers (Tom & Arulkumaran, 2013; Purohit et. al., 2011). Block diagram of fingerprint feature extractor is shown in Figure 6.3.

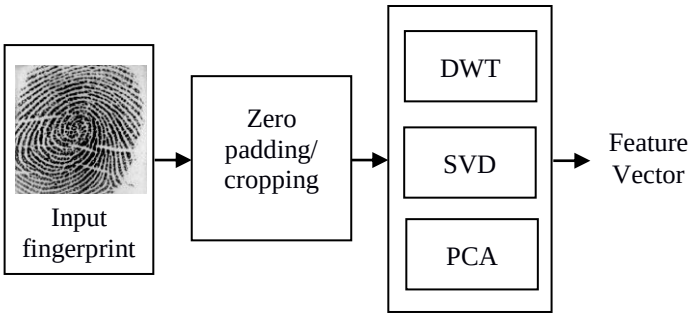

Figure 6.3 Block diagram of DWT/SVD/PCA based fingerprint feature extractor.

6.2.3 Gender Classification

In the present research work, BPNN (Haykin, 1999) model has been trained and tested for the male and female fingerprint images. The algorithm helped to increase the performance of the system and to decrease the convergence time for the training of the network. The training stage of a DWT/SVD/PCA based gender classification system optimized using GA is shown in Figure 6.4.

In the DWT based classifier, samples of training fingerprint images were subjected to three-level DWT to obtain ten subbands. For each image, energy of all subbands were calculated and arranged in such a way to form feature vector of length ten. These feature vectors were fed as input to the BPNN for training the classifier. Performance of the classifier could be improved by providing better training to the NN. This was done by optimizing the wavelet filter coefficients for decomposing the image into subbands having enhanced energy features to offer better classification

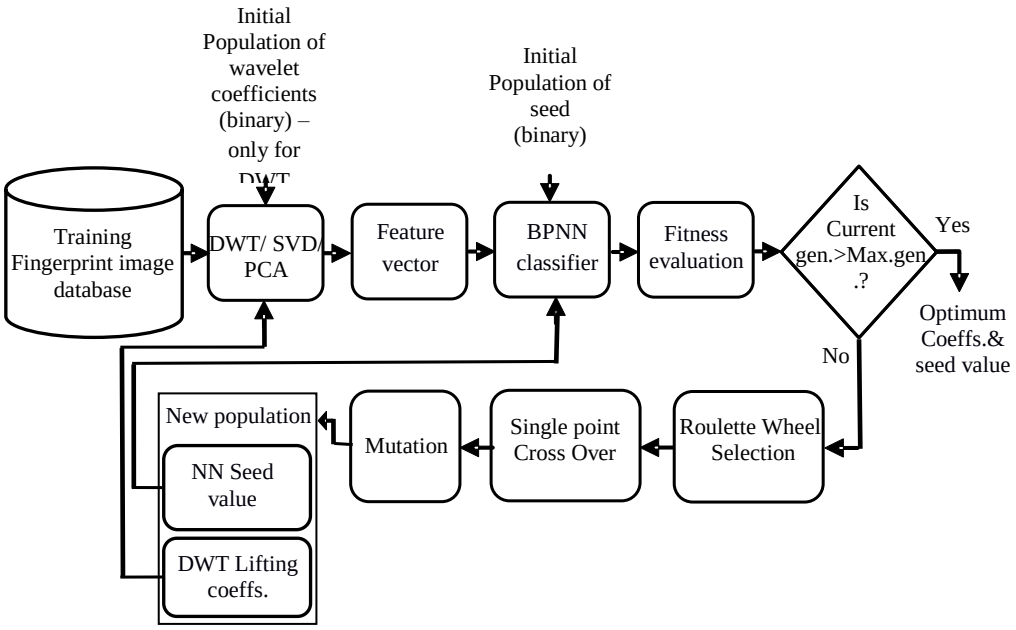

Figure 6.4 Training stage of a DWT/SVD/PCA and GA based gender classification system.

rate. The optimization was done by using GA. Error rate or accuracy is the term usually used for measuring the performance of a fingerprint classification system (Maltoni et al., 2009). Here, accuracy has been used as fitness function for the GA evolution.

$$Error\ rate = \frac{number\ of\ misclassified\ fingerprints}{total\ number\ of\ fingerprints} \times 100\ \% \qquad (6.2)$$

$$Accuracy\ = 100 - Error\ rate \qquad (6.3)$$

where, Accuracy and Error rate are in percent.

It has been observed that due to randomization of initial seed value, the NN gives different classification rates in different runs of the algorithm. However, in the proposed algorithm, an optimum seed value has been evolved using GA. Both optimum coefficients and optimum seed value have been evolved for maximum accuracy by running the algorithm till the end of the maximum number of generations. The proposed algorithm employs binary GA based optimization.

Accuracy of the classifier has been employed as the fitness function for GA evolution.

The initial population of wavelet coefficients was created by randomly mutated copies of the symmetrical lifting coefficients of cdf 9/7 wavelet. A random population was used as the initial population of seed value to the NN. Each wavelet coefficient was represented by 17 bits. The first bit characterizes the sign and the remaining 16 bits correspond to the coefficient value. The seed value was represented by 18 bits. The P_{size} for GA evolution was fixed as 30 and the number of generations, 50. The algorithm employed roulette wheel selection. The crossover was 'single point'. Rate of crossover was P_c = 0.7, rate of mutation P_m= 0.0075 and elitism was 1.

SVD and PCA based gender classifiers are similar to the wavelet based classifier. Here, instead of the WT block, an SVD or PCA block was used. So, there was no need for optimizing the wavelet coefficients. However, the initial seed for the NN classifier was optimized using GA. In the training stage, samples of training fingerprint images were decomposed using SVD or PCA and feature vectors were formed. As in the previous case, the initial seed value of the NN, represented by 18 bits, was generated randomly. In both cases, the GA parameters were the same and accuracy of classification computed using equation (6.3) worked as fitness function for GA evolution.

The testing stage of a DWT/SVD/PCA and GA based gender classification system is shown in Figure 6.5. In this stage, for the DWT based system, the input fingerprint with unknown gender is subjected to three-level DWT using the optimized wavelet coefficients. Energies of the subbands were calculated to form the feature vector. The feature vector was fed to the trained NN with seed value optimized for maximum accuracy. For the SVD or PCA based system the SVD or PCA components make the corresponding feature vectors. The trained NN with initial seed value optimized using GA for maximum accuracy provided more accurate gender information.

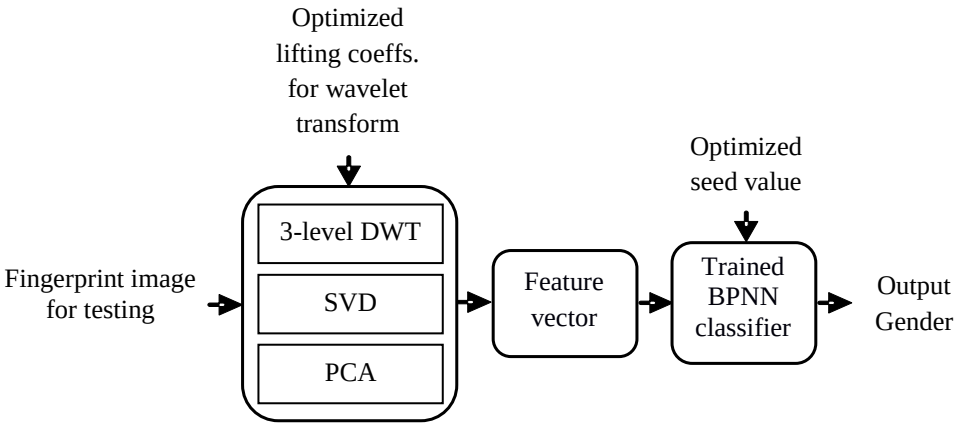

Figure 6.5 Testing stage of a DWT/SVD/PCA and GA based gender classification system.

6.2.4 Decision Based Gender Classifier

It has been observed that the outputs of the three classifiers described above are not unique. For certain input fingerprints, the classifiers outputs might be different. To be specific, for a particular fingerprint, some classifier(s) gave correct output and the other(s) gave incorrect output. This gave scope for further improvement in classification accuracy, which could be achieved by making decisions based on the outputs of the individual classifiers. Figure 6.6 shows a three variable truth table and Karnaugh map constructed to implement the decision box for the improved classifier. Here, the Boolean input variables D, S and P are actually the output of the DWT, SVD and PCA based classifiers respectively forming the inputs to the decision box. '0' represents male gender and '1' represents female gender. Figure 6.7 shows the decision box with the simplified Product-Of-Sums (POS) output expressions for gender determination.

6.3 Results and Discussion

6.3.1 DWT Based NN Classifier

In DWT based gender classifier, fingerprint images were decomposed into ten subbands using three levels of DWT. Both the wavelet lifting filter coefficients for DWT and the initial seed value for NN were optimized using GA evolution. The

evolved coefficients are:

$$0.920987579,\ 0.1857966857,\ -0.6954557939,\ 0.4403515732.$$

Inputs			*Output*
D (DWT)	*S (SVD)*	*P (PCA)*	*Y*
0	0	0	0
0	0	1	0
0	1	0	0
0	1	1	1
1	0	0	0
1	0	1	1
1	1	0	1
1	1	1	1

(a)

	$\overline{D}\,\overline{S}$	$\overline{D}S$	DS	$D\overline{S}$
$\overline{P}$	0	0	1	0
P	1	1	1	1

(b)

Figure 6.6 (a) Truth table and (b) Karnaugh map for decision-making to implement the improved classifier.

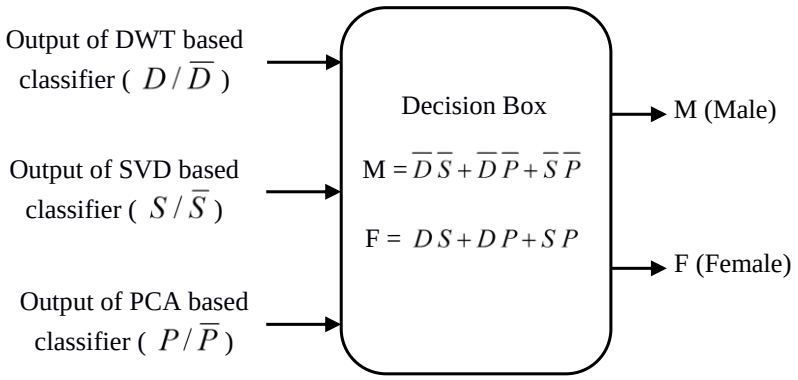

Figure 6.7 Decision box

The initial seed has been evolved as 214,960. Confusion matrix for the classical DWT based NN classifier and for the GA optimized NN classifier is shown in Table 6.1. Having done several trials, the overall accuracy of the classifier without optimization has been found to be 75.76%. With optimized coefficients and seed value, 90.91% of male and 81.82% of female genders have been correctly classified. The overall classification accuracy has been 86.36% showing an improvement of 10.6% over the classical DWT based classifier. Researchers in their earlier works on DWT based gender classification used six-level DWT decomposition giving 19 subbands. With 19 subbands the NN took 1.56 seconds. Time taken for NN classification in the proposed work, with DWT feature vector having 10 components obtained from three DWT levels, was 1.41 seconds only. There is 9.6% improvement in the speed with which the classification is done.

Table 6.1 Confusion matrix for DWT based NN classifier.

Actual/ estimated	*Total*	*Classical DWT-based NN classifier*			*GA optimized DWT-based NN classifier*		
		Male	*Female*	*Accuracy %*	*Male*	*Female*	*Accuracy %*
Males	33	28	5	84.84	30	3	90.91
Females	33	11	22	66.67	6	27	81.82
Total	66	39	27	**75.76**	36	30	**86.36**

Figure 6.8 shows the plot of overall classification accuracy for various numbers of female and male fingerprint samples computed with the evolved lifting coefficients and initial seed value given above. The number of female and male fingerprint samples has been successively increased in steps and the overall classification accuracy has been computed using lifting coefficients without GA optimization and using lifting coefficients and initial seed value after GA optimization, in each case. As shown in the figure, in all cases, the classification accuracy is far better with GA optimized lifting coefficient and seed value.

6.3.2 SVD Based NN Classifier

Table 6.2 shows the confusion matrix for the SVD based NN classifier without GA optimization and with GA optimization. The overall accuracy of the classifier without

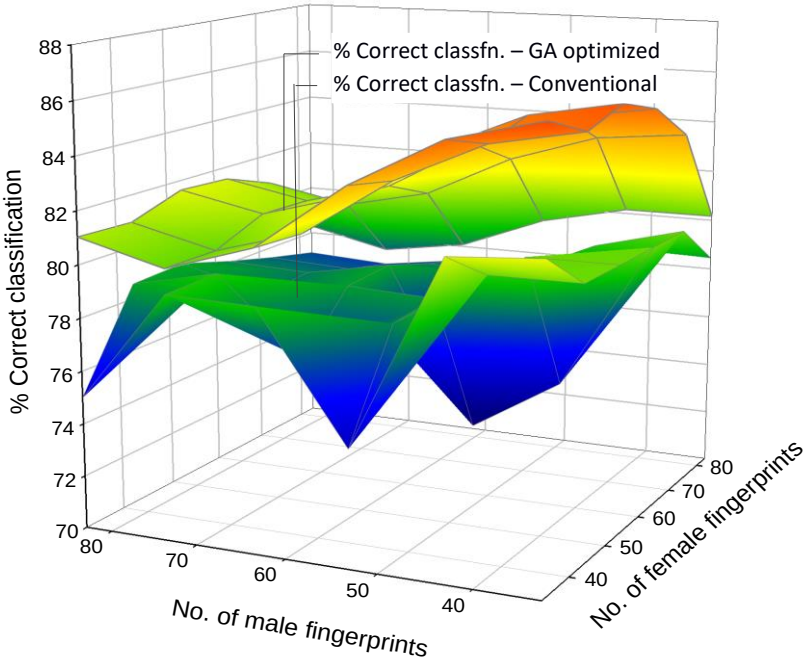

Figure 6.8 % classification accuracy of DWT based NN classifier for various numbers of female and male fingerprint samples.

Table 6.2 Confusion matrix for the SVD based NN classifier.

Actual/ estimated	*Total*	*SVD-based NN classifier*			*GA optimized SVD-based NN classifier*		
		Male	*Female*	*Accuracy %*	*Male*	*Female*	*Accuracy %*
Males	33	25	8	75.75	26	7	78.79
Females	33	12	21	63.64	7	26	78.79
Total	66	37	29	**69.69**	33	33	**78.79**

optimization has been obtained as 69.69%. With an optimized initial seed value of 251596, there is 9.1% improvement in classification accuracy, which gives an overall accuracy of 78.79%. The individual accuracy in classifying male and female is also 78.79%. In the previous works using SVD, the feature vectors were made up of all the 256 SVD components and the NN classifier took 55.8 seconds. In the present work the feature vectors have been formed by the first 12 significant SVD

components, as it gave the best result. This, in turn, reduced the time required for classification to 1.43 seconds, resulting 97.44% enhancement in speed.

The overall classification accuracy of conventional and GA optimized SVD based NN classifier using the optimized seed value of 251,596 for various numbers of female and male fingerprint samples is plotted in Figure 6.9. It is seen that the classification accuracy is superior along with GA optimized SVD based NN classifier.

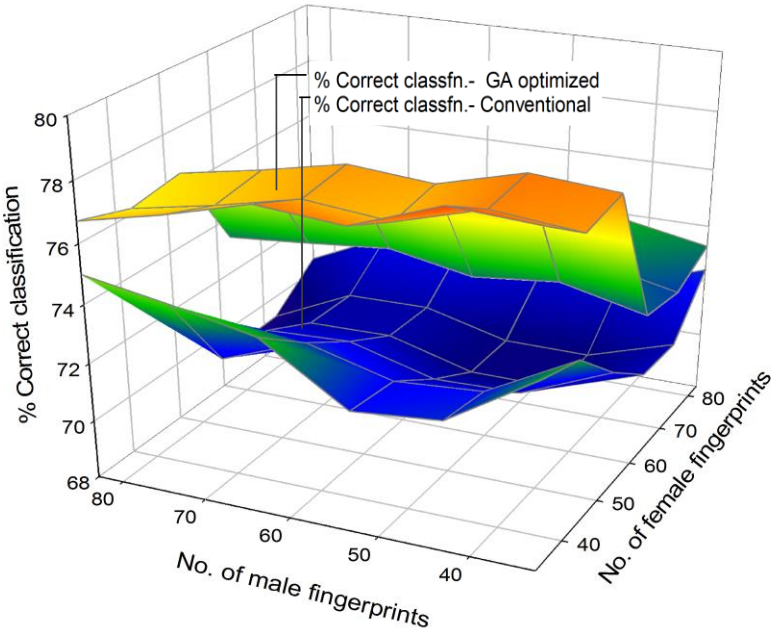

Figure 6.9 % classification accuracy of SVD based NN classifier for various numbers of female and male fingerprint samples.

6.3.3 PCA Based NN Classifier

Confusion matrix for the PCA based NN classifier without GA optimization and with GA optimization is shown in Table 6.3. The overall accuracy of the classifier without optimization is 77.27%. An optimized initial seed value of 144,322 gave overall classification accuracy of 83.33%. The overall classification accuracy has been improved by 7.8%. The classification accuracy for male is 84.85%, while that of female is 81.82%. In the case of PCA also, the previous works used feature vectors made up of 256 PCA components and the NN classifier took 97.17 seconds. In the

Table 6.3 Confusion matrix for the PCA based NN classifier.

Actual/ estimated	*Total*	*PCA-based NN classifier*			*GA optimized PCA-based NN classifier*		
		Male	*Female*	*Accuracy %*	*Male*	*Female*	*Accuracy %*
Males	33	23	10	69.69	28	5	84.85
Females	33	5	28	84.85	6	27	81.82
Total	66	28	38	**77.27**	34	32	**83.83**

current work, the feature vectors have been formed by the first PCA component, since it provided the best output. Consequently, the time required for classification has been cut down to 1.29 seconds, causing 98.7% enhancement in speed.

The overall classification accuracy of conventional and GA optimized PCA based NN classifier using the optimized seed value of 144,322 for various numbers of female and male fingerprint samples is plotted in Figure 6.10. A few instances are noticed where for higher numbers of female and male fingerprint samples the classification accuracy with conventional PCA based NN classifier become equal or sometimes better than GA optimized PCA based NN classifier. However, in most cases the classification accuracy is higher with GA optimized PCA based NN classifier.

6.3.4 Decision Based Hybrid NN Classifier

Confusion matrix for the decision based hybrid gender classifier is shown in Table 6.4. The overall accuracy of the classifier is 93.94%. Male genders have been classified with an accuracy of 90.91% and females, with accuracy 96.97%. The best overall gender classification accuracy reported in literature (Marasco, Lugini &

Table 6.4 Confusion matrix for the decision based improved gender classifier.

Actual/estimated	*Males*	*Females*	*Total*	*Accuracy %*
Males	30	3	33	90.91
Females	1	32	33	96.97
Total	31	35	66	**93.94**

Note: Best overall accuracy as reported in literature (Marasco et al. 2014): 88.7%

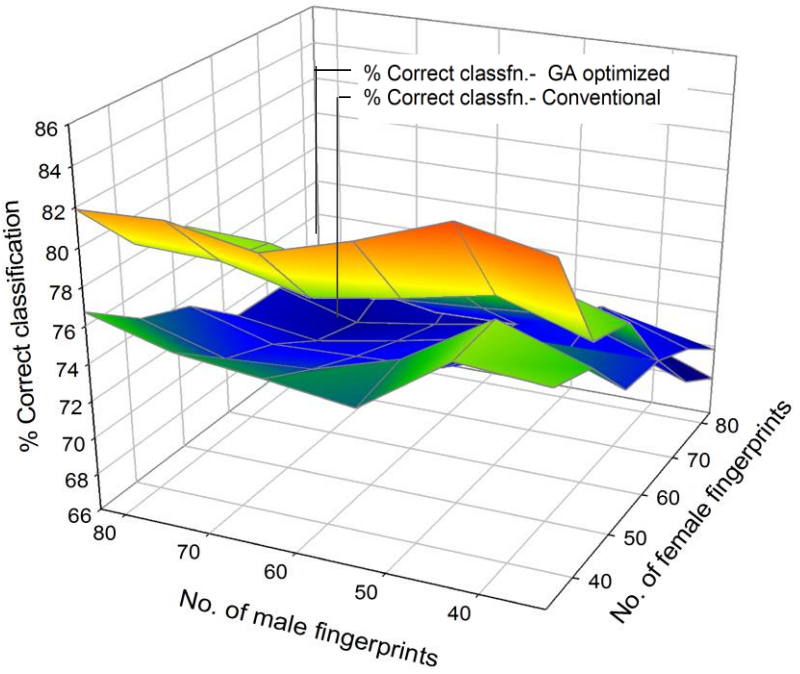

Figure 6.10 % classification accuracy of PCA based NN classifier for various numbers of female and male fingerprint samples.

Cukic, 2014) was 88.7%. So, the proposed method offers 5.24% improvement in gender classification accuracy, over the previous result. Comparison of the results with the previous works is shown in Table 6.5.

Table 6.6 compares the speed of classifiers based on the different techniques explained above. The overall improvement in classification speed of GA optimized decision based hybrid classifier is 97.33% above that of the decision based combined conventional classifier.

6.4 Chapter Summary

A multilevel approach for better classification of male and female gender from fingerprint images was presented in this chapter. In the first level, DWT, SVD and PCA transform based feature vectors were used as inputs to three independent BPNN classifiers for simultaneous gender classification. In the DWT based system, GA

Table 6.5 Comparison of the results with the previous works on gender classification.

Reference	**Classifier**	**Feature vector components**	**Fingerprint database**	**Best Accuracy %**
Badawi, et. al (2006)	FCM, LDA and NN	Ridge count, RTVTR, white lines count, ridge count asymmetry	10 fingerprint images of 1100 males and 1100 females	88.5
Verma & Agarwal (2009)	SVM	ridge width, ridge density, RTVTR	200 male samples and 200 female samples	88
Gnanasivam & Muttan (2012)	K-nearest neighbour	DWT, SVD	1980 male samples and 1590 female samples	88.28
Omidiora, et. al (2012)	NN	RTVTR, Ridge Count	10 fingerprint images of 100 males and 100 females	80
Kaur, et. al (2012)	-	FFT, DCT, PSD	110 male samples and 110 female samples	84.54
Gornale, et. al (2013)	-	FFT, Eccentricity, Major Axis Length	450 male samples and 550 female samples	79
Tom & Arulkumaran (2013)	Minimum distance	DWT, PCA	200 male samples and 200 female samples	70
Proposed method	NN	DWT, SVD, PCA	100 male samples and 100 female samples	93.94

* The authors used their own internal database, since no standard database was available.

Table 6.6 Comparison of time taken for classification (seconds).

Classifier type	*Using conventional method*	*Using GA optimization*	*% improvement in speed*
DWT alone	1.56	1.41	9.60
SVD alone	55.80	1.43	97.44
PCA alone	97.17	1.29	98.70
Decision-based	154.53	4.13	**97.33**

optimized cdf 9/7 wavelet lifting coefficients were used to decompose the fingerprint images into subbands. The NN employed GA optimized initial seed value and lesser number of subbands. The use of lifting coefficients and lesser number of subbands increased the speed of the classifier. Compared to the conventional method, the overall classification rate of the GA optimized DWT based gender classifier got

enhanced by 10.6%. The proposed SVD and PCA based systems having optimized initial seed values used merely the first twelve SVD components and the first PCA component respectively. Besides the hike in the speed of the classifiers, there were 9.1% and 7.8% improvements in classification accuracy compared to the conventional gender classifiers based on SVD and PCA respectively. Moreover, the use of the optimized lifting coefficients and the initial seed values produced better classification accuracy on a large number of additional fingerprint samples.

Since the outputs of the three classifiers were not unique, the next level of the system combined these outputs to take a better decision on gender. This decision-based improved hybrid gender classifier provided overall accuracy of 93.94%, which is 5.24% above the best result, reported in literature. The improvement in classification speed of GA optimized decision based hybrid classifier is 97.33% above that of the decision based conventional classifier. The proposed techniques can also be extended to classify the male and female genders to different age groups.

Chapter 7

Conclusion and Scope for Further Work

This chapter presents the main conclusions of this research work and the scope for further work.

7.1 Introduction

It is well established that substantial improvement in picture quality at different CRs can be achieved due to better energy compaction property of WTs. By designing suitable wavelets, this property can be enhanced. In this work basic cdf9/7 wavelet has been modified and optimized using GA to maximize the energy compaction property of the wavelet to get better picture quality (i.e., PSNR). Evolution time is proportional to the size and the number of images in the training set. It is clearly seen that the difference between the evolution time taken with 5 images and the average of 4 cropped images increases with the size of the images and hence the evolution using 4 cropped (256 x 256) and averaged images is faster. Similarly, the use of lifting coefficients and lesser number of DWT subbands increase the speed of the DWT based classifier. Speed of the SVD and PCA based classifiers' is also high due to the optimization of the number of SVD and PCA components. By using GA optimized wavelet coefficients and initial seed values, the classification accuracy also increases.

7.2 Fingerprint Image Compression by Optimized Wavelet Coefficients

Wavelet based image compression is very promising, since it examines the image signal at different resolutions. DWT decomposes the original image to horizontal, vertical and diagonal components. Biorthogonal wavelet has both symmetry and compact support. Many wavelets and techniques have been reported in literature till date. The hand-designed classical cdf 9/7 biorthogonal wavelet (or Bior 4.4) introduced in 1992 by Cohen, Daubechies, and Feauveau (cdf) is used by the FBI fingerprint compression standard. This wavelet employs four sets of coefficients, that are denoted as Lo_D, Hi_D, Lo_R and Hi_R. In fact, the cdf 9/7 classical wavelet can be represented by 16 coefficients of Lo_D and Hi_D filter sets. The other filter coefficient sets Lo_R and Hi_R can be derived from these filter coefficients.

The orientation field of fingerprints has specific characteristics that discern the fingerprint images from other kinds of images. So, the fingerprint images make a specific class of images possessing distinct characteristics. A few researchers

exploited this property of fingerprints and evolved optimized wavelet coefficients for fingerprint image compression. Most of their works employed coefficients optimized from the classical cdf 9/7 wavelet using GA.

The optimization of classical cdf 9/7 wavelet coefficients is computationally complex as it requires 16 multiplications to transform every pair of subband samples. Due to the large computational complexity and hence the large evolution time involved, the researchers were strained to use even supercomputers for evolving optimized wavelet coefficients. However, the amount of time consumption can be reduced by employing LS of cdf 9/7 wavelet in which the equivalent symmetric lifting structure has just four lifting coefficients. So, in this work coefficients similar to symmetric lifting coefficients of cdf 9/7 wavelet were evolved to find the optimum coefficient values for fingerprint image compression under conditions subject to quantization.

Image compression and reconstruction under quantization necessitates the simultaneous minimization of MSE (or maximization of PSNR) and file size. So, it is an MOO problem. The image IE provides a precise calculation of the size of the compressed file and the computation of IE is very fast compared to file size calculation. Since PSNR and IE are two conflicting objectives, the optimization demands high PSNR with low IE value for the compressed image.

The work started with the wavelet optimization for a single-level DWT with a single training image and a quantization step size q = 64, using binary GA. The resultant PSNR obtained for the training image as well as the average PSNR over the 80 fingerprint images in the DB1_B of FVC 2000 database using the optimized coefficients are far better than that offered by the corresponding classical wavelet. Seeking for better results, in the next part of the work four training images were used with single-level transform and q = 64. The results were much promising as the optimized coefficients gave better performance than that given by a single training image. The subsequent work optimized coefficients for three-level transform and as expected, the results of the proposed work outperformed the previous results in literature.

Due to the contradictory nature of PSNR and IE, the desirable increase in PSNR causes simultaneous increase in the IE (a measure of file size). However, by keeping the IE or the compression ratio at a constant value the dual-objective problem can be converted into a single-objective problem and an accurate measure of the improvements in PSNR can be performed. So, the next proposed algorithm used PSNR as a single-objective of GA. Fixing CR = 16:1 takes only 1/16 (or 6.25%) numbers of most significant transform coefficients for reconstruction. This helps to reduce the computational complexity by reducing the GA evolution time.

Both single and multilevel WTs with single training image using the optimized lifting coefficients in each case were accomplished and the resulting PSNRs were compared with that of the corresponding classical wavelets. Several runs of the algorithm were performed to get the best results in each case.

Optimizations of coefficients for single-level to four-level compression using single training images (i.e., 101_1.tif of size 300 x 300 from DB1_B fingerprint database of FVC 2000) were performed. To ensure proper convergence in higher levels of MRA, the algorithm requires higher numbers of generations and population sizes.

The optimized coefficients offered better PSNRs when used for compressing images of certain other databases and also for certain other CRs (other than 16:1) too. The amount of PSNR improvement was the highest with the coefficients optimized for four-level MRA. Furthermore, with classical wavelet coefficients, there were no additional improvements in PSNR for five levels or above MRA compared to four levels. So, the maximum level of compression used for evolving coefficients was limited to four levels.

It was found that the coefficients optimized for higher levels of MRA performed better. The coefficients optimized for single-level showed an adverse effect on higher levels of compressions as they caused severe degradation of average PSNRs at these levels. The optimized coefficients, corresponding to other compression levels, (i.e., two-level to four-level) was found to be unsuitable for single-level compression as they resulted in degrading the average PSNR at that level.

This indicates that the coefficients optimized for single-level through four-level compressions are not appropriate for general compression purposes. This issue was circumvented by using multiple training images in GA evolution.

So, the next work presents techniques for faster evolution of wavelet coefficients optimized for better compression and reconstruction of fingerprint images.

Usually, full size images are being used for evolving wavelet coefficients. This evolution process is too slow. To speed up this, wavelets were optimized with different image sets like resized, cropped, resized-average and cropped-average images. Comparing the PSNRs offered by the optimized wavelets, it was found that the cropped images outperformed the resized images and is at par with the results reported so far. Wavelet lifting coefficients optimized from an average of four 256 x 256 centre-cropped images took less than $1/5^{th}$ the evolution time reported in literature. Besides increasing the computational speed by 81.35%, the optimized coefficients offered 1.009 dB improvements in average PSNR over 80 fingerprint images in the database. At the cost of a very small amount of PSNR, additional reduction in evolution time could be achieved. Except in few cases, the coefficients evolved for the database DB1_B of FVC 2000 offered better average PSNR when applied to the other fingerprint databases of different sizes and clarity. The evolved coefficients exhibited improvement in PSNR for other CRs too. For higher CRs, they outperformed the classical wavelets in compressing degraded images. There was reasonable improvement in PSNR when evolved coefficients were used with SPIHT algorithm. The coefficients optimized for thresholding conditions (i.e., single-objective problem) gave better average PSNR and better average IE under quantization conditions (i.e., dual-objective problem) for the database DB1_B and for most of the other fingerprint databases in FVC 2000. The optimized coefficients offered improvement in SSIM of the compressed images.

7.3 Gender Classification System using Genetic Algorithm

Apart from the fingerprint image compression, male/female gender classification is another promising area where optimization using genetic algorithm finds significant applications. Proceeding in this direction presents a multilevel approach for better classification of male and female gender from fingerprint images. In the first level, DWT, SVD and PCA transform based feature vectors were used as inputs to three independent BPNN classifiers for simultaneous gender classification. In the DWT based system, GA optimized cdf 9/7 wavelet lifting coefficients were used to decompose the fingerprint images into subbands. The NN employed GA optimized initial seed value and features derived from lesser number of subbands. Use of lifting coefficients and lesser number of subbands increased the speed of the classifier. Compared to the conventional method, the overall classification rate of the GA optimized DWT based gender classifier got enhanced by 10.6%. The proposed SVD and PCA based systems having optimized initial seed values used merely a few SVD and PCA components. Besides the hike in the speed of the classifiers, there were 9.1% and 7.8% improvements in classification accuracy compared to the conventional gender classifiers based on SVD and PCA respectively. Moreover, use of the optimized lifting coefficients and initial seed values produced better classification accuracy on a large number of additional fingerprint samples.

Since the outputs of the three classifiers were not unique, the next level of the system combined these outputs to take a better decision on gender. This decision based improved hybrid gender classifier provided overall accuracy of 93.94%, which is 5.24% above the best result, reported in literature. The improvement in classification speed of GA optimized decision based hybrid classifier was 97.33% above that of the decision based conventional classifier.

7.4 Scope for Further Work

In the proposed work, a faster algorithm for evolving optimized lifting coefficients from cdf 9/7 wavelet using GA to provide better performance on fingerprint image compression was presented. This work can be extended to evolve application-specific

optimized wavelets for medical, satellite, and digital photography applications. One of the factors which improve the performance of the evolved wavelet is a properly designed training data set. Therefore, techniques can be developed to design an optimum training data set, which improves the compression performance.

Regarding the gender classification problem, it will be very much useful if one could identify the age of the persons in addition to their gender information. The individuality of fingerprints in different age group can be exploited in forensic and non-forensic applications such as criminal identification, security problems, financial and identity misleading, etc. As such, the proposed gender classification techniques can be extended to classify the male and female genders to different age groups. By doing this, the database for searching a person can be further narrowed as it requires searching either a female or male database of a particular age group alone. This, in turn, can reduce the time for searching an individual in a large database. Thus, after a person is identified as female or male, more specific classifications can be done based on different age groups so that the search time for the particular person in the huge database can be reduced to a great extent.

REFERENCES

Acharya, T., & Tsai, P.-S. (2005). *JPEG2000 Standard, in JPEG2000 Standard for Image Compression: Concepts, Algorithms and VLSI Architectures*. Hoboken, NJ, USA: John Wiley & Sons, Inc.

Acree, M.A. (1999). Is there a gender difference in fingerprint ridge density?.*Forensic Science International*, *102*(1), 35–44.

Addison, P.S. (2002). *The Illustrated Wavelet Transform handbook: Introductory Theory and Applications in Science, Engineering, Medicine and Finance*. London: IOP Publishing Ltd.

Agnihotri, A.K, Jowaheer, V. , & Allock, A. (2012). An analysis of fingerprint ridge density in the Indo-Mauritian population and its application to gender determination. *Medicine, Science and the Law*, *52*(3),143-147.

Aldridge, S., Babb, B., Moore, F., & Peterson, M. (2010). Evolved image compression transforms, *Proc. of the SPIE 7704 Evolutionary and Bio-Inspired Computation: Theory and Applications IV*, 77040C.

Alrashed, H.F., & Berbar, M.A. (2013). Facial Gender Recognition Using Eyes Images, *Int. J.of Adv. Research in Computer and Comm.Engg.*, *2*(6),2441-2445.

Andina, D., & Pham, D.T. (2007). *Computational Intelligence for Engineering and Manufacturing*. New York, Springer.

Annadurai, S., & Shanmughalakshmi, R (2007). *Fundamentals of Digital Image Processing*, India: Pearson Edn.

Aware Biometric Software, (n.d.). http://www.aware.com/biometrics/awarewsq 1000.html. (Accessed 23 March 2015).

Babb, B. J. (2007). Evolved Transforms Surpass the FBI Wavelet for Improved Fingerprint Compression and Reconstruction, *Proc. of the 2007 Conf. Companion on Genetic and Evolutionary Computation, London*, 2603–2606.

Babb, B., & Moore, F. (2007). The Best Fingerprint Compression Standard Yet. *IEEE Int. Conf. on Systems, Man and Cybernetics*, ISIC,2911 –2916.

Babb, B.J., Moore, F. W., & Marshall, P. (2007). Evolved Multiresolution Analysis Transforms for Improved Image Compression and Reconstruction under Quantization. *Proc. of the 2007 IEEE Symp. on Computational Intell. in Image and Signal Processing*, 202-207.

Babb, B., Moore, F, & Peterson, M.(2009a). Optimized satellite image compression and reconstruction via evolution strategies. *Proc. of the SPIE, Evolutionary and Bio-Inspired Computation: Theory and Applications III*, Vol. 7347, article id. 73470O.

Babb , B. J., Moore , F. W., & Peterson, M. R. (2009b). Improved multiresolution analysis transforms for satellite image compression and reconstruction using evolution strategies. *Proc. of the 11th Annual Conf. Companion on Genetic and Evolutionary Computation Conference: GECCO '09* , 2547-2552.

Back, T. (1996). *Evolutionary Algorithms in Theory and Practice: Evolution Strategies, Evolutionary Programming, Genetic Algorithms*. NY: Oxford University Press, Inc.

Badawi, A., Mahfouz, M., Tadross, R., & Jantz, R. (2006). Fingerprint-Based Gender Classification. *Proc. of the 2006 Int. Conf. on Image Processing, Computer Vision and Pattern Recognition*, Vol. 1, 41-46.

Baker, K. (2013). *Singular Value Decomposition Tutorial.* Retrieved October 25, 2013 from http://www.ling.ohiostate.edu/~kbaker/pubs/Singular_Value_Decomposition_Tutorial.pdf

Bansal, A. , Agarwal, R. & Sharma R.K. (2014). Predicting Gender Using Iris Images. *Research Journal of Recent Sciences, 3*(4), 20-26.

Barua, S., Kotteri, K. A., Bell, A. E., & Carletta, J. E. (2004). Optimal quantized lifting coefficients for the 9/7 wavelet. *Proc. IEEE Int. Conf. Acoustics, Speech, Signal Processing*, Vol. 5,193-196.

Basha, A.F., & Jahangeer, G.S.B. (2012). Face Gender Image Classification Using Various Wavelet Transform and Support Vector Machine with various Kernels. *IJCSI Int. Journal of Computer Science Issues*, *9*(6), 2, 150-157.

Bishop, C.M. (1995). *Neural Networks for Pattern Recognition*. Oxford: Clarendon Press.

Bochner, S., & Chandrasekharan, K. (1949). *Fourier Transforms*. Princeton Uty. Press.

Bradley, J., Brislawn, C., & Hopper, T. (1993). The FBI Wavelet/Scalar Quantization Standard for Gray-scale Fingerprint image Compression. *SPIE Proc. Visual Information Processing II*, 1961, 293–304.

Brown, W. M. , Hines, M., Fane, B. A., & Breedlove, S. M. (2002). Masculinized Finger Length Patterns in Human Males and Females with Congenital Adrenal Hyperplasia. *Hormones and Behavior*, *42*(4), 380–386.

Bull, D.R., (2014). *Communicating Pictures: A Course in Image and Video Coding*.UK: Elsevier Ltd.

Burrus, C.S., Gopinath, R.A., & Guo, H. (1998). *Introduction to Wavelets and Wavelet Transforms: A primer*. NJ: Prentice Hall.

Castleman, K.R. (1996). *Digital Image Processing*. Prentice Hall.

Chand, P., & Sarangi, S. K. (2013). A Novel Method for Gender Classification Using DWT and SVD Techniques. *Int. J. of Computer Technology and Applications*, *4*(3), 445-449.

Chanda, B., & Majumder, D. D. (2000). *Digital Image Processing and Analysis*. Prentice-Hall of India.

Chen, C. & Ross, A., (2011). Evaluation of gender classification methods on thermal and near-infrared face images. *IEEE Int. Joint Conf. on Biometrics (IJCB)*, pp. 1-8.

Chui, C. K. (1992). *An Introduction to Wavelets*. San Diego: Academic Press.

Chun-Lin, L. (2010). *A Tutorial of the Wavelet Transform*. Retrieved October 20, 2013 from http://disp.ee.ntu.edu.tw/tutorial/WaveletTutorial.pdf.

Criminal Justice Information Services (CJIS). (1997). *WSQ Gray-scale Fingerprint Image Compression Specification*, FBI, Washington, D.C.

Coello, C. A. C., Lamont, G. B., & Veldhuizen, D. A. V. (2007). *Evolutionary Algorithms for Solving Multi-Objective Problem* (2nd ed.), NY: Springer-Verlag.

Cohen, A., Daubechies, I., & Feauveau, J.C. (1992). Biorthogonal Bases of Compactly Supported Wavelets. *Communications on Pure and Applied Mathematics*, *45*(5), 485-560.

Coley, D. A. (1999). *An Introduction to Genetic Algorithms for Scientists and Engineers*. Singapore: World Scientific Publishing Co. Pte. Ltd.

Daubechies, I. (1992). *Ten Lectures on Wavelets*. Philadelphia, Pennsylvania: SIAM.

Daubechies, I. (1998). Orthonormal Bases of Compactly Supported Wavelets. *Communications on Pure and Applied Mathematics*, *41*, 909-996.

Daubechies, I., & Sweldens, W (1998). Factoring wavelet transforms into lifting steps. *Journal of Fourier analysis and applications*, *4*(3), 247-269.

G. M. Davis, & A. Nosratinia. (1999). Wavelet-based image coding: an overview, *Appl. Comp. Control, Signal & Circuits*, B. N. Datta (ed), Birkhauser, 205–269, 1999.

Dhungana, H. N., &S ahu, K. K. (2013). Bayesian Approach for Gender Differentiation by Finger Ridges Count. *Research & Reviews: Journal of Statistics (STM Journals)*, *2*(2), 12- 15.

Dorigo, M., & Gambardella, M.L. (1997). Ant Colony System: A Cooperative Learning Approach to the Traveling Salesman Problem. *IEEE Transactions on Evolutionary Computation*, *1*(1), 53-66.

Eberhart, R., & Kennedy, J. (1995). Particle Swarm Optimization. *Proc. of IEEE Int. Conf. on Neural Networks*, IV, 1942-1948.

Emmanuel, B. S., Mu'azu, M. B., Sani, S. M., & Garba, S. (2014). A Review of Wavelet-Based Image Processing Methods for Fingerprint Compression in Biometric Application. *British Journal of Mathematics & Computer Science*, *4*(19), 2781-2798.

Erçal, F., Gokmen, M., & Ersoy, I. (1999). A model-based approach for compression of fingerprint images. *Proc. of Int. Conf. on Image Processing (ICIP)*, *2*, 973-977.

Eshak, G. A., Zaher, J. F. , Hasan, E. I., & Ewis, A. A. E. A. (2013). Sex identification from fingertip features in Egyptian population. *J. Forensic and Leg. Med.*, *20* (1), 46–50.

Fausett, L. V. (1994). *Fundamentals of Neural Networks: Architectures, Algorithms, and Applications*. USA: Prentice-Hall.

Ferreira, A. J., & Figueiredo, M. A. T. (2006). On the use of independent component analysis for image compression. *Signal Processing: Image Communication*, *21*(5), 378–389.

Fidler, A., Skaleric, U., & Likar, B. (2006). The impact of image information on compressability and degradation in medical image compression. *Med. Phys. 33*(8), 2832-2838.

Fieguth, P. (2011). *Statistical Image Processing and Multidimensional Modeling*. NY: Springer.

Fisher, Y. (1995). *Fractal Image Compression-Theory and Applications*. NY: Springer-Verlag.

Fonseca, C.M., & Fleming, P.J. (1995). An overview of evolutionary algorithms in multiobjective optimization. *Evolutionary Computation, 3*(1), 1-16.

Freeman J.A., & Skapura D.M. (1991). *Neural Networks: Algorithms, Applications and Programming Techniques*. USA: Addison Wesley Longman Publishing Co., Inc.

Funk, W., Arnold, M., Busch, C., & Munde, A. (2005). Evaluation of Image Compression Algorithms for Fingerprint and Face Recognition Systems. *Proc. from the Sixth Annual IEEE SMC Information Assurance Workshop, IAW '05*, 72 – 78.

Fingerprint Verification Competition FVC2000. (2000). Retrieved February 2, 2006, fromhttp:/bias.csr.unibo.ir/fvc2000.

Fingerprint Verification Competition FVC2002. (2002). Retrieved March 10, 2007, fromhttp:/bias.csr.unibo.ir/fvc2002.

Fingerprint Verification Competition FVC2004. (2004). Retrieved March 10, 2007, fromhttp:/bias.csr.unibo.ir/fvc2004.

Garcia, E. (2006). Singular Value Decomposition (SVD) A Fast Track Tutorial. Retrieved August 22, 2013 from https://www.ce.yildiz.edu.tr/personal/banud/file/1200/singular-value-decomposition-fast-track-tutorial.pdf.

Gnanasivam, P., & Muttan, S. (2012). Fingerprint Gender Classification Using Wavelet Transform and Singular Value Decomposition. *Int. Journal of Computer ScienceIssues*, *9*(2),3, 274-282.

Goldberg, D.E. (2004). *Genetic Algorithm in Search, Optimization & Machine Learning*. India: Pearson Edn.

Gonzalez, R.C., & Woods, R. E. (2008). *Digital Image Processing*. Pearson Education Inc., third edition.

Gornale, S. S., Geetha, C.D., & Kruthi, R. (2013). Analysis of Fingerprint Image for Gender Classification Using Spatial and Frequency Domain Analysis. *American Int. J. of Research in Science, Technology, Engineering & Mathematics (AIJRSTEM), 1*(1), 46-50.

Gornale, S. S., Humbe, V. T., Manza, R. R., & Kale, K.V. (2008). Fingerprint Image Compression using Retain Energy (RE) and Number of Zeros (NZ) through Wavelet Packet (WP). *Int. J. of Computer Science and Security, 1*(2), 35-42.

Gornale, S.S., Manza, R. R., Humbe, V., & Kale, K.V. (2007). Performance Analysis of Biorthogonal Wavelet Filters for Lossy Fingerprint Image Compression. *Int. J. of Imaging Science and Engineering (IJISE), 1*(1),16-20.

Goswami, J.C., & Chan, A.K. (1999). *Fundamentals of Wavelets: Theory, Algorithms, and applications.* New Delhi: Wiley India (P) Ltd.

Graps, A. (1995). An Introduction to Wavelets. *IEEE Transactions on Computer Science and Engineering, 2*(2), 50-61.

Grasemann, U. & Mikkulainen, R. (2005). Effective Image Compression using Evolved Wavelets. *Proc. of the 7th Annual Genetic and Evolutionary Computation Conference (GECCO'2005), Washington, DC, 2*, 1961-1968, ACM.

Gungadin, S. (2007). Sex Determination from Fingerprint Ridge Density. *Internet Journal of Medical Update, 2*(2), 4-7.

Hajek, M. (2005). *Neural Networks*. University of KwaZulu-Natal.

Haykin, S. (1999). *Neural Network: A Comprehensive Foundation*. NJ: Prentice-Hall, Inc.

Holder, E.H., Robinson, L.O., Laub, J.H., & National Institute of Justice (U.S.) (2011). *The Fingerprint Sourcebook*. Washington, DC: U.S. Dept. of Justice, Office of Justice Programs, National Institute of Justice.

Holland, J.H. (1975). *Adaptation in natural and artificial systems.* Ann Arbor: University of Michigan Press.

Huang, S., Ward, M.O., & Rundensteiner, E.A. (2005). Exploration of dimensionality deduction for text visualization. *Proc. of the IEEE Third Int. Conf. on Coordinated and Multiple Views in Exploratory Visualization (CMV '05)*, 63–74.

Ientilucci, E.J. (2003). Using Singular Value Decomposition. Retrieved August 22, 2013 from http://www.cis.rit.edu/ ~ejipci/Reports/svd.pdf.

Islam, M. R., Bulbul, F., & Shanta, S.S. (2012). Performance analysis of Coiflet-type wavelets for a fingerprint image compression by using wavelet and wavelet packet transform. *Int. J. of Computer Science & Engineering Survey (IJCSES), 3*(2),79-87.

Jain, A. K. (1989). *Fundamentals of Digital Image Processing*. Pearson Education Inc.

Jain, A. K., Ross, A., & Prabhakar, S. (2004). An Introduction to Biometric Recognition.*IEEE Trans. on Circuits and Systems for Video Technology, 14*(1), 4-20.

Jaswante, A., Khan, A.U., & Gour, B. (2013). Gender Classification Technique Based on Facial Features using Neural Network. *Int. J. of Computer Science and Information Technologies (IJCSIT), 4*(6),839-843.

Jeong, D. H., Ziemkiewicz, C., Ribarsky, W., & Chang, R. (2009). *Understanding Principal Component Analysis Using a Visual Analytics Tool*. Charlotte Visualization Center, UNC Charlotte.

Jolliffe, I.T. (1986). *Principal Component Analysis.* NY: Springer-Verlag.

Kaiser, G. (1994). *A Friendly Guide to Wavelets*. Birkhäuser.

Kampfer , A. M., Stogner , H., & Uhl, A. (2007). Comparison of Compression Algorithms' Impact on Fingerprint and Face Recognition Accuracy. *Proc. of SPIE 6508 Visual Communications and Image Processing*, 650810, doi:10.1117/12.699199.

Kasaei, S., Deriche, M., & Boash, B, (2002). Novel Fingerprint Image compression technique using Wavelet packets and Pyramid Lattice Vector Quantization. *IEEE Transactions on Image Processing, 11*(12), 1365-1378.

Kaur, R., Mazumdar, S. G., & Bhonsle, D. (2012). A Study on Various Methods of Gender Identification Based on Fingerprints. *Int. J. of Emerging Technology and Advanced Engineering, 2*(4), 532-536.

Keinert, F. (2003). *Wavelets and Multiwavelets*. Studies in advanced mathematics, CRC Press.

Khalid Sayood (2006). *Introduction to Data Compression*. San Francisco, CA: Elsevier.

Khan, M.N.A, Qureshi, S.A., & Riaz, N. (2013). Gender Classification with Decision Trees. *Int. J. of Signal Proc., Image Proc. and Pattern Recog., 6*(1), 165-176.

Kirkpatrick, S.,Gelatt, C.D., & Vecchi, M. P. (1983). Optimization by Simulated Annealing. *Science, 220*(4598), 671-680.

Kobayashi, M. (1998*). Wavelets and their Applications: Case Studies*. Society for Industrial and Applied Mathematics (SIAM), USA.

Koren, Y., & Carmel, L. (2003). Visualization of Labeled Data Using Linear Transformations. *Proc. of the IEEE conf. on Information Visualization (INFOVIS'03)*,121-128.

Koza, J.R. (1992). *Genetic Programming: On the Programming of Computers by Means of Natural Selection*.Cambridge, London: MIT Press.

Kröse, B., & Smagt, P. (1996). *An Introduction to Neural Networks*. University of Amsterdam.

Kumar, P., Jakhanwal, N., Bhowmick, B., & Chandra, M. (2011). Gender Classification Using Pitch and Formants. *Proc. of the 2011 Int. Conf. on Communication, Computing & Security (ICCCS '11)*, 319-324.

Lakshmi, F. G. P., Chandulal, J.A., & Patro, Y. G. K. (2012). Finger Print Image Compression for Extracting Texture Features and Reconstructing. *IOSR Journal of Computer Engineering (IOSRJCE), 3*(2),44-46.

Lewis, A.S., & Knowles, G. (1992). Image Compression Using the 2D Wavelet Transform. *IEEE Transactions on Image Processing, 1*, 244–250.

Li, B., Lian, X.-C., & Lu, B.-L. (2012). Gender classification by combining clothing, hair and facial component classifiers. *Neurocomputing, 76*(1), 18-27.

Li, J., & Kuo, C.C.J. (1995). *Fingerprint Compression Using Embedded Wavelet Packet Transform.* Rockwell conference on signal processing, Thousand Oak, CA.

Lian, H-C., & Lu,B-L. (2006). Multi-view Gender Classification Using Local Binary Patterns and Support Vector Machines. *Advances in Neural Networks, Lecture Notes in Computer Science, 3972*, 202-209.

Lu, J., Wang, G., & Huang, T.S. (2012). Gait-Based Gender Classification in Unconstrained Environments. *21st IEE Int. Conf. on Pattern Recognition (ICPR)*, 3284 – 3287.

Madsen, R. E., Hansen, L. K., &, O. (2004). Singular Value Decomposition and Principal Component Analysis. Retrieved May 12, 2013 from www2.imm.dtu.dk/pubdb/views/ edoc_download.php/4000/pdf.

Mallat, S. (1989a). A Theory for Multiresolution Signal Decomposition: The Wavelet Representation. *IEEE Trans. on Pattern Analysis and Machine Intelligence, 11*, 674–693.

Mallat, S. G. (1989b). Multifrequency channel decompositions of images and wavelet models. *IEEE Trans. on Acoustics, Speech, and Signal Proc., 37*(12), 2091-2110.

Mallat, S. (1999). *A Wavelet Tour of Signal Processing*. San Diego, California, USA: Academic Press, Elsevier.

Maltoni, D., & Jain, A.K. (2004). Biometric Authentication. *Proc. of ECCV 2004 Int. Workshop, BioAW 2004*.Prague, Czech Republic: Springer.

Maltoni, D., Maio, D., Jain, A.K., & Prabhakar, S. (2009). *Handbook of Fingerprint Recognition* (2nd ed.). London, UK: Springer-Verlag.

Marasco, E., Lugini, L., & Cukic, B. (2014). Exploiting quality and texture features to estimate age and gender from fingerprints. *SPIE Defense+ Security, Int. Society for Opticsand Photonics*, 90750F.

McFadden D., & Shubel E. (2002). Relative lengths of fingers and toes inhuman males and females. *Hormones and Behavior*, *42*(4),492–500.

Meena, K., Subramaniam, K., & Gomathy, M. (2013). Gender Classification in Speech Recognition using Fuzzy Logic and Neural Network. *The Int. Arab Journal of Information Technology*, *10*(5), 477-485.

Meyer, Y. (1992). *Wavelets and Operators*.Cambridge: Cambridge University Press.

Michel, M., Yves, M., Oppenheim, G., & Poggi, J.M. (2007). *Wavelets and their Applications*. United States: ISTE Ltd.

Michie, D., Spiegelhalter, D. J., & Taylor,C. C. (1994). *Machine learning, neural and statistical classification*. NY: Ellis Horwood.

Moallem, P., & Mousavi, B. S. (2013). Gender Classification by Fuzzy Inference System. *Int. J. of Advanced Robotic Systems*, *10*(89), 1-7.

Moore, F., Marshall, P., & Balster, E. (2005). Evolved Transforms for Image Reconstruction. *The IEEE Congress on Evolutionary Computation*, *3*, 2310- 2316.

Mozaffari, S., Behravan, H., & Akbari, R., (2010). Gender Classification Using Single Frontal Image Per Person: Combination of Appearance and Geometric Based Features. *20th IEEE Int. Conf. on Pattern Recognition (ICPR)*, 1192 – 1195.

Muhsen, Z., Dababneh, M., & Nsour, A. A. (2011). Wavelet and Optimal Requantization Methodology for Lossy Fingerprint Compression. *The Int. Arab Journal of Information Technology*, *8*(4),383-387.

Nanavati, S., Thieme, M., & Nanavati, R. (2002). *Biometrics: Identity verification in a networked world*. USA: John Wiley & Sons.

Nayak, V.C., Rastogi, P., Kanchan, T., Lobo, S.W., Yoganarasimha, K., Nayak, S., Rao, N.G., Kumar, G. P., Shetty, B. S. K., & Menezes, R.G. (2010a). Sex differences from fingerprint ridge density in the Indian population. *J. Forensic Leg. Med.*, *17*(2), 84-6.

Nayak, V.C. , Rastogi, P., Kanchan, T., Yoganarasimha, K., Kumar, G.P., & Menezes, R.G. (2010b). Sex differences from fingerprint ridge density in Chinese and Malaysian population. *Forensic. Sci. Int.*, *197*(1), 67-69.

Nazir, M., Ishtiaq, M., Batool, A., Jaffar, M.A., & Mirza, A.M. (2010). Feature Selection for Efficient Gender Classification. *Proc. of the 11th WSEAS Int. Conf. on Neural Networks, Evolutionary Computing and Fuzzy Systems*, pp.70-75.

Ng, C.B., Tay, Y.H., & Goi, B..M. (2012). Vision-based human gender recognition: a survey. In Anthony, P., Ishizuka, M., Lukose, D. (Eds.). *Trends in Artificial Intelligence*. PRICAI.

Novakovic, J., & Rankov, S. (2011). Classification Performance Using Principal Component Analysis and Different Value of the Ratio R. *Int. J. of Computers, Communications & Control, VI (2)*,317-327.

Omidiora, E.O., Ojo, O., Yekini, N.A., & Tubi, T.O. (2012). Analysis, Design and Implementation of Human Fingerprint Patterns System Towards Age & Gender Determination, Ridge Thickness To Valley Thickness Ratio (RTVTR) & Ridge Count On Gender Detection. *Int. J. of Adv. Research in Artificial intell*., *2*(4),532-536.

Orandi, S., Libert, J.M., Grantham, J.D., Ko, K., Wood, S.S., Byers, F.R., Bandini, B., Harvey, S.G., & Garris, M.D. (2014). Compression Guidance for 1000 ppi Friction Ridge Imagery. *US: NIST Special Publication 500-289.*

Perez, C., Tapia, J., Estevez, P., & Held, C. (2012). Gender classification from face images using mutual information and feature fusion. *Int. J. of Optomechatronics*, *6*(1), 92-119.

Perumal. V., & Ramaswamy, J. (2009). An Innovative Scheme For Effectual Fingerprint Data Compression Using Bezier Curve Representations. *Int. J. of Computer Science and Information Security (IJCSIS), 6*(1), 149-157.

Peterson, M. R., Lamont, G.B., & Moore, F. (2006). Improved Evolutionary Search for Image Reconstruction Transforms. *IEEE Congress on Evolutionary Computation*, Canada, pp. 2880-2887.

Planetbiometrics, (n.d.). Retrieved March 23, 2015 fromhttp://www.planetbiometrics.com/ article-details/i/2253/.

Polikar, R. (1996). The Wavelet Tutorial Part III, Multiresolution analysis & The Continuous Wavelet Transform. Retrieved November 8, 2014fromhttps://ccrma.stanford.edu/ ~unjung/mylec/WTpart1.html.

Prasad, B., & Prasanna, S.R.M. (2008). *Speech, Audio, Image and Biomedical Signal Processing using Neural Networks*. Berlin: Springer-Verlag.

Purohit, R. V., Imam, S. A., & Beg, M. T. (2011). Recognizing Gender with Fingerprints. *Int. J.of Advanced Engineering Technology(IJAET), 2*(4),239-241.

Rabbani, M., & Jones, P.W. (1991). *Digital Image Compression Techniques*. The Society of Photo-Optical Instrumentation Engineers (SPIE). Bellingham, WA.

Rahman, M.H., Chowdhury, S., & Bashar, M.A. (2013). An Automatic Face Detection and Gender Classification from Color Images using Support Vector Machine. *J. of Emerging Trends in Computing and Information Sciences*, *4*(1),5-11.

Rai P., & Khanna, P. (2012). Gender classification techniques: a review. *Advances in Computer Science Eng. & Appl., Adv. Intell. Soft Comput. (AISC). Springer-Verlag, 166*, 51–59.

Rajasekaran.S., & Vijayalakshmi Pai, G.A. (2012). *Neural Networks, Fuzzy Logic, and Genetic Algorithms: Synthesis and Applications*. New Delhi: PHI Learning Pvt. Ltd.

Randy L.Haupt, & Sue Ellen Haupt (2004). *Practical Genetic Algorithms* (2nd Edn.), NJ: John Wiley & Sons, Inc.

Rao, K.R., & Yip, P.C. (2001). *The Transform and Data Compression Handbook*. USA: CRC Press.

Rao, R.M., & Bopadikar, A.S. (1998). *Wavelet Transforms: Introduction to Theory and Applications*. USA: Addison Wesley Longman, Inc.

Rastogi, P., & Pillai, K. R. (2010). A study of fingerprints in relation to gender and blood group. *J. Indian Acad. Forensic Med., 32*(1), 11-14.

Ravi, S., & Wilson, S. (2010). Face detection with facial features and gender classification based on support vector machine. *Proc. of IEEE Int. Conf. on Computational Intelligence and Computing Research*, pp. 125-130.

Rechenberg, I. (1973). *Evolution sstrategie: Optimierung Teehnischer Systemenach Prinzipien der Biologischen Evolution*. Stuttgart: Frommann-Holzboog.

Rioul, O., & Vetterli, M. (1991). Wavelets and signal processing. *IEEE signal processing magazine, 8*, 14-38.

Rojas, R. (1996). *Neural networks: a systematic introduction*. Berlin: Springer-Verlag.

Rumelhart, D.E., Hinton, G.E., & Williams, R.J. (1986). Learning representations by back-propagating errors. *Nature, 323,* 533–536.

Safonova, A., Hodgins, J. K., & Pollard, N. S. (2004). Synthesizing Physically Realistic Human Motion in Low-Dimensional, Behavior-Specific Spaces. *ACM Transaction on Graphics (TOG), 23*(3),514-521.

Said, A., & Pearlman, W.A. (1996). A New, Fast and Efficient Image Codec based on Set Partitioning in Hierarchical Trees. *IEEE Transactions on Circuits and Systems for Video Technology, 6*, pp. 243–250.

Salvador, R., Moreno, F., Riesgo, T., & Sekanina, L. (2011). Evolutionary approach to improve wavelet transforms for image compression in embedded systems. *Eurasip J. Advances inSignal Processing*, 2011, 1-20, Article ID 973806.

Santhi, M., & Banu, R.S.D.W. (2010). Modified SPIHT Algorithm for Coding Color Images using Inter-color Correlation. *IJCSNS Int. J. of Computer Science and Network Security, 10*(3), 256-265.

Set Partitioning In Hierarchical Trees (SPIHT). (n.d.). Retrieved January 5, 2008, from http://www.cipr.rpi.edu/research/SPIHT.

Semmlow, J.L. (2004). *Biosignal and Biomedical Image Processing: MATLAB-Based Applications*. USA: Marcel Dekker, Inc.

Shahid, Z., Dupont, F., & Baskurt, A. (2009). A novel efficient Image Compression System based on Independent Component Analysis. *Proc. SPIE 7248, Wavelet Applications in Industrial Processing VI,* doi:10.1117/12.806159, http://dx.doi.org/10.1117 /12.806159.

Shakhakarmi, N. (2012). Quantitative Multiscale Analysis using Different Wavelets in 1D Voice Signal and 2D Image. *IJCSI Int. J. of Computer Science Issues, 9*(1), 2, 475-484.

Shan, C. (2012). Learning local binary patterns for gender classification on real-world face images. *Pattern Recognition Letters, 33*(4), 431-437.

Shan, C., Gong, S.., & McOwan, P.W. (2007). Learning gender from human gaits and faces. *IEEE Conf. on Adv. Video and Signal Based Surveillance (AVSS 2007)*, pp. 505 – 510.

Shannon, C.E.(1948). A Mathematical Theory of Communication. *Bell System Technical Journal, 27*, 379–423, 623–656.

Shao, G., Wu, Y. Yong, A., Liu, X., & Guo, T. (2014). Fingerprint Compression Based on Sparse Representation. *IEEE Trans. on Image Processing*, *23*(2), 489- 501.

Shapiro, J.M. (1993). Embedded Image Coding Using Zero trees of Wavelet Coefficients. *IEEE Transactions on Signal Processing*, *41*, 3445–3462.

Sheng, Y. (1996). *Wavelet transform. The Transform and Application Handbook*. Boca Raton, Fl (USA): CRC Press.

Sherlock, B. G., & Monro, D. M. (1996). Optimized Wavelets for Fingerprint Compression. *IEEE Proceedings of International Conference on Acoustics, Speech, and Signal Processing (ICASSP-96)*, *3*, pp. 1447 – 1450.

Shi, Y. Q., & Sun, H.(2000). *Image and video compression for multimedia engineering: fundamentals, algorithms, and standards.* CRC Press.

Shobeirinejad, A., & Gao, Y. (2010). Gender Classification Using Interlaced Derivative Patterns. *20th International Conference on Pattern Recognition (ICPR),*1509 -1512.

Shoniregun, C. A., & Crosier, S. (2008). *Securing biometrics applications*. USA: Springer.

Singh, G. (2012). Determination of Gender Differences from Fingerprints Ridge Density in Two Northern Indian Population of Chandigarh Region. *J. Forensic Res.*, *3*(3).

Sivanandan, S.N., & Deepa, S.N., (2008). *Introduction to Genetic Algorithms*. Berlin: Springer-Verlag.

Soman, K.P., & Ramachandran, K.I. (2006). *Insight into Wavelets : From Theory to Practice* (2nd edn.). India: PHI Pvt. Ltd.

Stewart, D., Pass, A., & Zhang, J. (2013). Gender classification via lips: static and dynamic features. *IET Biometrics*, *2*(1), 28 – 34.

Stolojescu, C., Railean, I., Moga, S., & Isar, A. (2010). Comparison of Wavelet Families with Application to WiMax Traffic Forecasting. *Proc.of 12th Int. Conf. on Optimization of Electrical and Electronic Equipment (OPTIM), Brasov, Romania,* pp. 932-937.

Strang, G. (1988). *Linear Algebra and its Applications* (3rd Edn.). USA: Thomson Learning, Inc.

Strang G. (2009). *Introduction to Linear Algebra (4th Edn.*). USA: Wellesley- Cambridge Press.

Sudhakar.R, S., & Jayaraman.S, J. (2008). Fingerprint Compression Using Multiwavelets. *World Academy of Science, Engineering and Technology, International Science Index* 19, *2*(7), 968 - 977.

Sung, T. Y., & Hsin, H. C. (2007). A Hybrid Image Coder Based on SPIHT Algorithm with Embedded Block Coding. *IEICE Transactions Fundamentals, E90-A* (12), 2979-2984.

Suresh, G.R., Sudha, S., & Sukanesh, R. (2009). Shape Adaptive Wavelet Transform for Magnetic Resonance Images Coding. *International Journal of Electronics*, 96, 613–622.

Sweldens, W. (1996). The Lifting Scheme: A custom-design construction of biorthogonal wavelets. *J. Applied and Computational Harmonic Analysis*, *3*(2), 186-200.

Sweldens, W. (1997). The Lifting Scheme: A construction of second-generation wavelets. *SIAM Journal of Mathematical Analysis*, *29*(2),511-546.

Taubman, D., & Marcellin, M. (2002). *JPEG2000: Image Compression Fundamentals, Standards, and Practice*. Boston/Dordrecht/London: Kluwer Academic Publishers.

Theodoridis, S., Pikrakis, A., Koutroumbas, K., & Cavouras, D. (2010). *Introduction to Pattern Recognition : A MATLAB Approach*. Academic Press.

Tom, R. J., & Arulkumaran, T. (2013). Fingerprint Based Gender Classification Using 2D Discrete Wavelet Transforms and Principal Component Analysis. *International Journal of Emerging Trends and Technology*, *4*(2), 199-203.

Topiwala, P. N. (1998). *Wavelet Image and Video Compression*. USA: Kluwer Academic Publishers.

Turk, M., & Pentland, A. P. (1991). Face recognition using eigenfaces. *Proc. IEEE Computer Society Conf. on Computer Vision and Pattern Recognition*, pp. 586 – 591.

UIDAI Committee on Biometrics (2009). *Biometric Design Standards for UID Applications. Version 1.0*, New Delhi: Unique Identification Authority of India.

Veerakumar, T., Esakkirajan, S., Sudhakar, R., & Murugan, V. S. (2007). Fingerprint Compression Using Contourlet Transform and Self Organizing Feature Map. *Iranian Journal of Electrical and Computer Engineering*, *6*(2), 133-140.

Verma, M., & Agarwal, S. (2009). Fingerprint Based Male-Female Classification. *Proc. of the Int. Workshop on Computational Intelligence in Security for Information Systems (CISIS'08) Advances in Soft Computing*, 53, pp. 251-257.

Vetterli, M., & Herley, C. (1992). Wavelets and Filter Banks: Theory and Design. *IEEE Trans. on Signal Processing*, *40*(9), 2207-2232.

Vetterli, M., & Kovacevic, J. (1995). *Wavelets and Subband Coding*. Englewood Cliffs, NJ: Prentice-Hall.

Villasenor, J., Belzer, B., & Lia, J. (1995). Wavelet filter evaluation for image compression. *IEEE Trans. on Image Processing*, 2, 1053-1060.

Wang, Z., Bovik, A. C., Sheikh, H. R., & Simoncelli, E. P. (2004). Image quality assessment: From error visibility to structural similarity. *IEEE Trans. Image Process.*, *13*(4), 600-612.

Watson, A. B. (1994). Image Compression Using the Discrete Cosine Transform. *Mathematica Journal*, *4*(1), 81-88.

Wei, L. (2008). Fingerprint Classification Using Singularities Detection. *Int. Journal of Mathematics and Computers in Simulation. 2*(2), 158-162.

Welstead, S. (1999). *Fractal and Wavelet Image Compression Techniques*. The Society of Photo-Optical Instrumentation Engineers (SPIE), Bellingham, WA.

Willis, M. J., Hiden, H. G., Marenbach, P., McKay, B., & Montague, G. A. (1997). Genetic programming: an introduction and survey of applications. *2nd Int. conf. on Genetic Algorithms in Engg. Systems: Innovations and Applications (GALESIA)*, pp. 314-319.

Woodward, J. D. Jr., Orlans, N. M., & Higgins, P.T. (2003). *Biometrics: The ultimate Reference*. New Delhi: Dreamtech Press.

Wu, M., & Yuan, Y. (2014). Gender Classification Based on Geometry Features of Palm Image. *The Scientific World Journal*, 2014, 1-7, doi:10.1155/2014/734564.

YooJH., Hwang D., & Nixon M.S. (2005). Gender Classification in Human Gait Using Support Vector Machine. In: Blanc-Talon J., Philips W., Popescu D., Scheunders P. (eds). *Advanced Concepts for Intelligent Vision Systems. ACIVS 2005*. *Lecture Notes in Computer Science*, 3708. Springer, Berlin, Heidelberg.

Yoon, S., & Jain, A. K. (2013). Is there a fingerprint pattern in the image? *In* Proceedings - 2013 International Conference on Biometrics, ICB 2013 *[6613023] IEEE Computer Society*. DOI: 10.1109/ICB.2013.6613023.

Young, R.K. (1993). *Wavelet Theory and its Applications*. NY: Springer Science+Business Media.

Zeng , W., Yu , H., & Lin, C.Y. (2006). *Multimedia Security Technologies for Digital Rights Management*. Orlando, FL: Academic Press, Inc.

Zhang, B. L., Zhang, H., & Ge, S. S. (2004). Face Recognition by Applying Wavelet Subband Representation and Kernel Associative Memory. *IEEE Transactions on Neural Networks*, *15*(1),166-177.

Zhao, S., & Wang, X. F. (2009). Fingerprint Image Compression Based on Directional Filter Banks and TCQ. *Second International Workshop on Knowledge Discovery and Data Mining, (WKDD 2009)*, pp.660 – 663.

Zhou, Y., Guo, T., & Wu, M. (2010). Fingerprint image compressionalgorithm based on matrix optimization. *Proc. 6th International Conference on DigitalContent, Multimedia Technology and its Applications*, pp. 14–19.

LIST OF PUBLICATIONS

Journal Papers

1. K.T. Shanavaz & P. Mythili (2013). Faster techniques to evolve wavelet coefficients for better fingerprint image compression, *International Journal of Electronics, Taylor & Francis*, *100* (5) : 655-668.

2. K.T. Shanavaz & P. Mythili (2016), A fingerprint-based hybrid gender classification system using genetic algorithm, *International Journal of Computational Vision and Robotics*, *6*(4) : 399-413.

Conference Papers

1. K.T. Shanavaz & P. Mythili (2010). An Improved Technique for Evolving Wavelet Coefficients for Fingerprint Image Compression, *Proceedings of IEEE International Conference on Communication Control and Computing Technologies (ICCCCT'10)*, pp. 665-669.

2. K.T. Shanavaz & P. Mythili (2012). Evolution of Better Wavelet Coefficients for Fingerprint Image Compression using cropped images, *Proceedings of IEEE International Conference on Advances in Computing and Communications (ICACC 2012)*, pp.126-129.